

IOWA STATE UNIVERSITY

Digital Repository

Retrospective Theses and Dissertations

Iowa State University Capstones, Theses and
Dissertations

1986

The glassy phase and reaction products of Iowa fly ashes

Kenneth Lynn Bergeson
Iowa State University

Follow this and additional works at: <https://lib.dr.iastate.edu/rtd>

 Part of the [Civil Engineering Commons](#)

Recommended Citation

Bergeson, Kenneth Lynn, "The glassy phase and reaction products of Iowa fly ashes " (1986). *Retrospective Theses and Dissertations*. 8058.
<https://lib.dr.iastate.edu/rtd/8058>

This Dissertation is brought to you for free and open access by the Iowa State University Capstones, Theses and Dissertations at Iowa State University Digital Repository. It has been accepted for inclusion in Retrospective Theses and Dissertations by an authorized administrator of Iowa State University Digital Repository. For more information, please contact digirep@iastate.edu.

INFORMATION TO USERS

This reproduction was made from a copy of a manuscript sent to us for publication and microfilming. While the most advanced technology has been used to photograph and reproduce this manuscript, the quality of the reproduction is heavily dependent upon the quality of the material submitted. Pages in any manuscript may have indistinct print. In all cases the best available copy has been filmed.

The following explanation of techniques is provided to help clarify notations which may appear on this reproduction.

1. Manuscripts may not always be complete. When it is not possible to obtain missing pages, a note appears to indicate this.
2. When copyrighted materials are removed from the manuscript, a note appears to indicate this.
3. Oversize materials (maps, drawings, and charts) are photographed by sectioning the original, beginning at the upper left hand corner and continuing from left to right in equal sections with small overlaps. Each oversize page is also filmed as one exposure and is available, for an additional charge, as a standard 35mm slide or in black and white paper format.*
4. Most photographs reproduce acceptably on positive microfilm or microfiche but lack clarity on xerographic copies made from the microfilm. For an additional charge, all photographs are available in black and white standard 35mm slide format.*

*For more information about black and white slides or enlarged paper reproductions, please contact the Dissertations Customer Services Department.

U·M·I Dissertation
Information Service

University Microfilms International
A Bell & Howell Information Company
300 N. Zeeb Road, Ann Arbor, Michigan 48106

8627093

Bergeson, Kenneth Lynn

THE GLASSY PHASE AND REACTION PRODUCTS OF IOWA FLY ASHES

Iowa State University

PH.D. 1986

University
Microfilms
International 300 N. Zeeb Road, Ann Arbor, MI 48106

PLEASE NOTE:

In all cases this material has been filmed in the best possible way from the available copy.
Problems encountered with this document have been identified here with a check mark ✓.

1. Glossy photographs or pages _____
2. Colored illustrations, paper or print _____
3. Photographs with dark background ✓
4. Illustrations are poor copy _____
5. Pages with black marks, not original copy _____
6. Print shows through as there is text on both sides of page _____
7. Indistinct, broken or small print on several pages ✓
8. Print exceeds margin requirements _____
9. Tightly bound copy with print lost in spine _____
10. Computer printout pages with indistinct print _____
11. Page(s) _____ lacking when material received, and not available from school or author.
12. Page(s) _____ seem to be missing in numbering only as text follows.
13. Two pages numbered _____. Text follows.
14. Curling and wrinkled pages _____
15. Dissertation contains pages with print at a slant, filmed as received _____
16. Other _____

University
Microfilms
International

**The glassy phase and
reaction products of Iowa fly ashes**

by

Kenneth Lynn Bergeson

**A Dissertation Submitted to the
Graduate Faculty in Partial Fulfillment of the
Requirements for the Degree of**

DOCTOR OF PHILOSOPHY

**Department: Civil Engineering
Major: Geotechnical Engineering**

Approved:

Signature was redacted for privacy.

In Charge of Major Work

Signature was redacted for privacy.

For the Major Department

Signature was redacted for privacy.

For the Graduate College

Iowa State University

Ames, Iowa

1986

TABLE OF CONTENTS

	Pages
INTRODUCTION	1
Problem Statement	1
Objectives	2
BACKGROUND AND LITERATURE REVIEW	3
Structure of Glass	3
Atomic Structure	3
Glass Formers and Modifiers	3
Glassy Phase of Fly Ash	8
GLASSY PHASE OF IOWA FLY ASHES	10
Composition	10
Chemical Relationships	26
Glassy Phase Reactivity	34
Summary	51
SECONDARY CHEMICAL ADDITIVE STUDY	54
Introduction	54
Previous Work	54
Effects of Reagent Grade Chemicals	60
Neal 2	60
Neal 4	63
Fertilizer Grade Chemicals	66
Neal 2	70
Neal 4	72
Ottumwa	77
Summary	83
REACTION MECHANISMS	84
CONCLUSIONS	103
BIBLIOGRAPHY	105
ACKNOWLEDGEMENTS	112
APPENDIX: FIGURES	113

INTRODUCTION

Problem Statement

In Iowa, the increased usage of western coals coupled with stringent pollution control requirements on power plants and new power plant designs have resulted in fly ashes of significantly different chemical properties than those of ten years ago. Many of the fly ashes now being produced in Iowa contain crystalline compounds somewhat analogous to compounds contained in portland cement. These compounds impart cementitious properties to the fly ashes and result in significant early compressive strength development. Many of the fly ashes now being produced should no longer be considered "pozzolans". Some are, in fact, more akin to low grade hydraulic cements in and of themselves. There is still much we do not know about the properties of the newer fly ashes.

Approximately 20 percent of the fly ash being produced in Iowa is utilized in the construction industry, primarily as a cement replacement in concrete. Utilization of the newer ashes in soil and subbase stabilization is still in its infancy but will probably increase dramatically in the next few years. Total utilization of fly ash in the construction and product manufacturing industries can be expected to increase significantly over the near term.

Since a major constituent of fly ash is glass,

[6, 8, 29] it follows that an understanding of the glass composition and structure is basic in order to gain some insight into its potential influence in concrete, soil, and subbase stabilization.

Past research [29] has indicated that the glassy phase constitutes approximately 75 percent of Iowa fly ashes. The principal elements present are calcium, aluminum, and silicon which are the building blocks of cementitious materials. If the liberation of these elements could be economically accelerated from the vitreous state and recombined into cementitious material, the effective utilization of the ashes in soil and subbase stabilization could potentially be dramatically increased.

Objectives

Recent research by Pitt et al. [30] and Schlorholtz and Boybay [39] established means of quantitatively analyzing the elemental and compound composition of several Iowa fly ashes. From these data, the composition of the glassy phase could be estimated. The objectives of this research is two-fold. First to evaluate the glassy phase of a range of different fly ashes from the Iowa area, and secondly to investigate the potential of using small quantities of secondary chemical additives to attack the glassy phase and enhance or accelerate cementitious product development.

BACKGROUND AND LITERATURE REVIEW

Structure of Glass

Atomic structure

Some of the current hypotheses [28] regarding glass formation in the oxide systems include Goldschmidt's radius ratio criteria, Zacharisen's random network theory, Smekal's mixed bonding hypothesis, and Sun's bond-strength criterion. The following discussion incorporates parts of these models.

The basic framework for the understanding of the structure of oxide glasses was set forth by Zacharisen [50] where he proposed that the principal difference between a crystal network and a glass network is that the crystal form has symmetry and periodicity in atomic arrangement which is not present in the glassy state. Glasses form extended random three-dimensional networks with the energy state of the glass network comparable to the energy state of the corresponding crystal form. Zacharisen's model of the atomic arrangement of glass has generally been accepted [28] with minor limitations. Figures 1a and 1b depicts a two-dimensional model of a silica crystal network and silica vitreous network [46] indicating the random network structure of the vitreous state.

Glass formers and modifiers

Only a few oxides are capable of being formed in a vitreous state by themselves. These oxides are B_2O_3 , SiO_2 ,

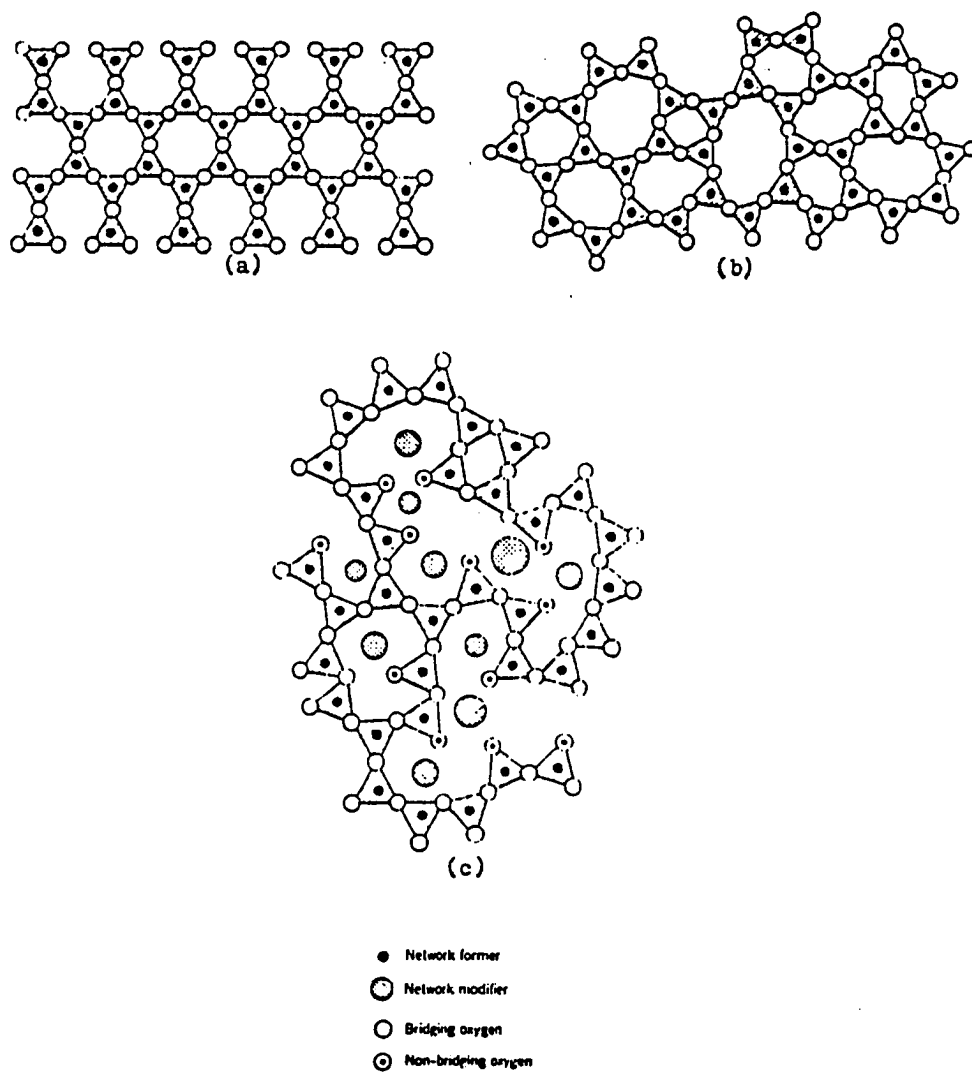


Figure 1. Schematic two-dimensional representation of (a) quartz crystal lattice, (b) silica glass network and (c) silica glass network with cation modifiers (adapted from Van Vlack [46])

GeO_2 , P_2O_5 , As_2O_3 , and Sb_2O_3 . Their network structure would generally be typified by Figure 1b. Other oxides may form a glass network when incorporated with a quantity of a second oxide. Included among this group of "conditional glass formers" is Al_2O_3 . Volf [47] terms these oxides "network dwellers".

The silica glass network shown in Figure 1b is seen to have varying size "holes" between network linked silica tetrahedra that exist in three dimensions. These "holes" may be occupied by various cations to satisfy non-bridging oxygen valencies depending on the number of non-bridging oxygens present. These cations are described as "network modifiers" and are shown in Figure 1c. In Figure 1c, it can be seen that covalent bonding is predominant in the linked network forming chain and ionic bonding is predominant in the structure incorporating cation network modifiers. Sun developed a hypothesis of glass formation based on bond strengths of oxide glass components [44]. Table 1 lists these oxides and their respective bond strengths. In Table 1, the oxides are divided into three groups.

Network Formers This group includes oxides capable of forming glass networks by themselves. Conditional glass formers (e.g., Al_2O_3) that require a second oxide to form a glass network are also included in this group.

Table 1. Bond strengths of oxide glass components [Sun, 44]

Oxide	Dissociation Energy kcal/mole	Coordination Number of cation	Bond Strength kcal/mole
Network formers			
B ₂ O ₃	356	3	119
GeO ₂	431	4	108
SiO ₂	424	4	106
V ₂ O ₅	449	4	112-90
P ₂ O ₅	442	4	111-88
Al ₂ O ₃	402-317	4	101-79
B ₂ O ₃	356	4	89
As ₂ O ₅	349	4	87-70
Sb ₂ O ₅	339	4	85-68
ZrO ₂	485	6	81
Intermediates			
TiO ₂	435	6	73
PbO ₂	145	2*	73
ZnO	144	2*	72
Al ₂ O ₃	402-317	6	67-53
ThO ₂	516	8	64
BeO ₂	250	4	63
ZrO ₂	485	8	61
CdO ₂	119	2*	60
Network modifiers			
Sc ₂ O ₃	362	6	60
La ₂ O ₃	406	7	58
Y ₂ O ₃	399	8	50
SnO ₂	278	6	46
Ga ₂ O ₃	267	6	45
In ₂ O ₃	259	6	43
ThO ₄	516	12	43
PbO ₄	232	6	39
MgO ₂	222	6	37
Li ₂ O	144	4	36
PbO	145	4	36
ZnO	144	4	36
BaO	260	8	33
CaO	257	8	32
SrO	256	8	32
CdO	119	4	30
Na ₂ O	120	6	20
CdO	119	4	20
K ₂ O	115	9	13
Rb ₂ O	115	10	12
HgO	68	6	11
Cs ₂ O	114	12	10

*assumed coordination number.

Intermediates These oxides are capable of entering into the network chain of a glass former. Aluminum, for example, can enter a silica glass network by two means. Aluminum ions can isomorphously substitute for silicon ions in the silica tetrahedral and function as a network former and/or octahedrally coordinated aluminum can be linked and incorporated into the silica tetrahedral chain network functioning as an intermediate [46].

Network Modifier These oxides do not enter the linking network chain but modify the network by occupying holes created by the network skeleton of linking polyhedra as indicated in Figure 1c.

In reviewing Table 1 and considering a combination of Zacharisen's random network theory and Sun's bond strength theory, we note that the more intermediate oxides that are incorporated in a network chain the less the total bond strength of the system, and further, that the more modifying cations incorporated into a network structure the less the total bond strength of the system.

The system becomes increasingly strained with a lower total bond strength as the amount of intermediate oxides and modifying cations that are incorporated into the system is increased.

It is also noted from Table 1 that Al_2O_3 is both a "conditional glass former" and an "intermediate", and

exhibits two bond strengths depending on whether it is substituted for silicon in the silica tetrahedron or is a part of the network chain in octahedral coordination.

Glassy Phase of Fly Ash

The glassy phase of fly ash and its influence on hydraulic properties is currently not understood. This is especially true for the newer high calcium ashes where significant amounts of calcium bearing crystalline compounds are present. Some of those compounds are analogous to those found in portland cement and react with water to produce insoluble cementitious materials. The interaction between the hydrating system of crystalline compounds and the glassy phase is a complex chemical process, much of which has yet to be explained.

The characterization of fly ash crystalline and glassy phases has been undertaken by a number of researchers [5, 6, 7, 8, 12, 17, 24, 26, 34] using a variety of techniques.

Diamond and Lopez-Flores [8] studied a series of fly ashes ranging from a low calcium ash derived from bituminous coals to high calcium ashes derived from lignitic and sub-bituminous coals. From x-ray diffraction studies, they observed that the amorphous halo in the diffractograms appeared quite different in comparison of the low calcium to high calcium ash. They postulated that there was a

substantial difference in the composition of the glassy phase. Further work by Diamond [6] on another series of low calcium to high calcium ashes indicated a progressive shift of the maxima of the amorphous halo corresponding to an increase in analytical calcium oxide content. Diamond postulated that the glassy phase in the low calcium ashes were predominantly siliceous in nature. He further postulated that the glassy component of the high calcium ashes were of a calcium aluminate structure and were possibly a more reactive glass. Mehta's [24] findings were in agreement with Diamonds.

Joshi et al. [17] studied the mineralogy and morphology of the various size fractions present in a fly ash containing 17 percent analytical calcium oxide. Results of his work indicated significant differences in the crystalline and glassy phases as a function of particle size. His results indicated that the amount of crystalline calcium bearing compounds decreased as the size of the particles increased. The glassy phase studies indicated approximately the same amount of glass present in each size fraction. The reactivity of the glassy phase of the larger sizes, however, appeared much less than the reactivity of the smaller size fractions.

GLASSY PHASE OF IOWA FLY ASHES

Composition

In order to gain some insight into the chemical composition and the glassy phase of fly ashes being produced in the Iowa area, a compilation of data was initiated. Fly ash sources and locations are given in Table 2.

Table 2. Fly ash sources and ASTM classifications

<u>Fly Ash Generating Station</u>	<u>Abbreviation</u>	<u>Location</u>	<u>ASTM C 618-80 Classification</u>
North Omaha	NO	Omaha, Nebr.	F
Clinton	Cl	Clinton, Ia.	F
Neal #3	N3	Sioux City, Ia.	Marginal F
Neal #2	N2	Sioux City, Ia.	Marginal F
Sherburn	Sh	Sherburn, Minn.	Marginal C
Ames	Am	Ames, Iowa	C
Ottumwa	Ot	Ottumwa, Iowa	C
Neal #4	N4	Sioux City, Ia.	C
Alma	Al	Alma, Minn.	C
Nebraska City	NC	Nebraska City, Nebr.	C
Council Bluffs	CB	Council Bluffs, Ia.	C
Lansing	La	Lansing, Iowa	C

Chemical names and notations that will be referred to are listed on Table 3.

Table 3. Chemical terminology

<u>Chemical Name</u>	<u>Common Name</u>	<u>Chemical Formula</u>
Calcium Oxide	Lime	CaO
Silicon Dioxide	Quartz	SiO ₂
Tricalcium Aluminate	---	3CaO-Al ₂ O ₃
Calc. Alum. Sulphate	---	3CaO-3Al ₂ O ₃ -CaSO ₄
Calcium Sulphate	Anhydrite	CaSO ₄
Aluminun Silicate	Mullite	3Al ₂ O ₃ -2SiO ₂
Magnesium Oxide	Periclase	MgO
Iron Oxide	Magnetite	Fe ₃ O ₄

The chemical properties of ashes are summarized in Table 4, referenced to each data source, including data generated as part of this research effort. The data base sources were selected to provide a full chemical composition spectrum of the ashes currently being produced. All test results and analysis were conducted in the Materials Analysis and Research Laboratory at Iowa State University utilizing essentially the same methods of testing.

Elemental composition was determined by quantitative

Table 4. Chemical properties of fly ash

	NO ¹	Cl ¹	N3 ¹	N2 ²	Sh ³
<u>Elemental Composition, expressed as oxides (%)</u>					
ASTM Class	F	F	F/C	F/C	C/F
SiO ₂	50.0	55.8	50.5	48.5	44.9
Al ₂ O ₃	27.7	19.2	18.1	16.8	18.0
Fe ₂ O ₃	14.6	18.1	7.9	6.2	6.3
Subtotal	92.3	93.1	76.5	71.5	69.2
CaO	1.5	4.3	13.6	14.8	21.1
MgO	1.4	1.3	3.1	1.8	3.3
K ₂ O	0.2	2.1	1.2	1.6	1.0
Na ₂ O	0.5	0.6	0.5	0.2	3.3
TiO ₂	0.7	0.8	0.7	0.5	-
SO ₃	-	-	-	1.8	1.0
Total	96.5	102.2	95.6	92.2	98.9
<u>Crystalline Compound Composition (%)</u>					
CaO	0.2	0.2	2.3	4.8	2.5
SiO ₂	9.9	8.2	7.0	15.6	10.2
C ₃ A	0.0	0.1	0.0	0.0	0.5
C ₄ A ₃ S	0.0	0.1	0.1	0.3	0.2
CS	0.3	0.2	0.3	0.9	0.7
Al ₆ Si ₂ O ₁₃	3.6	3.0	0.0	1.2	1.3
MgO	0.0	1.3	1.0	0.6	1.0
Fe ₃ O ₄	10.0	7.4	0.7	3.1	3.3
Total	24.0	20.5	11.4	25.3	19.7
Glass (%)	76	80	89	75	80

¹ J. M. Pitt et al. [29].

² Iowa Department of Transportation [14a].

³ J. M. Pitt and T. Demirel, Civil Engr. Dept., ISU, unpublished research report to Dean Skaugstad, Plymouth, Minnesota, November, 1982.

⁴ T. Demirel et al., Civil Engr. Dept., ISU, unpublished research report to City of Ames, Ames, Iowa, October, 1983.

Am ⁴	Ot ²	N4 ¹	Al ³	NC ¹	CB ¹	La ¹
C	C	C	C	C	C	C
38.5	35.0	32.1	33.3	34.1	29.7	30.0
18.3	20.2	19.7	16.8	21.1	20.3	19.7
5.6	5.3	5.8	5.9	5.5	5.1	5.9
62.5	60.5	57.6	56.0	60.7	55.1	55.6
23.7	25.2	29.5	29.7	30.3	31.5	31.1
6.0	5.1	7.7	6.9	5.8	5.8	6.2
0.7	0.4	0.3	0.4	0.3	0.3	0.4
2.5	1.7	2.2	2.1	1.8	1.8	1.8
1.2	1.5	1.2	-	1.4	1.4	1.3
3.7	1.7	-	2.5	-	-	-
100.0	96.1	98.5	97.6	100.3	95.9	96.4
1.7	0.6	0.8	2.5	0.1	1.4	2.1
12.4	8.6	8.0	9.6	7.1	5.3	10.1
2.9	6.9	4.9	5.4	0.5	6.0	5.2
1.1	0.4	1.1	1.4	0.0	0.2	2.3
1.4	1.2	1.3	2.4	0.1	0.9	1.7
0.0	2.2	2.3	0.4	2.9	0.0	0.9
2.9	1.1	3.2	4.1	0.4	2.0	2.8
0.0	0.0	0.0	0.9	0.0	0.2	1.0
22.4	21.0	21.6	26.7	11.1	16.0	26.1
78	79	78	73	89	84	74

x-ray fluorescence (QXRF). Crystalline compounds present were determined by x-ray diffraction. Amounts of the various compounds were determined by quantitative x-ray diffraction (QXRD) techniques utilizing sodium chloride as an internal standard. Details of the methods are given in other publications [25, 30, 39].

The ability to accurately measure crystalline compounds present in fly ash is complicated by the fact that the variation in background radiation on either side of crystalline compound peaks is high and that the quantity of some of the compounds being measured is small. These two factors combine to make accurate determinations of the amount of some of the compounds present difficult. Table 5 shows the results of several runs and replicates of tests for the Neal #4 fly ash. The results of the compound analysis given in Table 4, therefore, must be viewed with the understanding that the values given are at best reasonable estimates for some of the compounds. Results do, however, serve to indicate general trends.

The data in Table 4 represent the spectrum of ashes available in the Iowa area ranging from the low calcium ash from the North Omaha plant to the high calcium ashes from the Council Bluffs and Lansing plants. Several observations can be made from the elemental analysis data. All elemental analysis data are expressed as oxides. The term "analytical"

Table 5. Coefficient of variation of Neal #4 fly ash compounds for the average of 20 tests

<u>Compound</u>	<u>Average Weight, %</u>	<u>Coefficient of Variation (%)</u>
Lime	1.8	26
Quartz	9.8	13
Tricalcium Aluminate	3.2	20
Calc. Alum. Sulphate	0.8	100
Anhydrite	2.4	12
Mullite	2.0	61
Periclase	2.9	16
Magnetite	3.2	51

will be used herein and will refer to total elemental analysis data, expressed as oxides, and obtained by x-ray fluorescence (XRF). With the exception of the North Omaha ash, the analytical Al_2O_3 content remains fairly constant in the range of 18 to 20 percent Al_2O_3 for all the ashes. The analytical Fe_2O_3 content remains in the 5 to 7 percent range for the ashes with the exception of North Omaha and Clinton ashes. There is a general trend for increasing analytical MgO with increasing analytical CaO . SiO_2 decreases with increasing analytical CaO . This relationship is shown on Figure 2 and with the exception of the North Omaha ash indicates a linear trend on a one to one basis by weight.

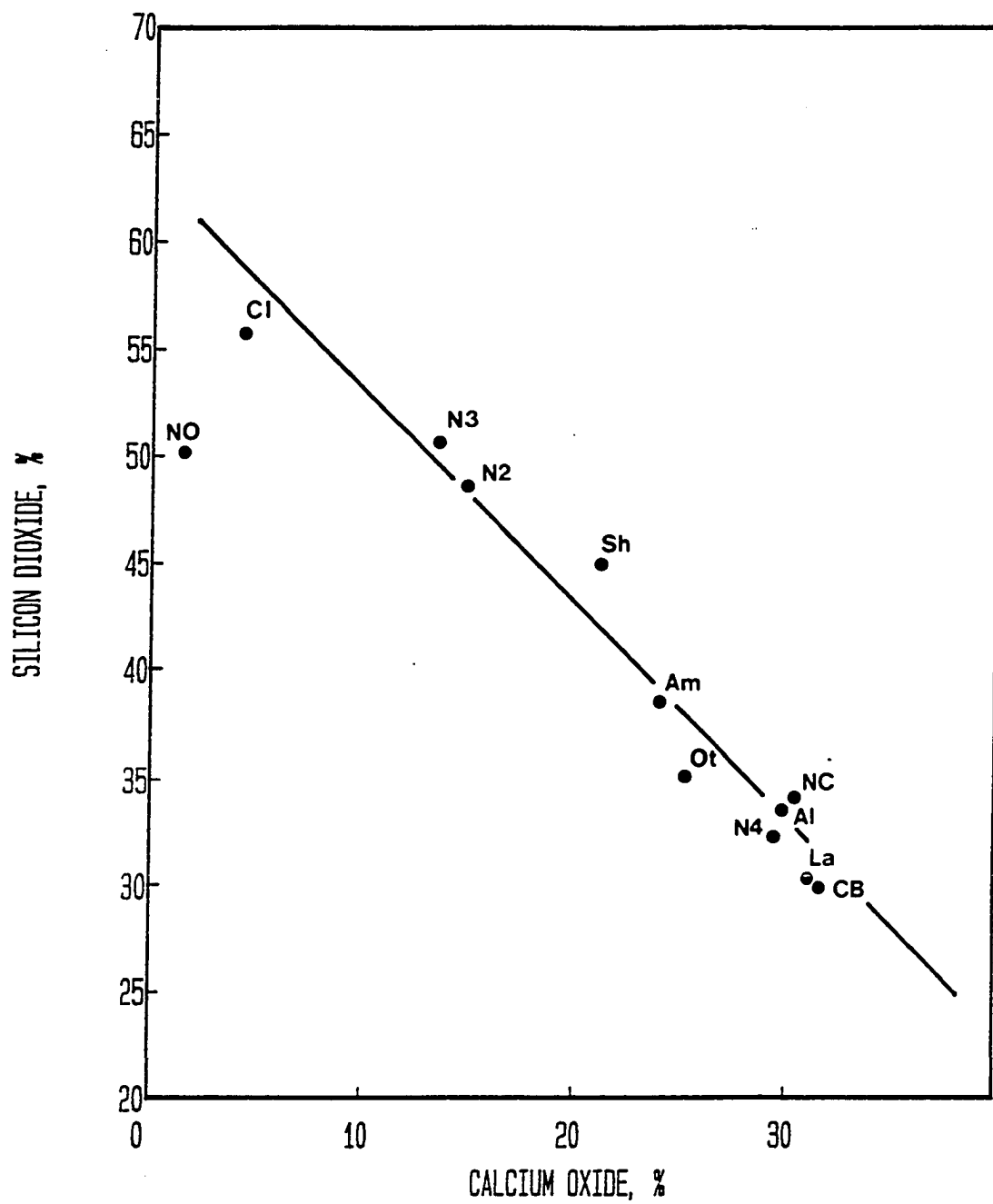


Figure 2. Total elemental silicon versus elemental calcium (expressed as oxides) comparison

The molar weight ratio of CaO to SiO_2 is 0.93 or nearly one to one. Figure 3 shows a graph of analytical $\text{SiO}_2 + \text{Al}_2\text{O}_3$ (glass network formers and conditional formers) versus analytical $\text{CaO} + \text{MgO}$ (glass network modifiers).

Interestingly, these oxide combinations also show a linear trend. These two figures illustrate the basic reason that the ASTM C-618 classification system functions to distinguish between low calcium and high calcium fly ash even though CaO is not a part of the method.

The crystalline compound data also reveal several trends. Crystalline uncombined lime generally remains low and below 2 percent for most of the ashes. The term "free lime" is deliberately not used here. Research by Schlorholtz and Demirel [40] has indicated that crystalline uncombined lime may be in a "hard burned" form and not be available for immediate reactions. On the average, quartz present is at about the 10 percent level for most of the ashes. There is a general trend for increasing tricalcium aluminate with increasing analytical CaO . Both calcium aluminum sulphate and anhydrite are present at less than 2 percent. Mullite contents vary from ash to ash with no trends evident. Periclase contents range from 0 to 4 percent and show no definite trend although higher periclase contents are generally found at higher analytical CaO amounts. Magnetite trends lower with increasing analytical CaO with substantial

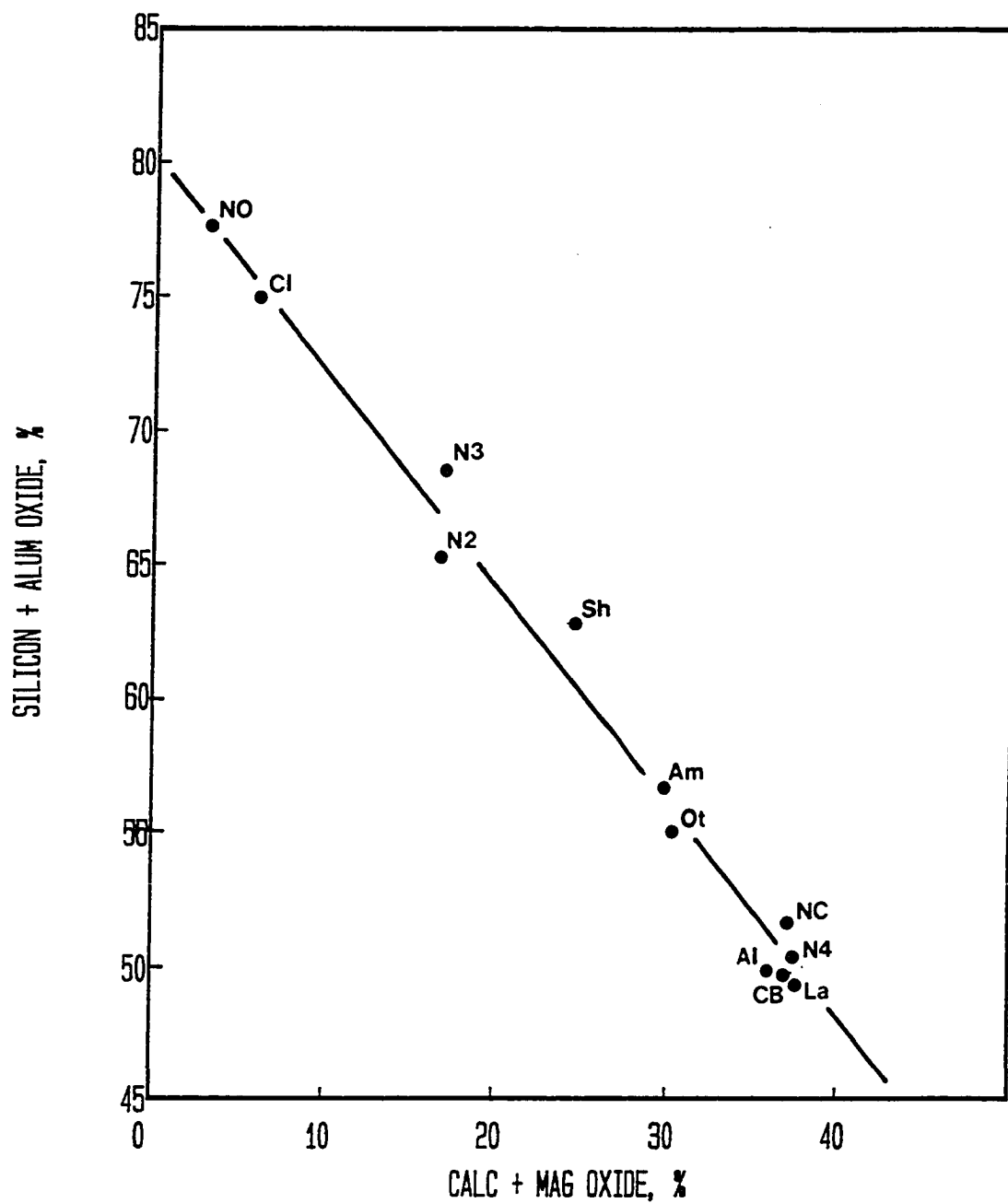


Figure 3. Total elemental silicon plus aluminum versus calcium plus magnesium (expressed as oxides) comparison

amounts present in the North Omaha and Clinton ashes.

Total quantities of crystalline compounds present range from 11 to 27 percent with an average of about 20 percent. By subtraction, the percent glass ranges from 74 to 89 percent with an average of 80 percent. A summation of all calcium bearing crystalline compounds indicates a range of 0.5 to 11.7 percent by weight. Correlation to analytical CaO or other elemental constituents (expressed as oxides) are not directly evident.

In order to derive an estimated composition of the glassy phase, the amount of individual oxides in the crystalline compounds was determined and subtracted from the total amount of each oxide obtained by x-ray fluorescence (XRF). These data are presented in Table 6. The glass composition shown has been divided into the three categories of network formers, dwellers, and modifiers. The total amount of the alkalis have been included in the glassy phase. It is recognized, however, that alkalis also exist in crystalline form [5] on the glassy surfaces of the fly ash particles. The division between the amount incorporated into the glass structure and the soluble crystalline phase is not known. The small amounts present currently precludes their separation.

The glass compositions were normalized to a basis of 100 percent in order to provide a means of comparison. On a

Table 6. Estimated glassy phase compositions of fly ash

	N0	C1	N3	N2
<u>Elements in crystalline compounds, expressed in oxides (%)</u>				
CaO	0.3	0.4	3.5	5.3
SiO ₂	10.9	9.0	7.0	15.9
Al ₂ O ₃	2.6	2.3	0.1	1.1
Fe ₂ O ₃	6.9	5.1	0.5	0.5
<u>Estimated glass composition (%)</u>				
Network Formers				
SiO ₂	39.1	46.8	43.5	32.6
Network Dwellers				
Al ₂ O ₃	22.5	16.9	18.0	15.7
Network Modifiers				
MgO	1.4	1.3	3.1	1.8
CaO	1.2	3.9	10.1	9.5
Na ₂ O	0.5	0.6	0.5	0.2
K ₂ O	0.2	2.1	1.2	1.6
Total Modifiers	3.3	7.9	14.9	13.1
Total	64.9	71.6	76.4	61.4
<u>Normalized Glass Composition</u>				
Network Formers				
SiO ₂	60.3	65.4	56.8	53.2
Network Dwellers				
Al ₂ O ₃	34.7	23.7	23.6	25.6
Network Modifiers				
MgO	2.1	1.8	4.1	2.9
CaO	1.8	5.4	13.2	15.4
Na ₂ O	0.8	0.8	0.7	0.3
K ₂ O	0.3	2.9	1.6	2.6
Total Modifiers	5.0	10.9	19.6	21.2
Total	100.0	100.0	100.0	100.0
<u>Normalized Glass composition, major oxides only</u>				
SiO ₂	62.3	69.2	60.7	56.5
Al ₂ O ₃	35.8	25.1	25.2	27.2
CaO	1.9	5.7	14.1	16.3

Sh	Am	Ot	N4	A1	NC	CB	La
3.2	4.5	5.1	4.7	7.3	0.5	5.5	6.9
10.6	12.4	9.2	8.6	9.7	7.9	5.3	10.4
1.2	1.7	4.4	4.1	2.1	2.3	2.5	3.8
2.3	0.0	0.0	0.0	0.6	0.0	0.1	0.7
34.3	26.1	25.8	23.5	23.6	26.2	24.4	19.6
16.8	16.6	15.8	15.6	14.7	18.8	17.8	15.9
3.3	6.0	5.1	7.7	6.9	5.8	5.8	6.2
17.9	19.2	20.1	24.8	22.4	29.8	26.0	24.2
3.3	2.5	1.7	2.2	2.1	1.8	1.8	1.8
1.0	0.7	0.4	0.3	0.4	0.3	0.3	0.4
25.5	28.4	27.3	35.0	31.8	37.7	33.9	32.6
76.6	71.1	68.9	74.1	70.1	82.7	76.1	68.1
44.8	36.8	37.4	31.6	33.6	31.7	32.0	28.9
21.9	23.3	22.9	21.1	21.0	22.7	23.4	23.3
4.3	8.4	7.4	10.4	9.8	7.0	7.6	9.1
23.4	27.0	29.1	33.5	32.0	36.0	34.2	35.5
4.3	3.5	2.5	3.0	3.0	2.2	2.4	2.6
1.3	1.0	0.6	0.4	0.6	0.4	0.4	0.6
33.3	39.9	39.6	47.3	45.4	45.6	44.6	47.8
100.0	100.0	100.0	100.0	100.0	100.0	100.0	100.0
49.7	42.3	41.8	36.7	38.8	35.1	35.7	33.0
24.3	26.6	25.6	24.5	24.2	25.1	26.1	26.6
1.9	5.7	32.6	38.8	37.0	39.8	38.2	40.4

normalized basis CaO , SiO_2 and Al_2O_3 comprise 86 to 97 percent of the glassy phase with an average of 91 percent for all of the ashes. The normalized data for these major components are also given on Table 6.

The normalized glassy phase chemical relationships are illustrated in Figures 4, 5, and 6. Figure 4 depicts SiO_2 versus CaO and a nearly linear relationship (North Omaha excepted) exists. Figure 5 plots network formers and intermediates of $\text{SiO}_2 + \text{Al}_2\text{O}_3$ versus the CaO network modifier with a very good linear relationship exhibited.

Figure 6 shows $\text{SiO}_2 + \text{Al}_2\text{O}_3$ versus $\text{CaO} + \text{MgO}$, in the glassy phase. A strong one to one ratio by weight is evident. The data in Figure 6 indicate that as the amount of $\text{SiO}_2 + \text{Al}_2\text{O}_3$ (network formers) increases the amount of $\text{CaO} + \text{MgO}$ (network modifiers) incorporated into the network decreases linearly. This indicates that the glassy phase of the North Omaha and Clinton ashes is principally composed of SiO_2 linked tetrahedra with Al_2O_3 , either linked into the network in its octahedral coordination as an intermediate or isomorphously substituted for silicon in the silica tetrahedron as a network former. In either case, the linked network contains only a small amount of CaO and MgO cations which act to modify and strain the network and lower the total bond strength. At the other end of the spectrum, the glassy phase of the Lansing ash comparatively has a much

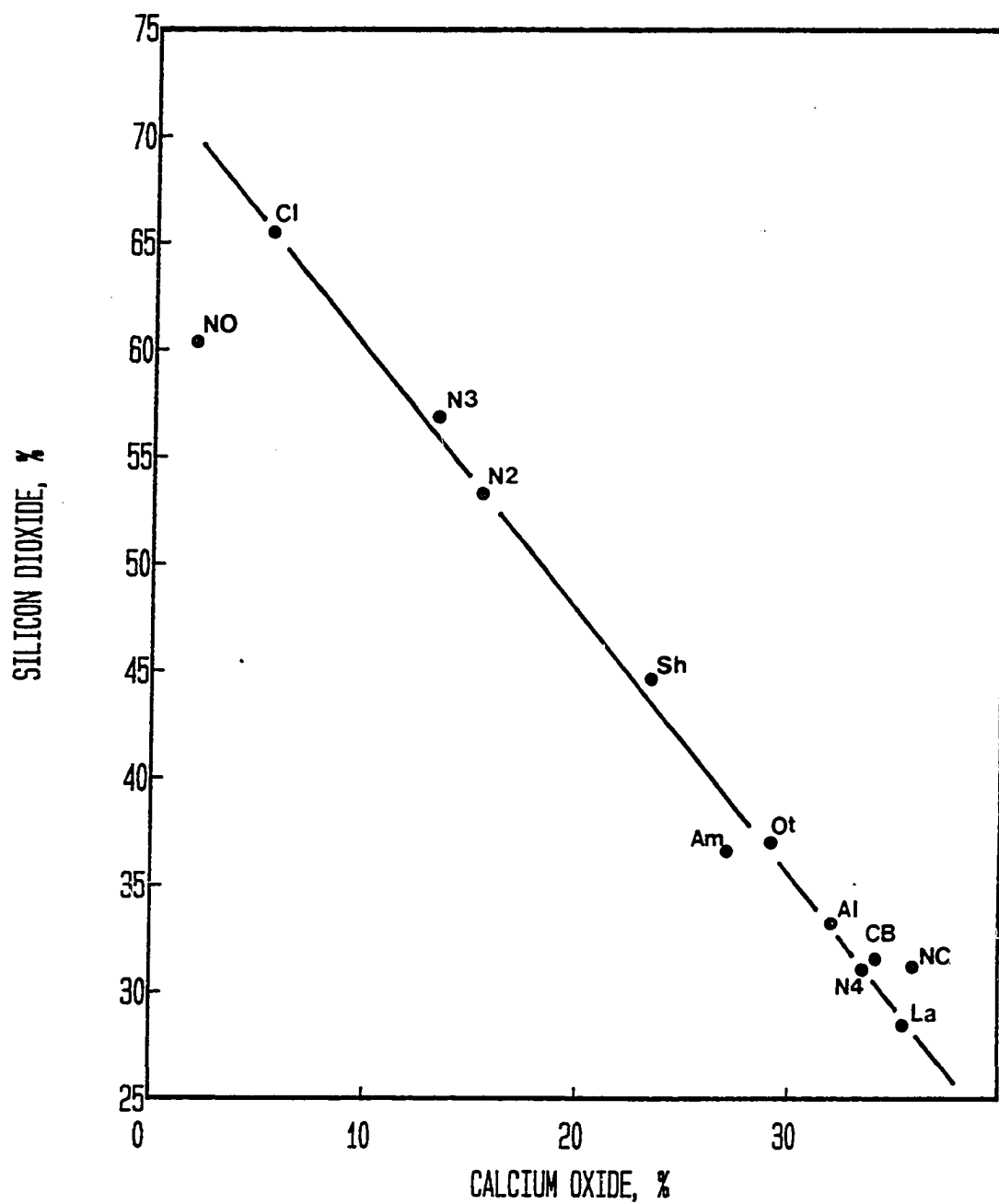


Figure 4. Glassy phase normalized data comparison of elemental silicon versus calcium (expressed as oxides)

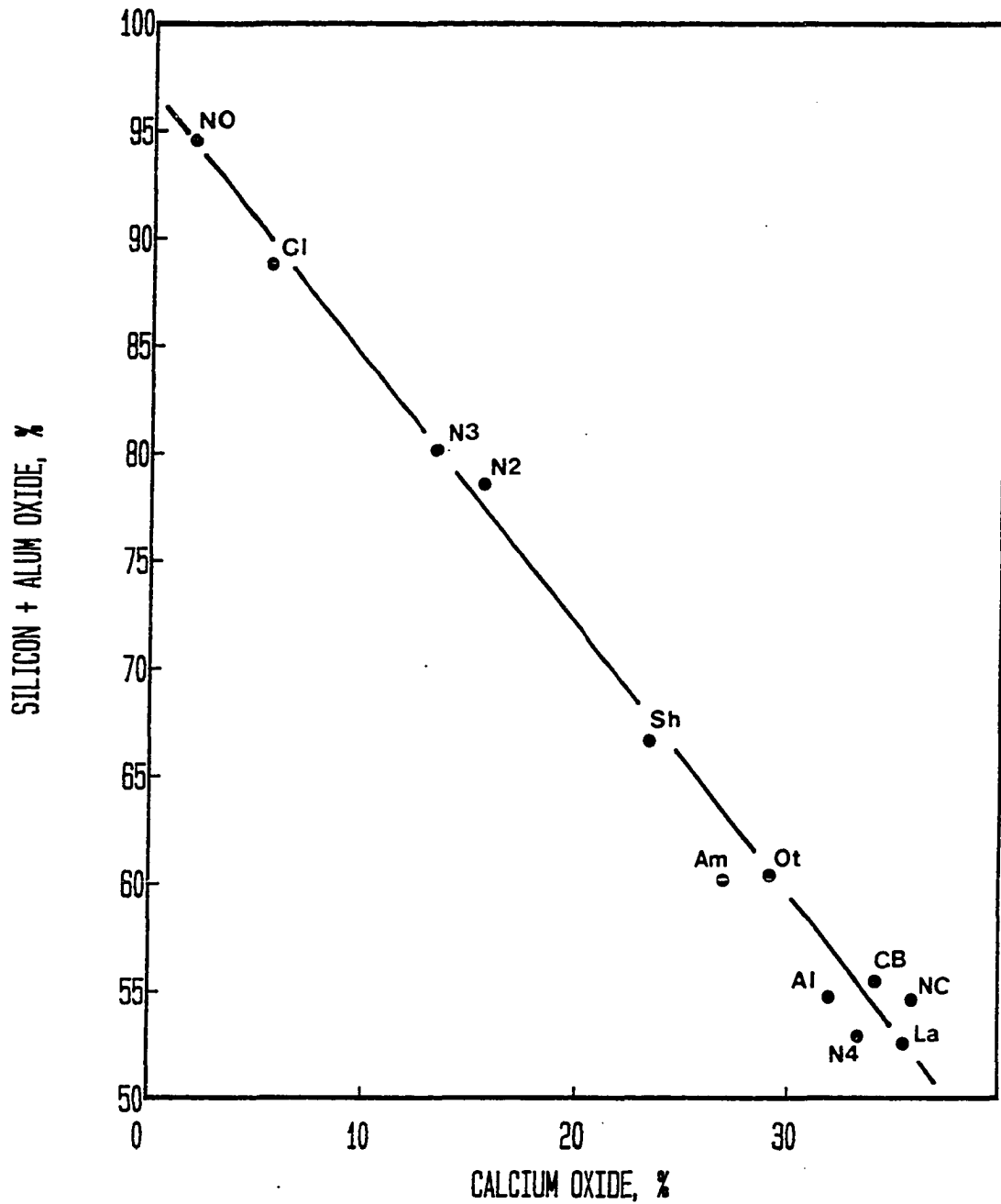


Figure 5. Glassy phase normalized data comparison of elemental silicon plus aluminum versus calcium (expressed as oxides)

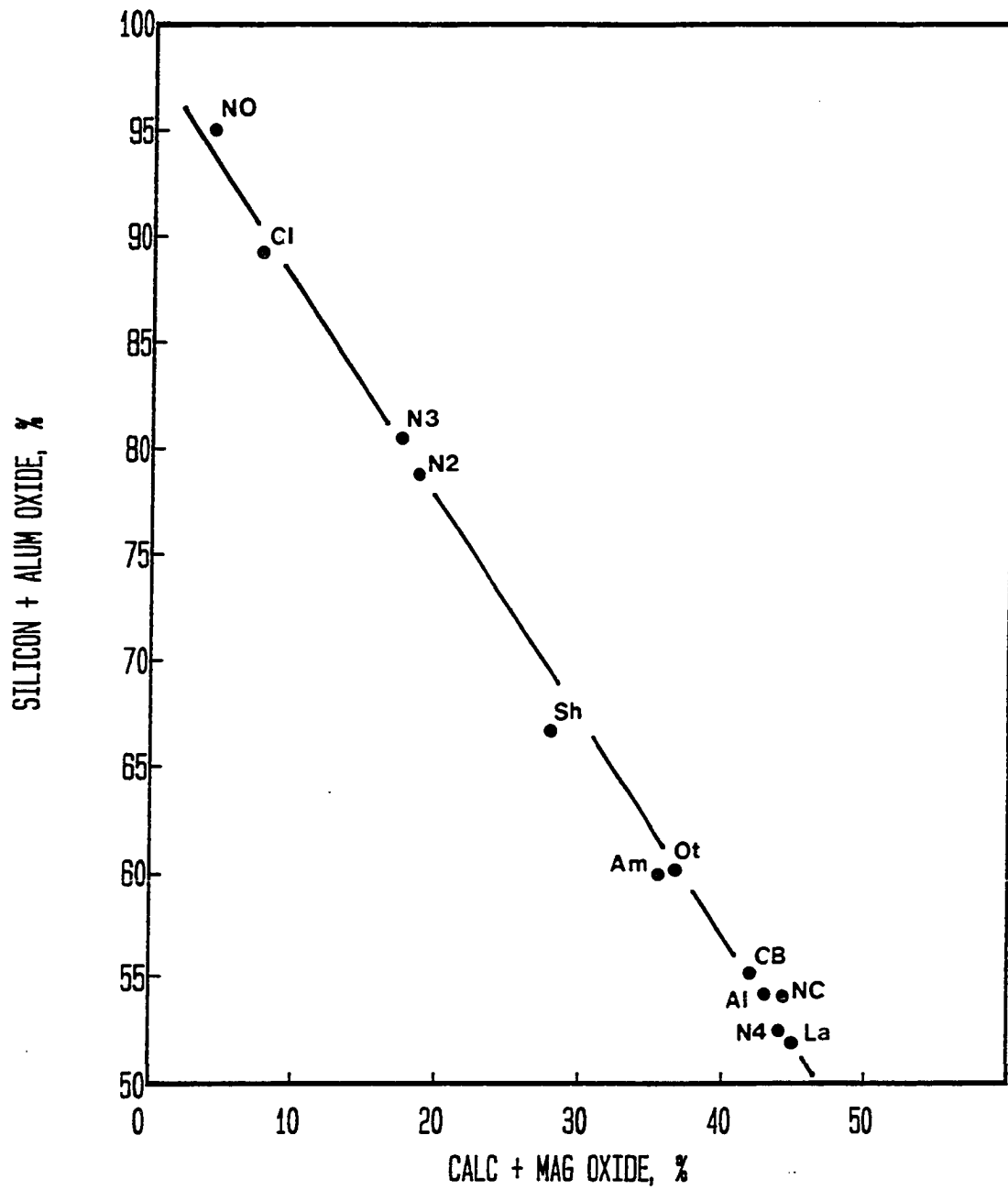


Figure 6. Glassy phase normalized data comparison of elemental silicon plus aluminum versus calcium plus magnesium (expressed as oxides)

lower amount of network forming SiO_2 and Al_2O_3 and a much greater amount of network modifying CaO and MgO cations. The glassy phase of the Lansing ash should then possess a much lower total bond strength and be in a much more chemically strained condition.

Chemical Relationships

Elemental and glassy phase chemical ratios are tabulated in Table 7. These ratios will be used for discussion here and will be referred to later.

It was previously noted that there is a strong relationship between analytical CaO + MgO and analytical SiO_2 + Al_2O_3 . Similar strong relationships have been shown for the glassy phase. To determine if simple XRF determinations of total elemental composition could be used to be predictive of the glassy phase makeup, a series of graphs were prepared. Since the glass network formers of SiO_2 and Al_2O_3 and the network modifiers of CaO and MgO are believed to be the principal controllers of the glass structure and a measure of its chemical strain, the glassy phase ratio (modifier/former) of $(\text{CaO} + \text{MgO})/(\text{SiO}_2 + \text{Al}_2\text{O}_3)$ was utilized. The higher the ratio the more strained the glass structure would be. Figure 7 is a plot of analytical CaO versus the modifier/former ratio of the glassy phase. There are two distinct linear portions to the graph which breaks at an analytical CaO content of about 15 percent. The reason for this is not yet

Table 7. Chemical ratios and combinations of fly ash

	N0	C1	N3	N2	Sh
<u>Elemental (expressed as oxides) Combinations</u>					
CaO/SiO ₂	0.03	0.08	0.27	0.31	0.47
CaO/SiO ₂ + Al ₂ O ₃	0.02	0.06	0.20	0.23	0.34
CaO + MgO/ SiO ₂ +Al ₂ O ₃	0.04	0.07	0.24	0.25	0.39
CaO + MgO	2.9	5.6	16.7	16.6	24.4
SiO ₂ +Al ₂ O ₃	77.7	75.0	68.6	65.3	62.9
<u>Crystalline Compound Combinations</u>					
CaO+C ₃ A + C ₄ A ₃ S ₃ +CS	0.5	0.6	2.7	6.0	3.9
<u>Glass (expressed as oxides) Combinations, normalized data</u>					
CaO/SiO ₂	0.03	0.08	0.23	0.29	0.52
CaO/SiO ₂ + Al ₂ O ₃	0.02	0.06	0.16	0.20	0.35
CaO+MgO/ SiO ₂ +Al ₂ O ₃	0.04	0.08	0.22	0.23	0.42
Modifiers/ Formers	0.05	0.12	0.24	0.27	0.50
CaO + MgO	3.9	7.2	17.3	18.3	27.7
SiO ₂ +Al ₂ O ₃	95.0	89.1	80.4	78.8	66.7

Am	Ot	N4	A1	NC	CB	La
0.62	0.72	0.92	0.89	0.89	1.07	1.04
0.42	0.46	0.57	0.59	0.55	0.63	0.63
0.52	0.55	0.72	0.73	0.65	0.75	0.75
29.7	30.3	37.2	36.6	36.1	37.3	37.3
56.8	55.2	51.8	50.1	55.2	50.0	49.7
7.2	9.1	8.1	11.7	0.7	8.5	11.3
0.73	0.78	1.06	0.95	1.14	1.07	1.23
0.40	0.48	0.64	0.59	0.66	0.62	0.68
0.59	0.61	0.83	0.77	0.79	0.75	0.85
0.66	0.66	0.90	0.83	0.84	0.81	0.92
35.4	36.5	43.9	41.8	43.0	41.8	44.6
60.1	60.3	52.7	54.6	54.4	55.4	52.2

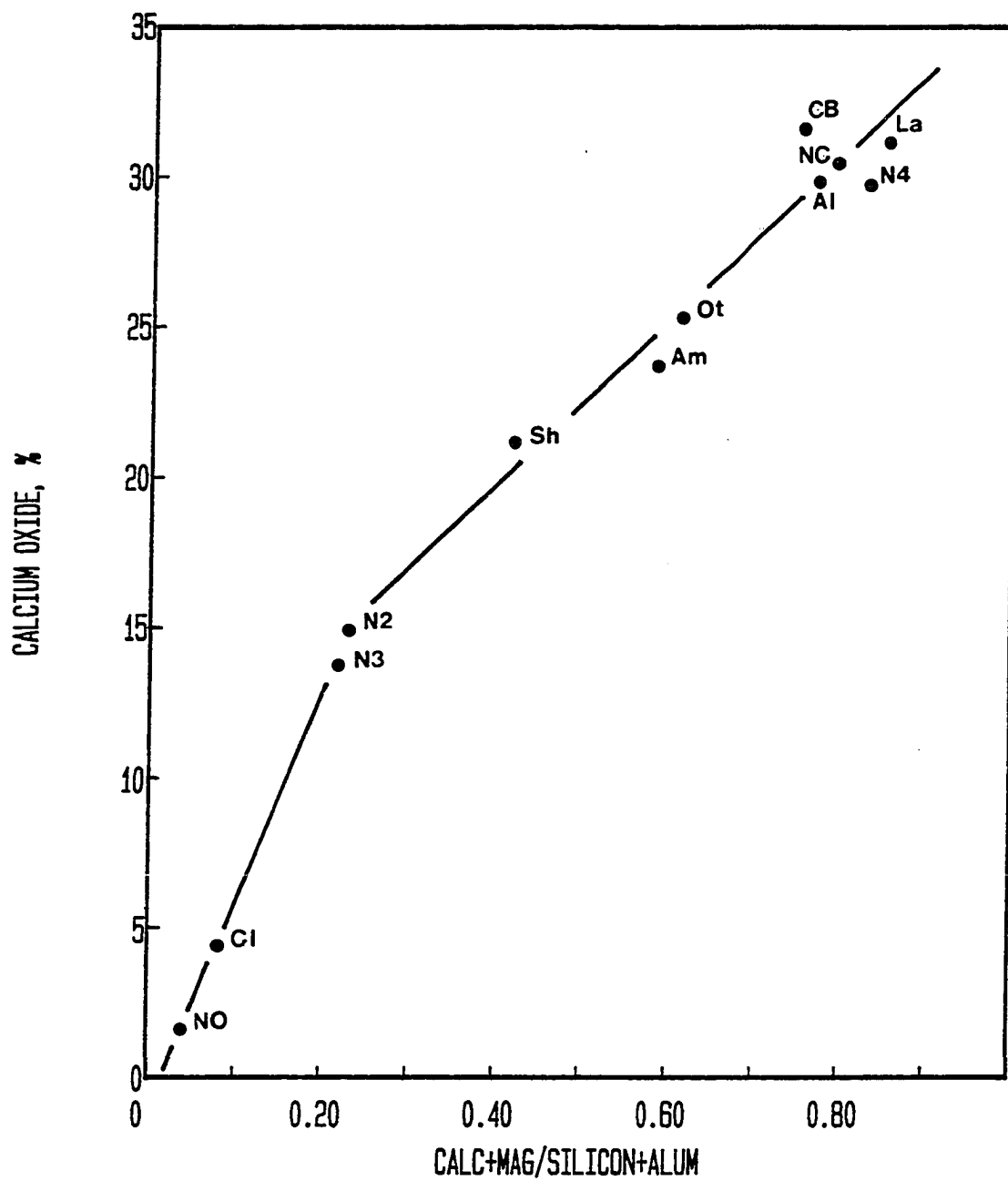


Figure 7. Total elemental calcium (expressed as an oxide) versus the normalized glassy phase ratio of calcium plus magnesium to silicon plus aluminum (expressed as oxides)

clear, but may be related to the shift in the XRD glassy halo noted by Diamond [6] at a 20 percent analytical CaO level.

Figure 8 compares the analytical modifier/former ratio with the glassy phase modifier/former ratio. Interestingly, a relatively strong linear fit is obtained. This implies that the relatively simple XRF elemental analysis data can be utilized to characterize the glassy phase chemical state of a fly ash and hence, its potential reactivity.

The calcium bearing phases of the fly ashes by source are given on Figure 9. They are ranked by increasing analytical CaO. The calcium contained in the glassy phase is also shown with the difference being the amount of CaO contained in the calcium bearing crystalline compounds.

Although there is a general trend for increasing CaO in the glassy phase and increasing amounts of calcium bearing compounds with analytical CaO, the trend is not absolute. The Nebraska City ash is a highly interesting anomaly. The glassy phase is calcium rich and silica lean, and should possess a reactive glass structure. It contains only a minor amount of calcium bearing compounds. The glassy phase of the Clinton ash, by contrast, is silica rich and calcium poor and should be stable and chemically durable. Figure 10 contrasts the calcium bearing compounds by ash source. Comparison of the Clinton and Nebraska City ashes indicate a similar total and individual amount of calcium bearing crystalline

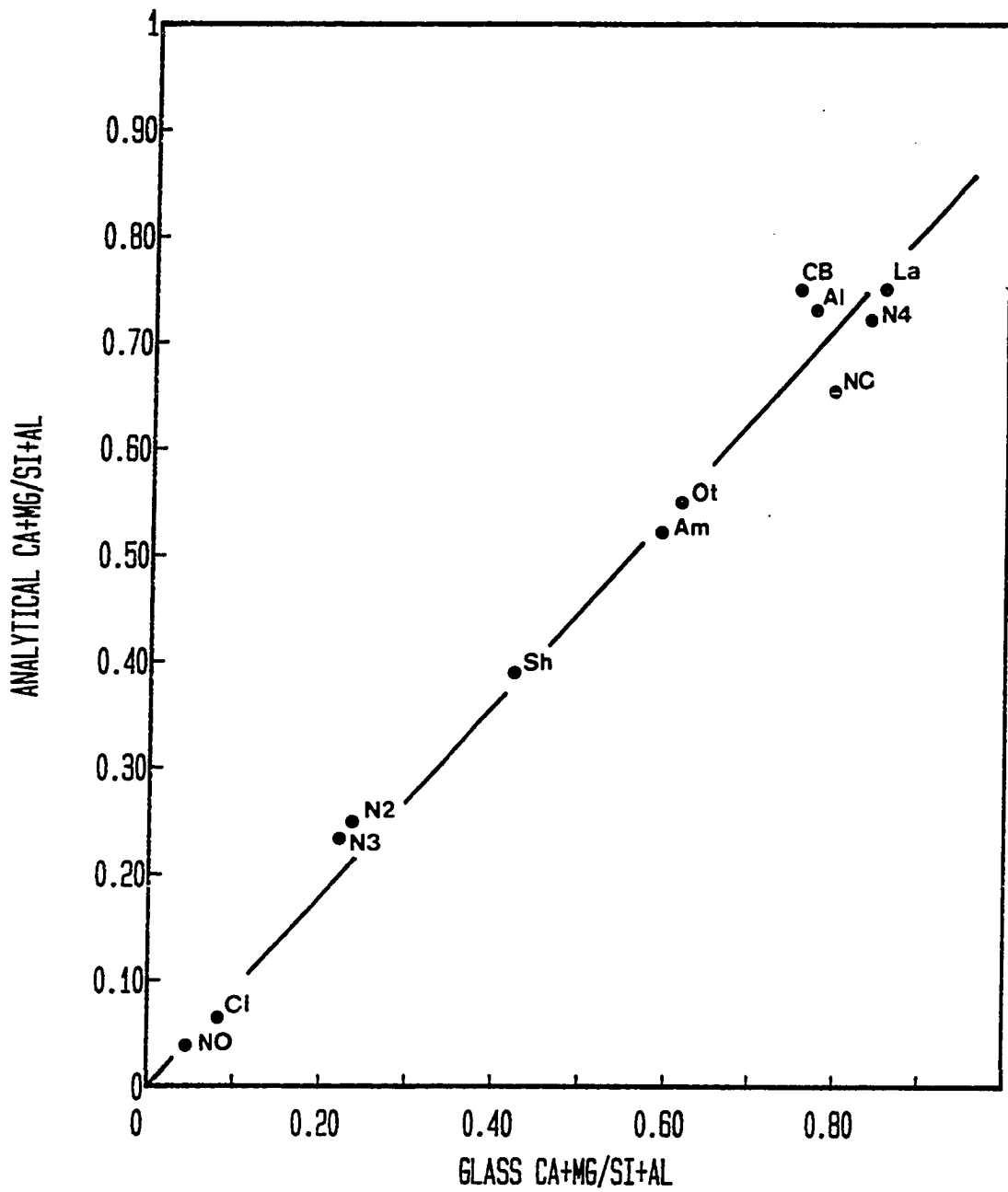


Figure 8. Total elemental ratio of calcium plus magnesium to silicon plus aluminum versus the normalized glassy phase ratio of the same elements (all expressed as oxides)

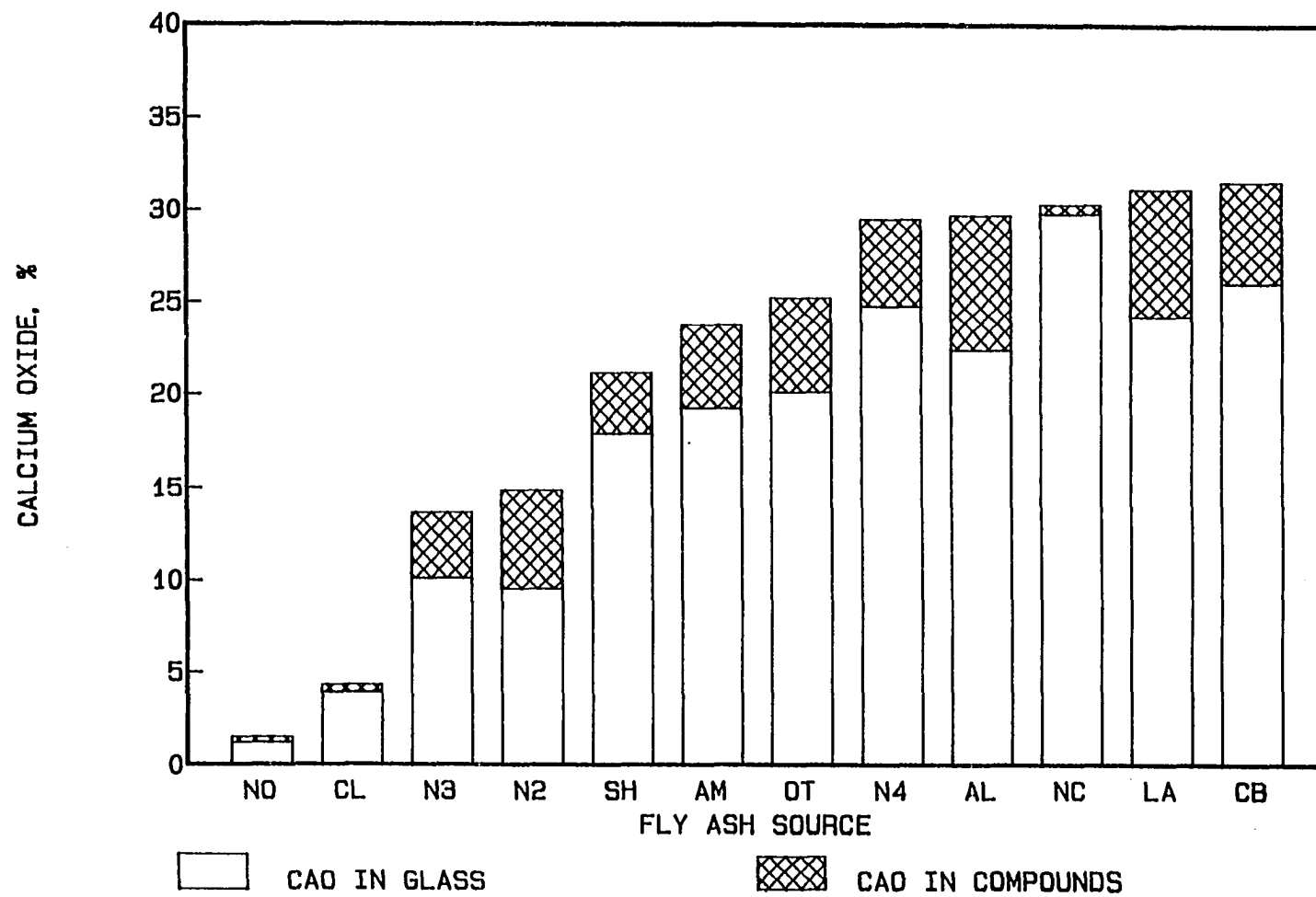


Figure 9. Calcium (expressed as an oxide) in crystalline compounds and the glassy phase versus fly ash source

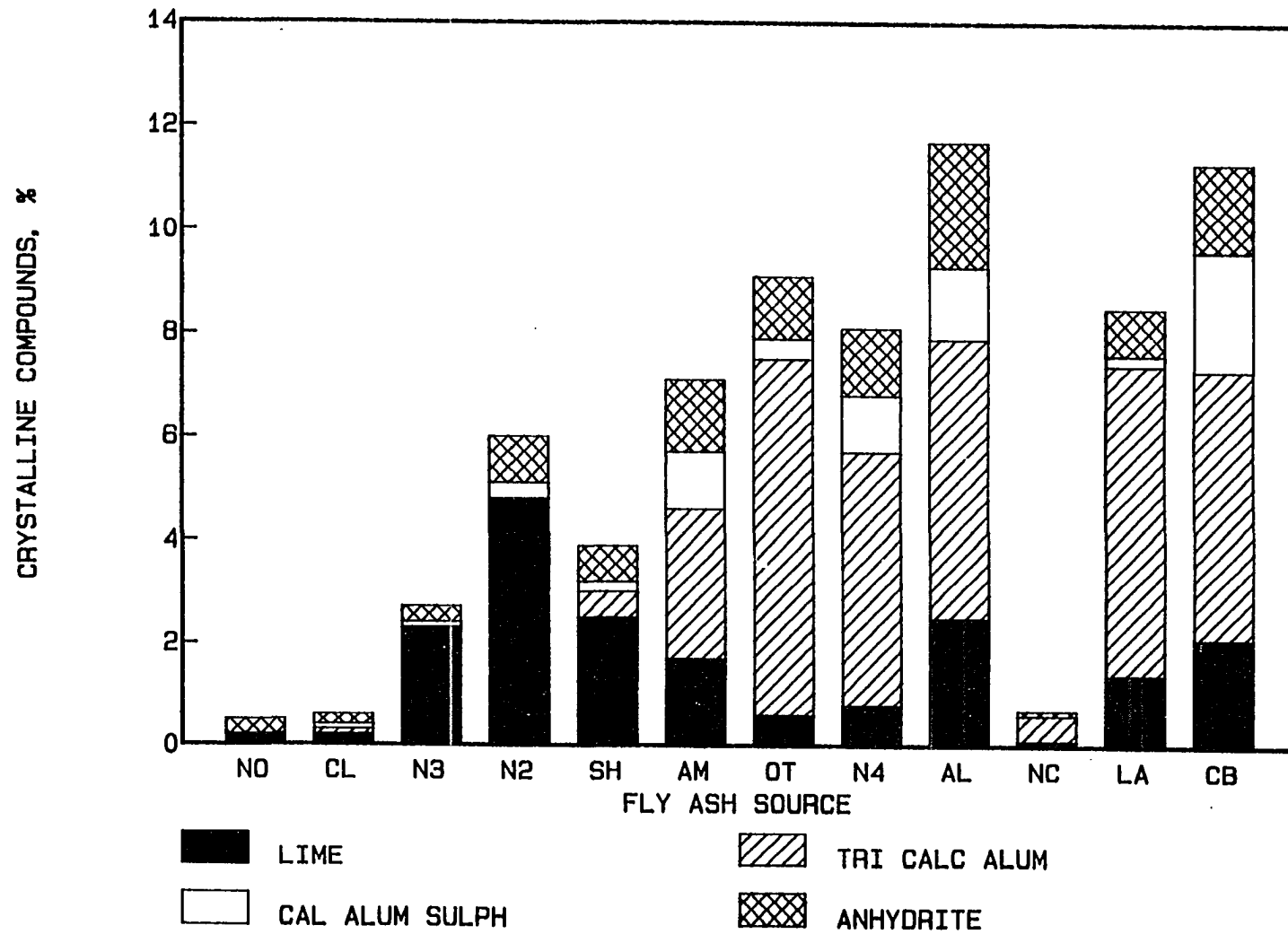


Figure 10. Calcium bearing crystalline compounds versus fly ash source

compounds present. Since the amount of compounds is small, it should be possible to directly evaluate the reactivity of the glassy phase of fly ash by incorporating a suitable activator into these ashes and monitoring hydration reaction by compressive strength development and XRD.

Glassy Phase Reactivity

Diamond [6] in a study of the glassy phase of a range of low calcium to high calcium fly ashes found a shift in the XRD maxima of the glassy halo with increasing analytical CaO . He postulated that this shift was due to a progressive change in glass structure from a predominantly siliceous glass in the low calcium ashes to a predominantly calcium aluminate glass, incorporating silica in its structure, for the high calcium ashes. Figure 11 depicts the glassy halo for Iowa area fly ashes showing similar trends in shift of the halo. Figure 12 depicts the normalized data for the major glassy components on a ternary $\text{CaO-Al}_2\text{O}_3\text{-SiO}_2$ diagram. Dunstan [9] used this technique in studies on blast furnace slags. The reader is again reminded that these data represent only an average gross composition of the glassy phase of the ash. It is known [8, 12, 17] and evidenced by the x-ray diffraction traces in Figure 11 that the glassy phase of individual fly ash particles can and does vary considerably and represents a range of compositions from durable silica rich and calcium lean particles to highly strained silica lean and

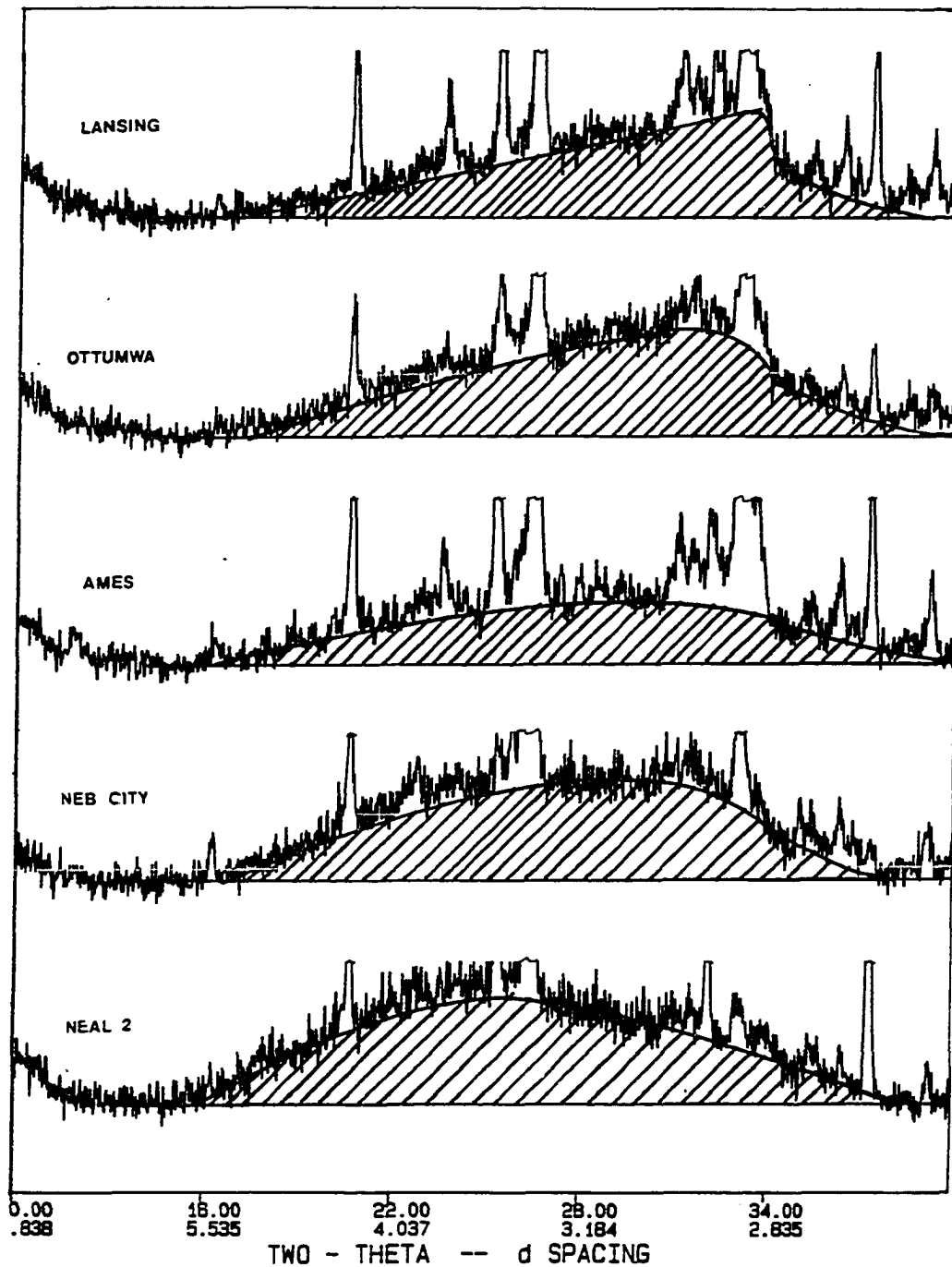


Figure 11. Typical Iowa fly ash glassy halos from x-ray diffraction

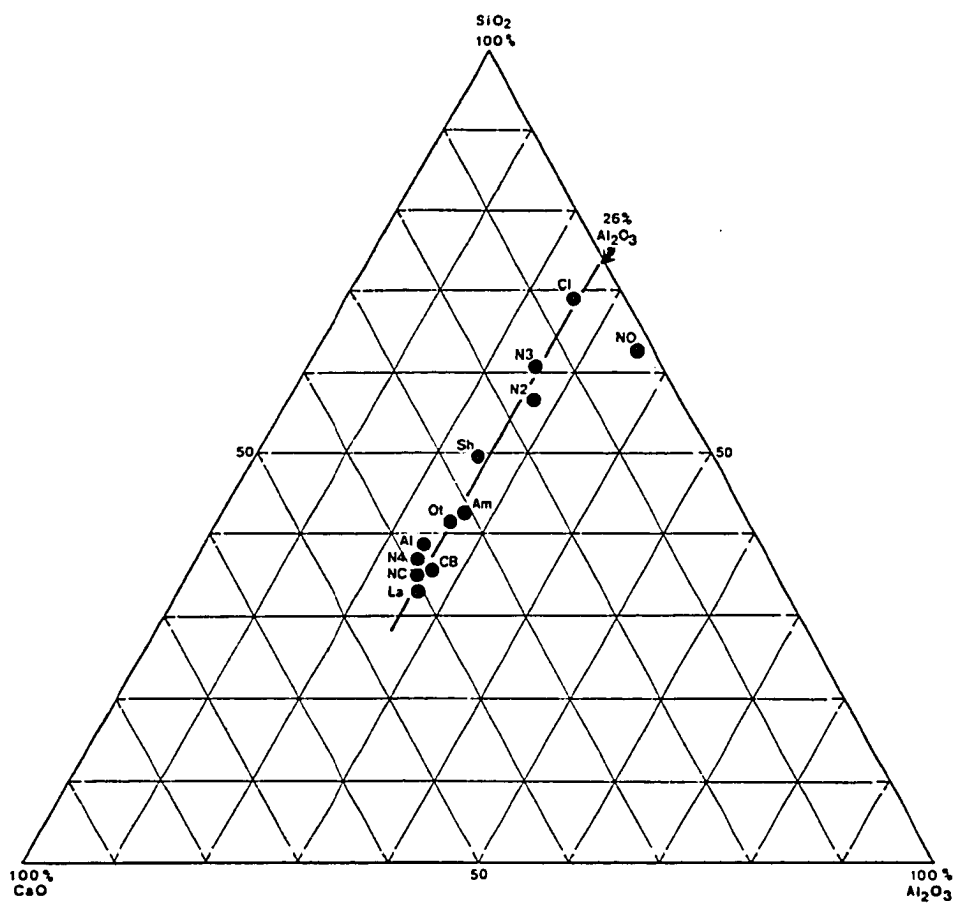


Figure 12. Normalized glass compositions in the ternary system $\text{CaO}-\text{Al}_2\text{O}_3-\text{SiO}_2$

calcium rich particles. This is also well-evidenced [5] from microscopic examinations of fly ash concrete of several years of age where fly ash spheres are present showing no evidence of any type of reaction. In viewing Figure 12 then, what Diamond [6] is suggesting is that a significant amount of the glassy phase of calcium rich fly ashes is of a calcium aluminate glass structure. For example, the glassy halo of the Nebraska City ash in Figure 11 is shown to have a broad glassy halo with no definitive maxima in the 24 to 32 degree two theta range. This implies that a significant portion of both calcium lean and calcium rich glasses are present. Referring to Figure 12 it is shown that the gross composition of the Nebraska City ash is plotted as one composition of 35 percent SiO_2 , 25 percent Al_2O_3 , and 40 percent CaO . From Diamond's work, however, a portion might be plotted directly, or nearly so, on the $\text{CaO-Al}_2\text{O}_3$ (range of calcium aluminate cements) and a portion on the $\text{SiO}_2\text{-Al}_2\text{O}_3$ axis (pozzolans) with portions of intergrade glasses between. Therefore, in the following discussions the foregoing must be kept in mind.

Although the normalized glassy compositional data shown in Figure 12 are averages only, it does allow us to gain an insight into the glassy phase and provides some basis for discussion and comparison.

The average glassy composition data plots nearly as a straight line along the average Al_2O_3 content of 26 percent.

The Clinton and North Omaha ashes fall in the mullite field. The Council Bluffs, Nebraska City and Lansing ashes fall in the gehlenite (borderline anorthite) field. The remaining glasses traverse the anorthite field.

The average glass compositions shown in Figure 12 will be discussed in relation to work conducted on the reactivity of glasses in these compositional ranges.

Buri et al. [3] studied a series of synthetically prepared glasses in the $\text{CaO-Al}_2\text{O}_3\text{-SiO}_2$ compositional system. The location of these glasses designated as series I, II, and III are shown on Figure 13. His research involved the structure and devitrification behavior of these glasses with the objective of showing that aluminum ions are principally present in tetrahedral coordination. From differential thermal analysis (DTA) studies for the series II and III glasses, Buri showed that the glass transition temperature decreased with increasing $\text{CaO}/(\text{Al}_2\text{O}_3+\text{SiO}_2)$ ratio. He attributed this to the glass structure moving from a quartz-like network, with aluminum in tetrahedral coordination, to an increasingly distorted network due to the modifier effect of the calcium ions. He concluded from his studies that at $\text{CaO}/\text{Al}_2\text{O}_3$ molar ratios less than 1, only 25 percent of excess aluminum ions would be in an octahedral coordination state.

Blast furnace slags are glassy materials of similar

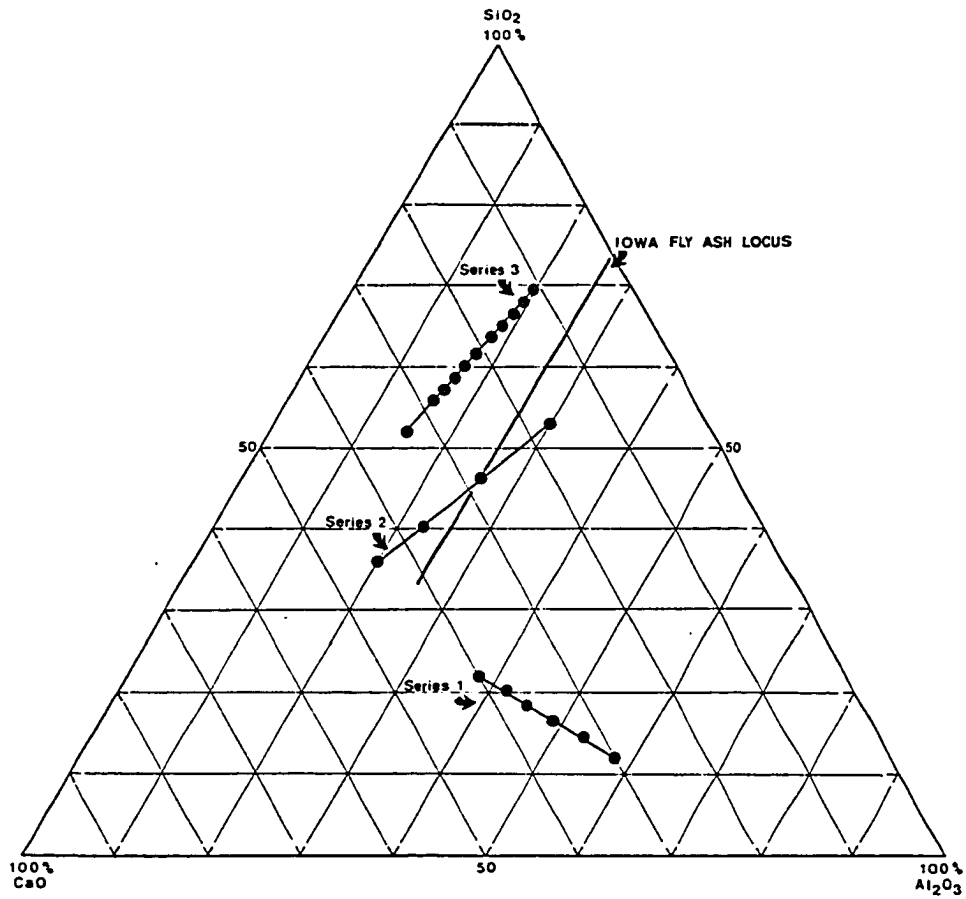


Figure 13. Glasses studied by Buri et al. [3]

glassy phase chemical composition although generally at a higher CaO content. Run-Zhang et al. [37] studied a variety of slags in the system $\text{CaO-MgO-Al}_2\text{O}_3\text{-SiO}_2$. Their efforts were directed at evaluating the structure and hydraulic activity of slags in this system by using a network energy and system bond energy approach. Their work is of interest because the glassy slags incorporate MgO into their structure and because of the bonding energy approach. Figure 14 shows the location of some of the slags they studied that correspond to the average composition of high calcium Iowa ashes. Results of their work indicated decreasing network bond energy and total system bond energy with increasing analytical CaO contents. As is recalled from Table 1, the bond strength of the CaO network modifier is only 32 kcal/mole compared to the network formers SiO_2 bond strength of 106 kcal/mole and tetrahedrally coordinated Al_2O_3 of 101 kcal/mole. Thus, as the amount of modifiers that are incorporated into the network increases, the amount of system energy should decrease. Run-Zhang's work indicates this is true for the slag glasses of his study and supports Buri's work from another approach. It also lends support to the hypothesis that the glassy phase of fly ash becomes increasingly strained, and hence, more reactive with increasing analytical CaO content.

Research conducted by Daugherty et al. [4] involved slag

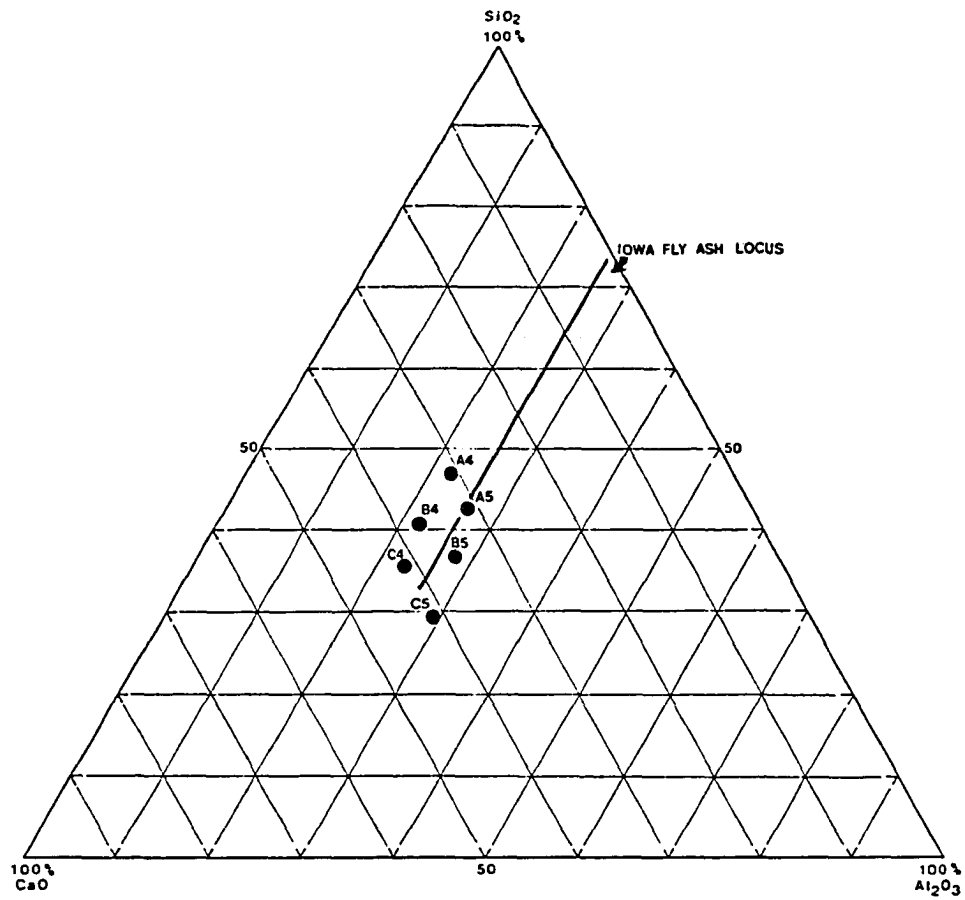


Figure 14. Glassy slags studied by Run-Zhang et al. [37]

glasses prepared in the $\text{CaO-MgO-Al}_2\text{O}_3\text{-SiO}_2$ system. Their work involved glass content and hydraulic activity of slags synthetically produced in the above system using varying base to acid (B/A) ratios calculated from $(\text{CaO}+\text{MgO})/(\text{SiO}_2+\text{Al}_2\text{O}_3)$. Theoretically as the B/A ratio decreases a glass is more easily produced. This work is of interest because it is believed that the composition and amount of the glassy phase is very important to hydraulic properties. Daugherty's work covered B/A ratios ranging from 0.80 to 1.30. He found that the amount of glass produced by melting at 1500 degrees centigrade and by quenching in ice water decreased dramatically with increasing B/A ratio. It had been hoped by using the B/A ratio from elemental XRF analysis data for fly ashes that the amount of glass present could be predicted. Reviewing the analytical $(\text{CaO}+\text{MgO})/(\text{SiO}_2+\text{Al}_2\text{O}_3)$ data from Table 7 indicate ratios ranging from 0.04 to 0.75 with no evident correlation to the percent estimated glass contents shown on Table 4. This may be due to differences in the conditions prevailing during the formation of glass between a power plant environment and Daugherty's controlled environment. What is interesting from Daugherty's work, however, is that the greatest hydraulicity was achieved with slags with the highest B/A ratio and the highest glass content. From Table 7 and Figure 8, it is noted that the analytical and glassy phase B/A ratios are directly related

and increase linearly from the low calcium to high calcium fly ashes. Daugherty's work is again believed to be evidence of the more strained and hydraulic nature of the glassy phase of Iowa ashes.

Run-Zhang and Qiong-Ying [35] in research on the structural features of slags and their hydraulic activity also reported increasing hydraulic activity as measured by compressive strength development, with increasing glass content and increasing modifying cation incorporation into the network.

Johansson [15] studied high glass content slags in the $\text{CaO-MgO-Al}_2\text{O}_3\text{-SiO}_2$ system. The slags contained glass contents ranging from 66 to 99 percent and MgO contents of around 8 to 10 percent. Figure 15 presents the location of some of the slags he studied normalized to the $\text{CaO-Al}_2\text{O}_3\text{-SiO}_3$ system. His work concentrated on comparing glass content and strength versus seven different ratios reported to represent hydraulic moduli of glass. He found that one of the better correlations with compressive strength was the FII modulus defined as $\text{FII} = (\text{CaO} + \text{MgO} + \text{Al}_2\text{O}_3) / \text{SiO}_2$. He also found the glass content to be important, with the correlation of FII to strength significantly improved by multiplying FII by the percent of glass. Johansson also determined that the higher the glass content of the slags the higher the strength gain. Little difference was noted in one day strengths but

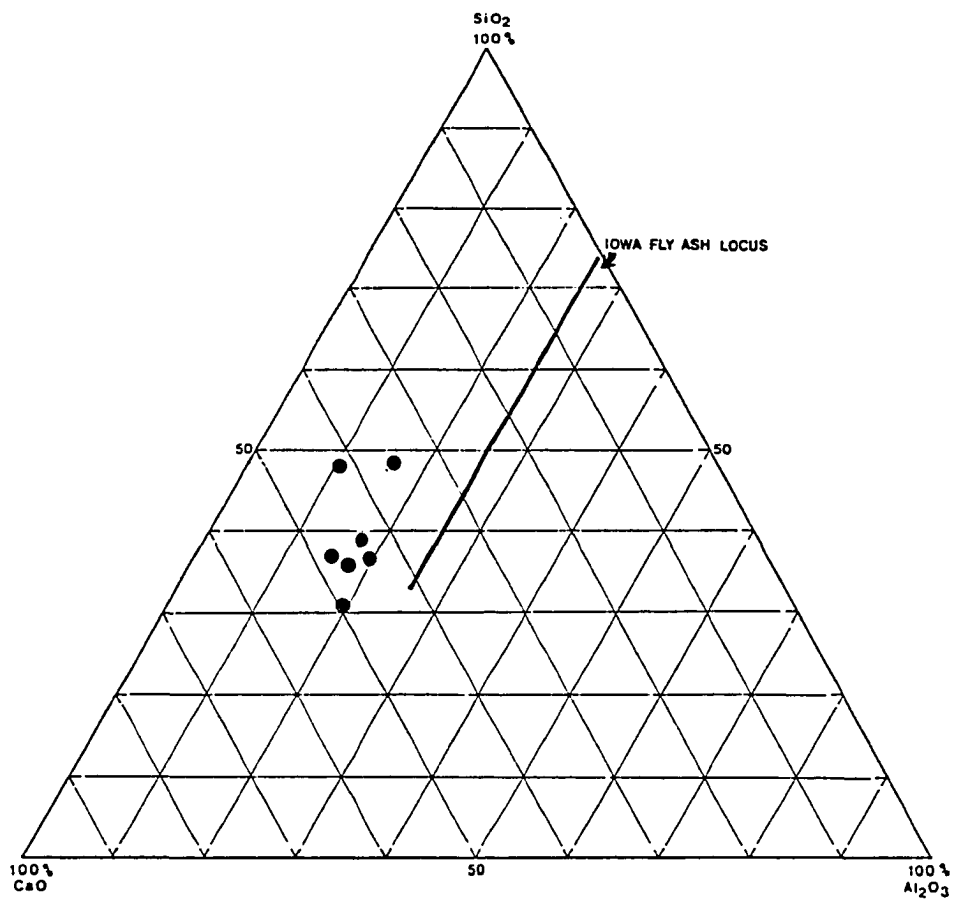


Figure 15. Glassy slags studied by Johansson [15]

significant differences in 28 day strengths were noted.

One of the most significant papers, in the writer's opinion, regarding hydraulic properties and hydration of glasses in the system $\text{CaO-Al}_2\text{O}_3\text{-SiO}_2$ is that of Locher [21]. Figure 16 depicts the range of glasses he studied. The letter "M" designates glasses containing 5 percent MgO . Included on Figure 16 are the locations of some of the normalized glassy phases of Iowa fly ashes (major oxides only). Figure 17 depicts contours of 28 day strengths of glasses activated with portland cement. It can be seen there are abrupt changes in strength development within relatively narrow changes in glass composition. Locher defines the three areas of high strengths as "silicatic", "silicoaluminatic", and "aluminatic" hardening regions. Locher activated these glasses with portland cement, anhydrite and calcium hydroxide. He also found widely varying response with the glasses depending on the activator used. For glass 22M (5 percent MgO incorporated in the glass), all three activators responded equally well. For glass 23M (containing MgO), cement and lime activation responded about the same as for glass 22M, but strength dropped drastically with sulphate activation. The incorporation of MgO in the glass had a very strong effect on activator response. For glass 23a (without MgO), cement activation was strongest, lime activation showing slightly

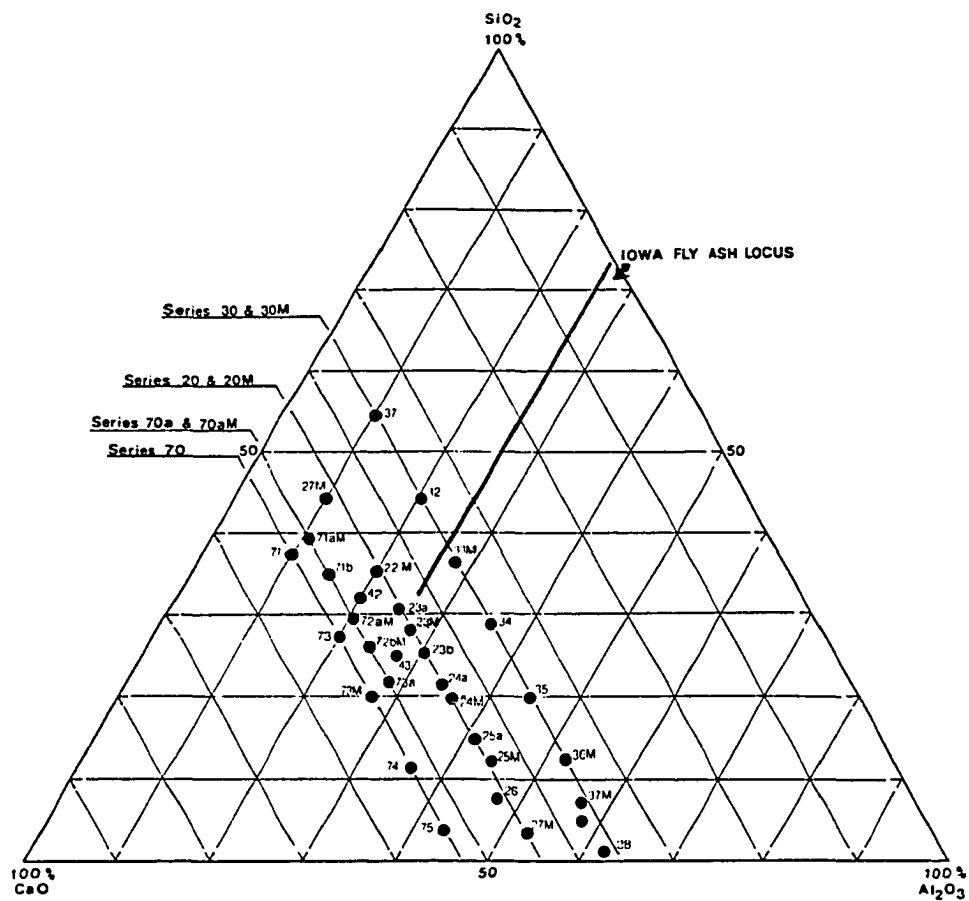


Figure 16. Glasses studied by Locher [21]

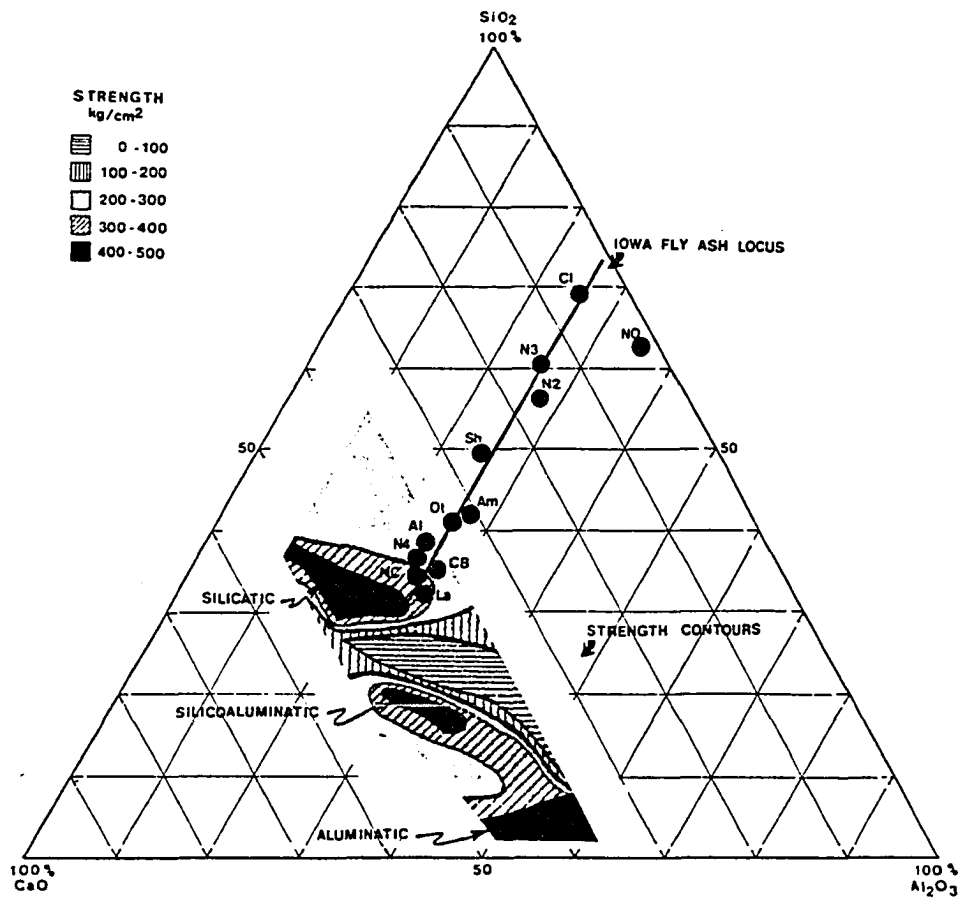


Figure 17. 28 day compressive strength contours of glasses activated with portland cement (adapted from Locher [21])

less strength development, and sulphate activation dropping drastically. Also, the abrupt strength drop noted for cement activation in glasses without MgO was not evident in the glasses containing 5 percent MgO. In efforts to explain the abrupt changes in hydraulic behavior, Locher assumed that the capacity of compounds to exhibit hydraulic characteristics presupposes that the compounds react with water or hydrous solutions with the compounds being dissolved and reformed into cementitious materials. Under this assumption, he postulated that either the dissolution behavior of the glasses changed dramatically with composition or that erratic changes in cementitious phases were occurring. In experiments on dissolution behavior in ammonium citrate solutions, he found continuous but no erratic changes in solubilities of a range of glasses. He, therefore, concluded that the changes were being caused by differing reaction product formation. By using XRD techniques, Locher showed that the abrupt changes were due to differing principal cementitious reaction products occurring in each region and that the regions between areas of high strength were transitional regions of different reaction product formation. In the silicatic field, the principal cementitious reaction product is calcium silicate hydrate, in the silicoaluminatic field gehlenite hydrate predominates and in the aluminatic field calcium aluminates are predominant. Locher also

reported that gehlenite hydrate is not stable in the presence of calcium hydroxide and converts to hydrogarnet while absorbing lime. Gehlenite hydrate is also not stable in lime-saturated gypsum solutions and converts to ettringite. He also concluded from his study that in the hydraulic properties of the glass the CaO of the activator is not used to form hydrate phases. In the hydrate phases, the only CaO that could be used for cementitious products was the CaO in the glass.

Idorn [13, 14] presents a significant conceptual viewpoint of fly ash relative to the ternary $\text{CaO-Al}_2\text{O}_3\text{-SiO}_2$ system. Figure 18 presents his concepts in relation to Iowa fly ash glassy phase compositions. Idorn views fly ash as a concrete admixture which possesses a progression of differing physical and chemical properties depending on its constitution. In the upper right hand area, the high silica-low lime ashes are considered to be alkali activated and produce reaction products of an amorphous, gel-like nature. Idorn relates this to the well-known alkali-silica reaction product gel. Towards the lower left are lime activated materials in which crystal like reaction products dominate the system. From the location of the Iowa fly ashes, it is seen that these glass compositions progress from the alkali activation area into the lime activation field. Idorn stresses that for proper utilization of fly ash in

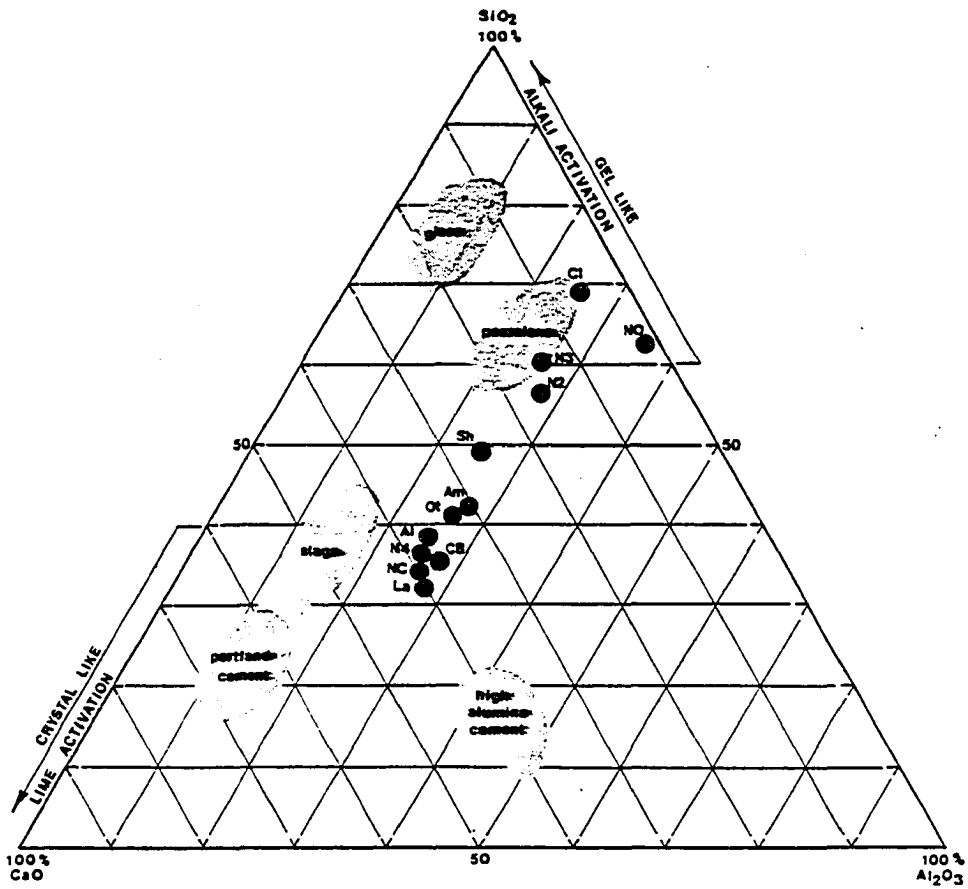


Figure 18. Glassy phase of Iowa fly ash in relation to Idorn's [13, 14] concepts

concrete we must recognize and design for the differing properties and reaction products.

Faber and Stirling [11] also stressed the differences between the low and high calcium ashes and the properties imparted to concrete. The low calcium ashes in concrete provide improved sulphate resistance, lower heat of hydration, decreased permeability, and retards early strength development. The high calcium ashes by contrast do not improve sulphate resistance or lower the heat of hydration. Because of crystal-like reaction products they are not as effective in densifying and decreasing the permeability of concrete. The high calcium ashes significantly improve early strength development and should perhaps be considered cement extenders.

It is clear that for proper utilization of Iowa fly ashes a classification system must be developed that recognizes and differentiates the ashes depending on desired properties. The system should also be capable of categorizing the marginal F/C or intergrade ashes. It would appear that at least four categories are necessary.

Summary

From the foregoing, we have seen that the glassy phase of Iowa fly ashes is composed principally of varying amounts of calcium, aluminum, and silicon which are the building

blocks of cementitious reactions products. It has been shown that the chemical composition of the glassy phase changes from a silica rich and calcium lean glass in the low analytical CaO ashes to a silica lean and calcium rich glass in the high analytical CaO ashes. Correspondingly, the structure of the glassy phase in the low analytical CaO ashes represents, on the average, a chemically durable and stable glass composed of a strong silica tetrahedral networking structure only partially modified and strained by small amounts of calcium and magnesium network modifying cations. At the other end of the spectrum are the high analytical CaO ashes. The glassy phase of these ashes represents, on the average, an unstable glass composed of a weak networking structure of silica tetrahedra highly strained by a significant amount of calcium and magnesium network modifiers.

Aluminum is incorporated in the glass structure of the low calcium and high calcium ashes either isomorphously substituted for silicon in the silica tetrahedron as a network former or incorporated as part of the network forming chain in octahedral coordination as an intermediate. Schlörholtz, Demirel and Pitt [41] postulate that aluminum in the high calcium ashes is more likely to be in its octahedral coordination as an intermediate. In the low calcium ashes, they contend that most of the aluminum is incorporated as a

network former isomorphously substituted for silicon in the silica tetrahedra frame. If this is true, this again would contribute to a more unstable glass structure in the high calcium ashes. From Table 1, it is noted that the bond strength of aluminum, in octahedral coordination, is about 34 kcal/mole less than that in the tetrahedral coordination.

SECONDARY CHEMICAL ADDITIVE STUDY

Introduction

The glassy phase of Iowa fly ashes have been shown to contain significant amounts of the cementitious building blocks of calcium, aluminum, and silicon. These elements have been shown to be present in varying amounts in the glass ranging from calcium lean-silica rich in the low calcium ashes, to calcium rich-silica lean in the high calcium ashes. The glassy phase network becomes progressively more strained, chemically unstable, and hence more reactive from the low calcium to the high calcium ashes. On the average, approximately 80 percent by weight of fly ash exists in the glassy phase.

Considering the foregoing, it was postulated that small amounts of secondary chemical activators could be economically utilized to accelerate the attack and dissolution of the glassy phase thereby releasing calcium, aluminum, and silicon for use in formation of cementitious calcium aluminate and calcium silicate hydrates. If this were possible, the efficient and economical utilization of the ashes in soil and subbase stabilization could be enhanced.

Previous Work

Chemical activators utilized in this study were selected based on economic considerations and on their expected

reactions being either to initiate chemical attack and dissolution of the glassy phase and/or to promote formation of cementitious compounds. From a chemical standpoint, the activators selected were expected to act as complexing agents, solid solutes, and buffers or catalysts in the decomposition of the glass and formation of cementitious hydration products.

In all, a total of sixteen different chemicals were used in concentrations (by weight of ash) of 0.1, 1.0, and 3.0 percent. The chemicals used are shown on Table 8.

All activators were commercially available reagent grade chemicals. The kiln dust was bypass material from kiln number 8 at the Lehigh plant, Mason City, Iowa. Water utilized for all sample preparation was deionized and distilled.

The fly ashes used in the preliminary work were the Neal 4 ash, selected to represent the high calcium ash, and the Neal 2 ash to represent the intermediate calcium content ashes. Chemical and physical properties of the ashes are given in the Appendix.

All test samples were prepared at a water/fly ash ratio of 0.24. Fly ash paste mixes were prepared and mixed in compliance with ASTM test method C-109. Chemicals, with the exception of kiln dust, were dissolved or completely

Table 8. Secondary chemical activator listing

1. Zinc Oxide
2. Aluminum Sulphate
3. Sodium Fluoride
4. Ammonium Phosphate (Dibasic)
5. Magnesium Oxide
6. Magnesium + Calcium oxide ($MgO/CaO=0.57$ by weight)
7. Kiln Dust (Lehigh, Mason City, Iowa)
8. Aluminum Ammonium Sulphate
9. Sodium Hydroxide
10. Ammonium Nitrate
11. Phosphoric Acid
12. Calcium Fluoride + Ammonium Nitrate ($CF/AN=2.0$ by weight)
13. Ammonium Bifluoride
14. Sodium Phosphate
15. Ammonium Fluoride
16. Cement, Type 1 (Monarch)

dispersed in the mix water prior to incorporation of the fly ash. The kiln dust samples were prepared by hand mixing the dry materials followed by machine mixing prior to the addition of water. Chemical concentration percentages are based on dry weight of fly ash.

As a preliminary screening measure, unconfined compressive strength testing was selected as a means to evaluate activator effectiveness. If an additive attacked the glassy phase and liberated calcium, aluminum, and silicon into a usable form, and new or additional cementitious products were formed then early 28 day strength would be expected to be enhanced.

Cylindrical unconfined compression test samples (1.5 inches in diameter by 3 inches in height) were cast in polyethylene split mold assemblies, rodded, overfilled slightly, and clamped between lucite plates. Six cylinders were cast for each test age. Cylinders were stripped within 24 hours of molding, and remained in the cure room until testing. Testing in unconfined compression was conducted at a controlled strain rate of 0.05 inches per minute.

To provide a rapid determination of setting properties and early strength gain in fly ash paste mortars, a Soiltest Model CL-700 pocket penetrometer was utilized. The procedure consisted of casting a fly ash paste sample into a four inch diameter by three-fourths inch deep metal pan and using the penetrometer to obtain periodic readings. When inserted into a material to a specified depth, this device gives an indirect measure of unconfined compressive strength in tons per square foot. Samples were left uncovered at room temperature and measurements made until a reading of 4.5 tons

per square foot was obtained. Figure 1 in the Appendix illustrates the results of one test. Typically, there is an initial period of slow hardening with time, after which the rate of hardening increased relatively rapidly. The data generally tended to plot as a straight line for both the initial slow-set period and for the accelerated-set period. The point of intersection of these lines has been defined as the time of "initial set". The point at which the penetrometer limit of 4.5 tons per square foot was reached was arbitrarily defined as "final set". Reaction time was measured from the time water was added.

Vial samples of the paste mixes were collected, sealed, and stored at room temperature at the time of molding. One vial sample was made for each group of six samples at each test age. Reaction product evaluations were conducted by step scan x-ray diffraction using monochromatic copper K alpha radiation at a 50 kv, 25 ma setting. Count time was two seconds with a step size of 0.05 degrees. The unit was equipped with a graphite monochromator and pulse height analyzer. Scanning electron microscopy (SEM) was selectively utilized for evaluation of reaction product morphology and additive effect on the glassy phase.

Results of the initial portion of this work have been published [2], and are briefly summarized as follows. For the Neal 4 ash, dibasic ammonium phosphate was effective in

retarding the initial setting time of the fly ash at a 1.0 percent concentration level with a reduction in compressive strength, and at a 3 percent concentration level, retarding final set while increasing strength by a factor of 2.5 times that of the untreated control sample.

Figures 2, 3 and 4 in the Appendix presents the XRD diffractograms of untreated and treated fly ash. Figure 2 shows the diffractogram of the raw air dry fly ash. Figure 3 shows that the major reaction products of hydrated, untreated Neal 4 fly ash is primarily in the form of ettringite. Comparing the ammonium phosphate treated pattern in Figure 4 with the hydrated untreated pattern in Figure 3 indicates the additional formation of relatively strong calcium aluminum silicate hydrate peaks (stratlingite). Relatively strong calcium aluminum oxide sulphate hydrate peaks were also evident (monosulfoaluminate). Comparison of the glassy halos also show a visible reduction in size (i.e., reduced amount) of the halo for the treated ash.

A scanning electron micrograph of the interior portion of the hydrated vial samples is shown on Figure 5 in the Appendix. Spiky ettringite crystals are evident in the untreated, hydrated Neal 4. SEM study of the ammonium phosphate treated ash clearly indicated disintegration and breakdown of the glassy phase as shown on Figures 6 and 7 in the Appendix. The formation of relatively massive

crystalline reaction products and monosulfoaluminate crystals was also evident.

Effects of Reagent Grade Chemicals

Neal 2

Ammonium nitrate was found to be one of the most effective strength enhancers for the Neal 2 ash. At a 3.0 percent treatment level, strength was increased 2.3 times that of the untreated controls while accelerating final set time from 125 minutes to 55 minutes.

The XRD results for hydrated samples of ammonium nitrate treated fly ash are shown on Figure 19 as compared to the XRD trace of fly ash hydrated with water only.

From the trace for hydrated fly ash treated with water only, (Figure 19a) it is seen that the principal crystalline reaction product is ettringite (E). Poorly crystalline to amorphous cementitious calcium aluminate hydrates (CAH), and calcium aluminum silicate hydrates (CASH) reaction products are generally recognizable by a hump or rise in the background in the 8 to 12 degree two theta range. Poorly crystalline to amorphous cementitious calcium silicate hydrates (CSH) are generally recognizable as a hump in the background of the XRD trace in the 26 to 36 degree two theta range. Evaluation of cementitious CSH formation in fly ashes is complicated by the fact that the glassy phase of air dry and untreated but hydrated fly ash produces a hump or halo in

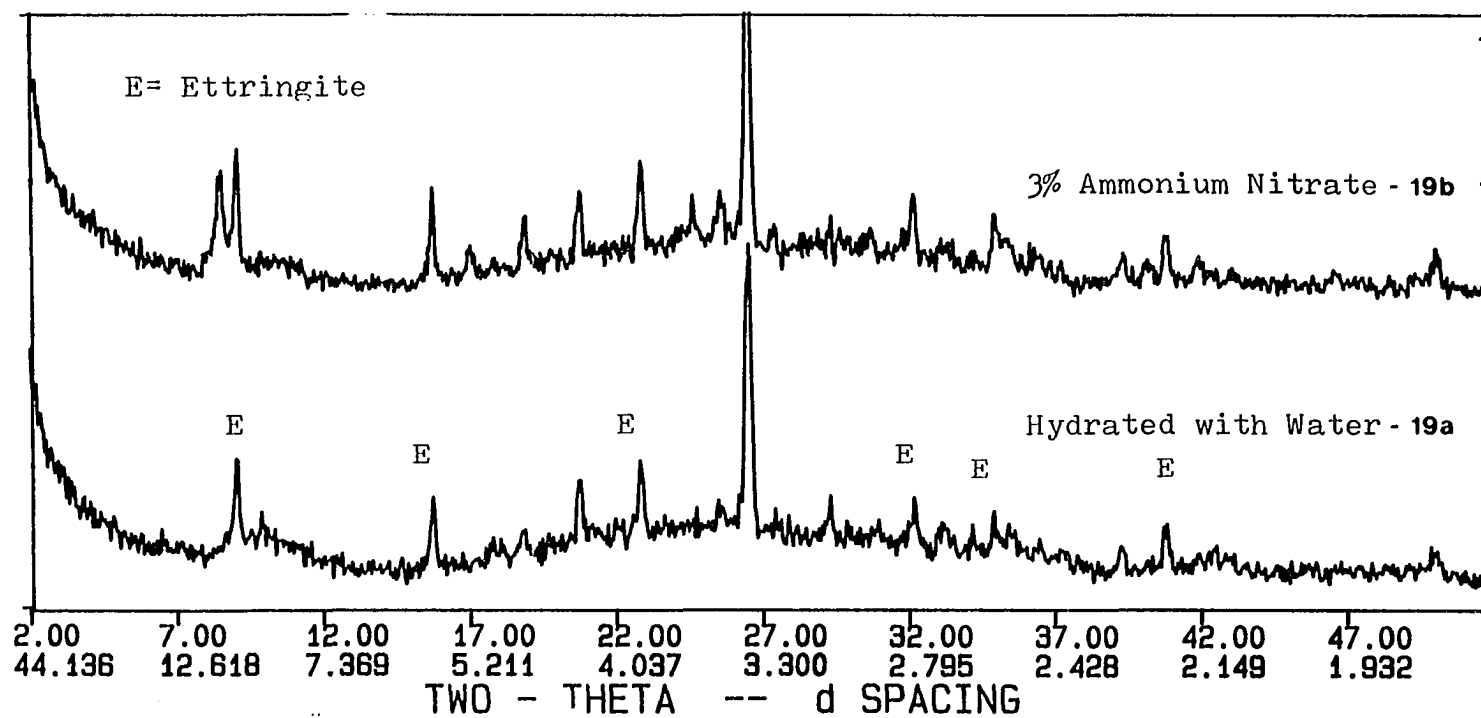


Figure 19. X-ray diffractograms, Neal 2 fly ash, untreated and ammonium nitrate treated

the background trace in the same general two theta range as cementitious CSH.

In comparing the ammonium nitrate treated fly ash (Figure 19b) to the control (fly ash hydrated with water only), the maximum intensity of the ettringite peak at 5.62 angstroms of the ammonium nitrate treated sample is 1.2 times stronger than the control. The amount of amorphous CAH appears reduced. There is a very strong peak present at 10.4 angstroms of the ammonium nitrate treated material that is not present in the control. After considerable search of JCPDS files, this material has yet to be clearly identified. This is primarily due to the difficulty in interpreting overlapping and conflicting XRD peaks occurring from the numerous compounds present. The material is believed to be cementitious and of a calcium aluminum silicate hydrate form (CASH). The increase or decrease in CSH, if present, is not evident. The strength increase appears to be resulting from formation of additional ettringite and the formation of a new crystalline cementitious product at 10.4 angstroms. The strength gain from these cementitious materials apparently outweigh the strength loss from the reduction in the amount of amorphous CAH. From SEM studies, the reaction products in Figure 19b appear to be forming on the surface of the fly ash particles with reaction products of needle-like and platelet morphology between particles. The fly ash particles do not

show surface reaction products, but appear to be blistering or peeling, and breaking down. Reaction products between particles appear more massive in nature. SEM micrographs are shown on Figure 8 in the Appendix.

Neal 4

In order to further evaluate the strength properties of ammonium phosphate (dibasic) treated Neal 4 fly ash, a series of pastes were prepared and tested at varying chemical concentrations. Mixes were made at a water/fly ash ratio of 0.24 and cured and tested as previously stated. The results of the 28 day strength tests are given on Figure 20 and are highly interesting in the fact that strength initially drops with additive addition rates up to 1.5 percent. Strength appears to plateau between 2.0 and 3.0 percent with a maximum of 3550 psi at 2.5 percent, and again drops dramatically to slightly under the untreated strength level. To investigate this behavior XRD analysis was conducted on the 0.1, 1.0, and 3.0 percent ammonium phosphate treated vial samples and are shown on Figure 21. Comparison of the reaction products from the XRD traces of the untreated hydrated fly ash with 0.1 percent ammonium phosphate treated samples indicate a slight increase in the ettringite intensities, and a decrease in the amorphous CAH hump in the two theta range of 9 to 12 degrees. The 1.0 percent treated trace compared to the 0.1 percent trace indicates an increase in ettringite intensity and a

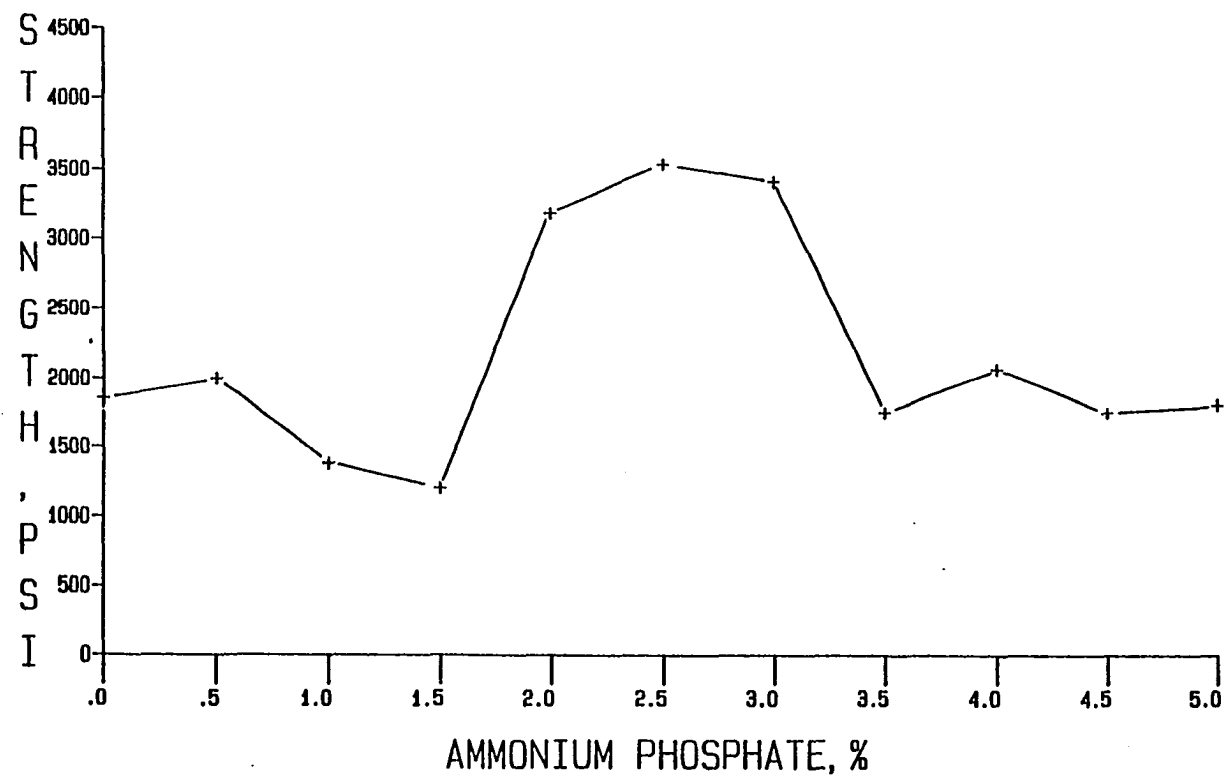


Figure 20. Compressive strength development of ammonium phosphate treated Neal 4 fly ash

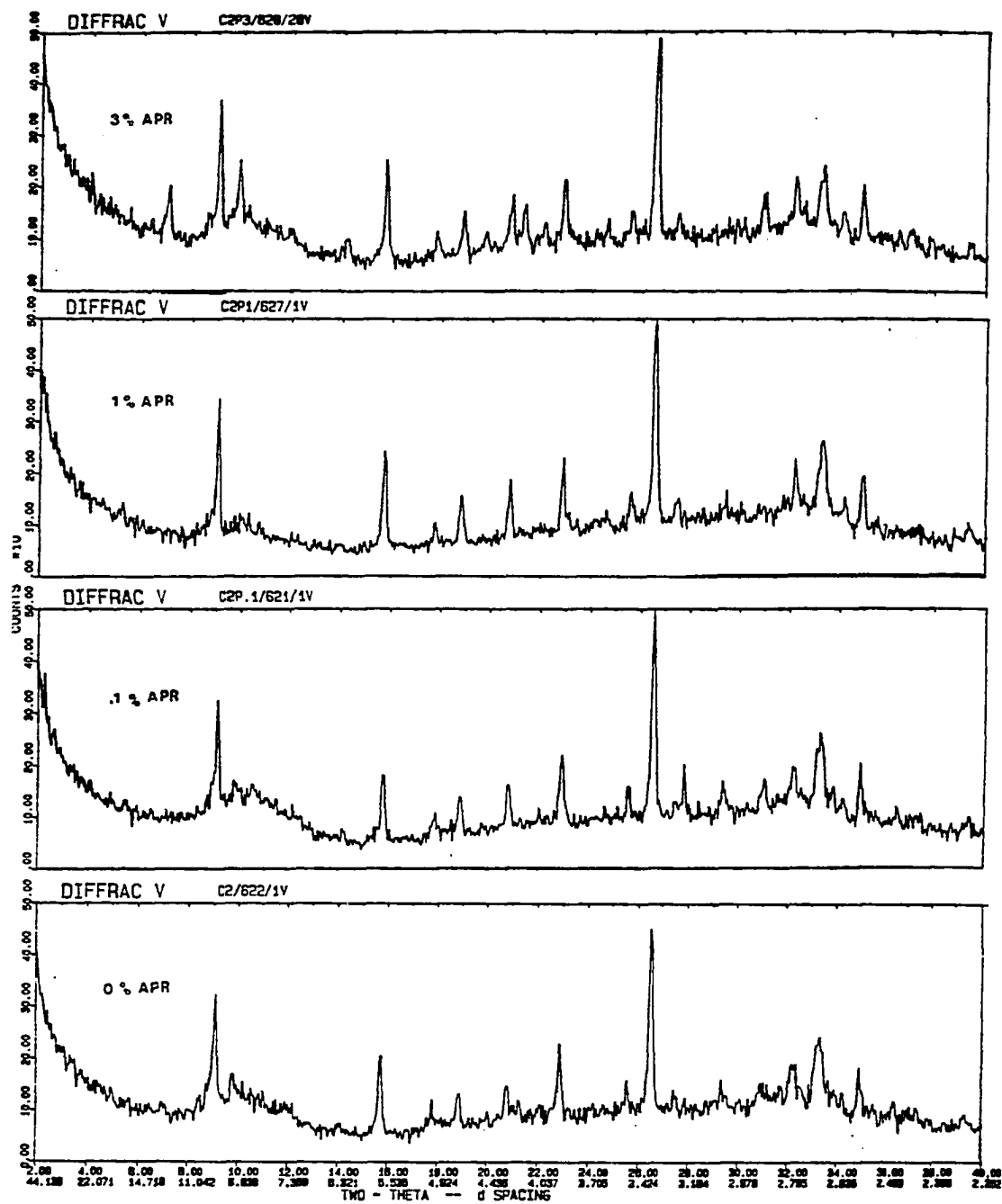


Figure 21. X-ray diffractograms of untreated and dibasic ammonium phosphate treated Neal 4 fly ash

reduction in amorphous CAH. For the 3.0 percent ammonium phosphate treated material, the ettringite intensities are about the same. A strong monosulfoaluminate peak is now present, however, at 8.92 angstroms, and a strong stratlingite peak is present at 12.5 angstroms. The dramatic strength increase is apparently the result of the formation of these new cementitious products. At the 3.0 percent addition level, any phosphate compounds would be detectable in XRD patterns. Inspection of Figure 21 does not indicate their presence. It is postulated that the phosphate tetrahedra may be substituting for the silica tetrahedra in the solid hydration phases. Initially the ammonium may be complexing aluminum and iron from the glass structure thereby making them, especially aluminum, available for formation of cementitious aluminosilicates.

The strength and XRD results also explain the changes in the setting properties at the different concentration levels noted previously. At low levels of concentration, ammonium phosphate appears to be functioning as a retarder of tricalcium aluminate hydration in the 1.0 percent treated materials. This action may be highly advantageous in field use of ammonium phosphate treated fly ash.

Fertilizer Grade Chemicals

Fertilizer grade ammonium nitrate was obtained in bag form from the State Nursery in Ames, Iowa, and produced by

N-REN Corporation-St. Paul Ammonia Products in South St. Paul, Minnesota. Figure 21a shows x-ray diffraction data (copper K alpha 50 KV @ 25 ma settings) for reagent grade and fertilizer grade ammonium nitrate. Comparison of peak locations for both samples indicate that ammonium nitrate is the principal compound present in both samples with no additional compound evident in the fertilizer grade material. Peak intensities were approximately the same for both samples. These data indicate that fertilizer grade ammonium nitrate, for all practical purposes, is chemically very similar to reagent grade material and would be expected to react similarly.

Fertilizer grade dibasic ammonium phosphate was obtained in bulk form from the Colo, Iowa feed and grain elevator. Comparison of x-ray diffraction data for dibasic ammonium phosphate fertilizer and reagent grade chemicals are given on Figure 22. The XRD trace for fertilizer indicates an additional compound present that is believed to be aluminum phosphate denoted by AL on the figure. Inspection and comparison of intensities indicate that the ammonium phosphate peaks are considerably lower in the fertilizer grade material implying either lower grain density and/or less of that compound present and presence of more absorbing ions. Fertilizer grade material, nevertheless, has a smaller concentration of ammonium phosphate present and contains

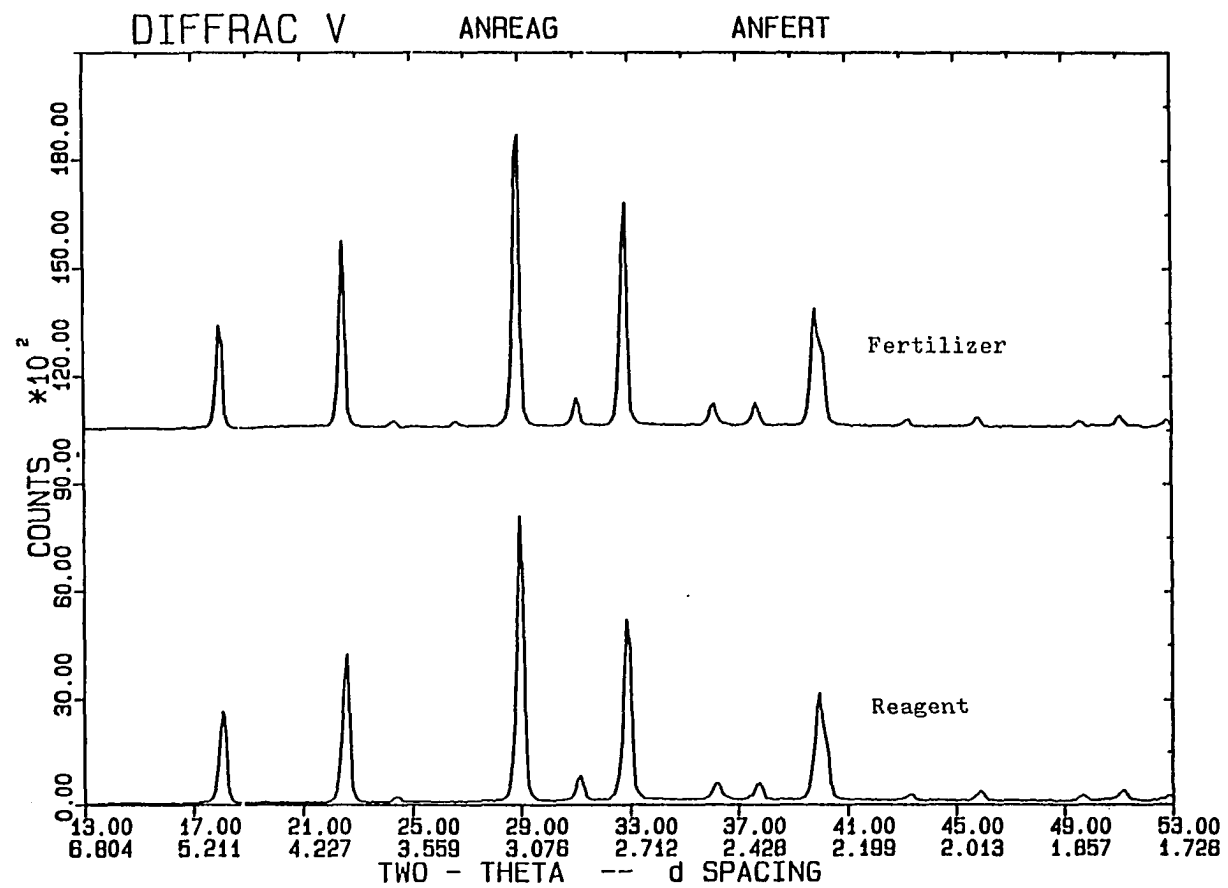


Figure 21a. X-ray diffractograms of ammonium nitrate chemicals

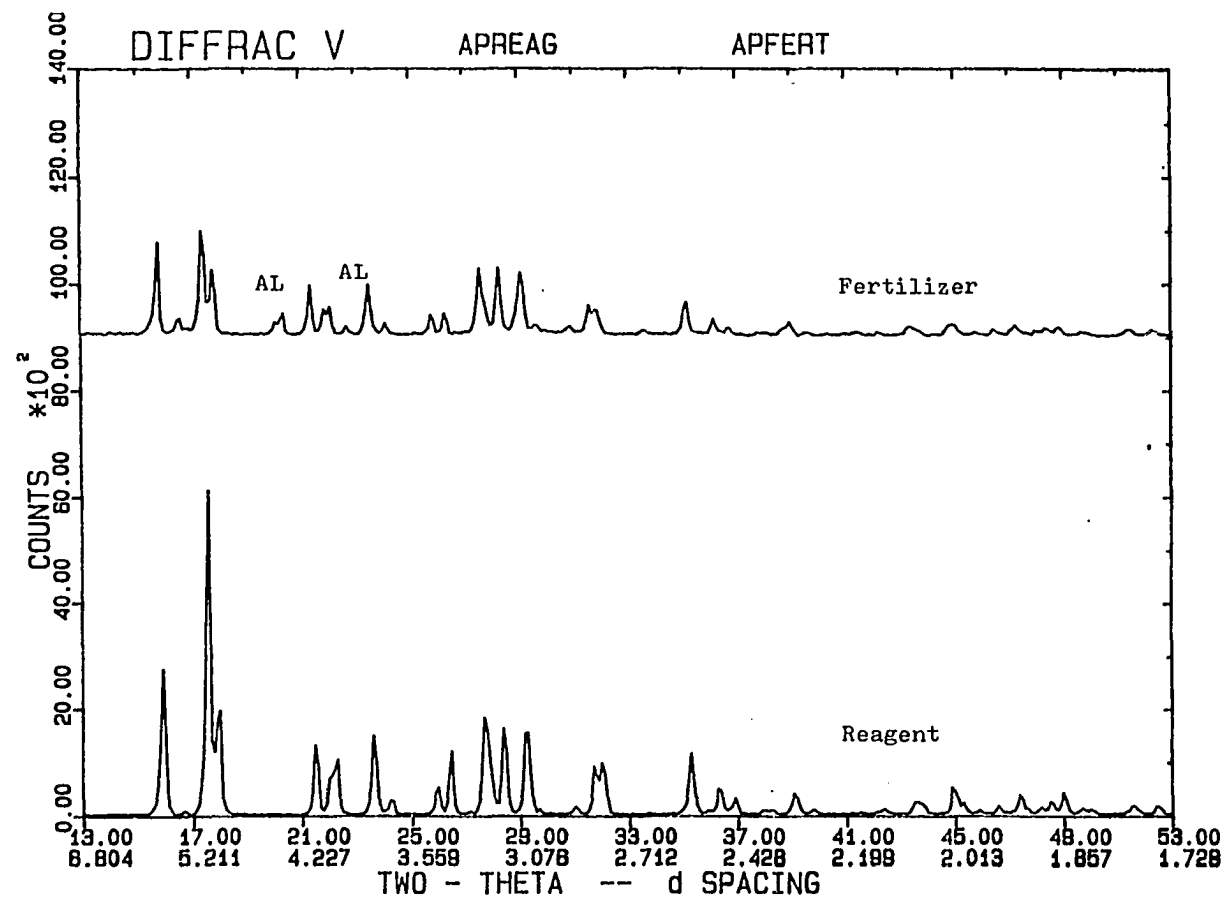


Figure 22. X-ray diffractograms of dibasic ammonium phosphate chemicals

other chemical compounds. These factors appear to have some influences on strength enhancement capabilities of fertilizer grade ammonium phosphate, and will be shown later in this study.

Ammonium nitrate (effective with Neal 2 ash), and dibasic ammonium phosphate (effective with the Neal 4 ash) are common chemicals utilized in the fertilizer industry. Fertilizer grade varieties of these chemicals are available in bulk quantities at many Iowa locations. If they could be utilized, the logistics and economics of secondary chemical activator treatment of the ashes would be easily feasible.

In order to evaluate their potential use, a series of investigations was initiated.

Neal 2

Figure 23 summarizes set time and strength data for the Neal 2 ash and ammonium nitrate fertilizer. At concentrations greater than 2.0 percent, final set time is accelerated and 28 day strength is enhanced by a factor of 5 to 6 times that of untreated ash. Acceleration of set time is desirable with this ash. The Neal 2 ash, however, is only weakly cementitious and exhibits a 28 day untreated strength of about 180 psi. Treatment dramatically increases early strength to 1000 psi and indicates it may have the potential to be utilized as an effective soil or subbase stabilizing agent.

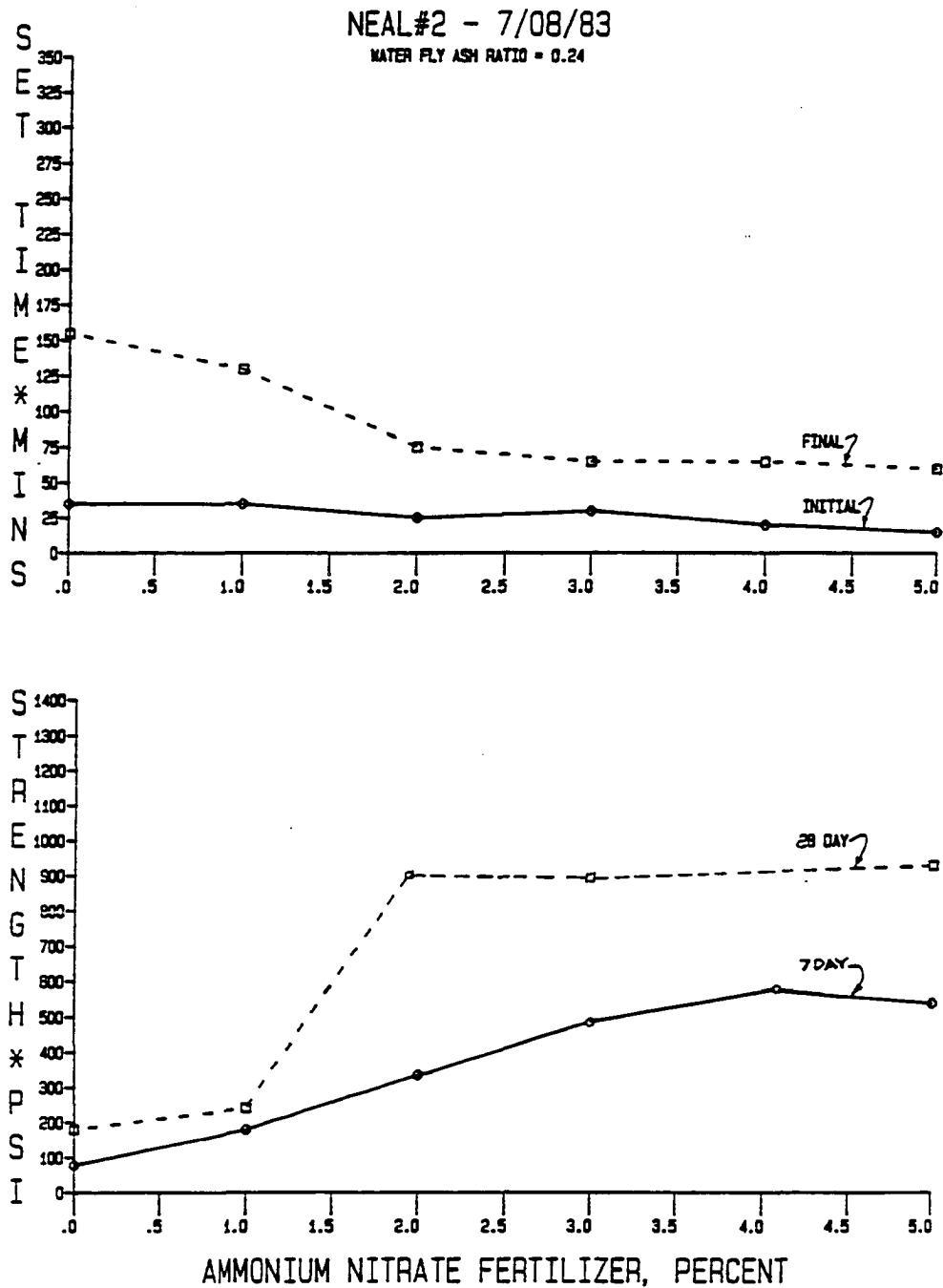


Figure 23. Set time and compressive strength of ammonium nitrate fertilizer treatment of Neal 2 fly ash

Neal 4

Data on dibasic ammonium phosphate treatment (reagent grade and fertilizer grade) of ash from the Neal 4 plant are summarized on Figures 24 through 27.

During the course of this study, it was necessary to obtain additional samples of the Neal 4 ash. Figure 24 presents results of reagent grade ammonium phosphate (APR) with the ash sampled 6/01/83 and presented previously. Figure 25 illustrates APR treatment of the Neal 4 ash sampled on 7/08/83 and showing that results are significantly different from those on Figure 24. The initial retardation of set time along with concurrent reduction in strengths are similar for both ashes. The strong increase in 28 day strength noted for the 6/01/83 ash in the 3 to 4 percent addition range are not evident for the 7/08/83 ash although strength appears to be increased at the 5 percent addition level. Figure 26 presents results of using dibasic ammonium phosphate fertilizer (APF) up to a 10 percent addition level with the 7/08/83 ash. Comparison of Figures 25 and 26 indicate similar trends in both set time effects and strength for APR and APF treatments up to the 5 percent treatments. From Figure 26, it is seen that strength is enhanced dramatically from 4 to 7 percent addition and is approximately twice that of the untreated controls at the 10 percent treatment. Similar trends are noted on Figure 27 for

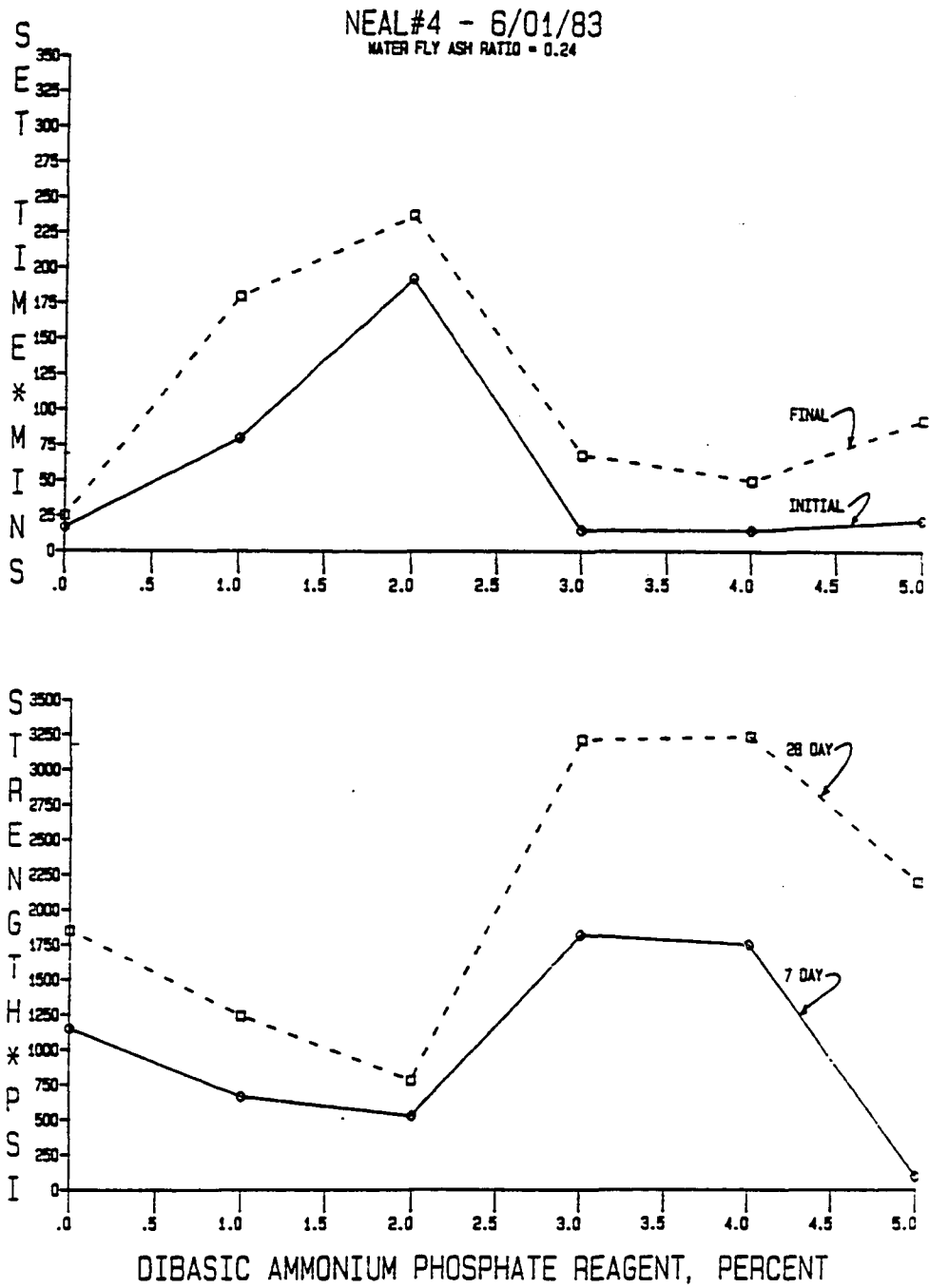


Figure 24. Set time and compressive strength of dibasic ammonium phosphate reagent and 6/01/83 Neal 4 fly ash

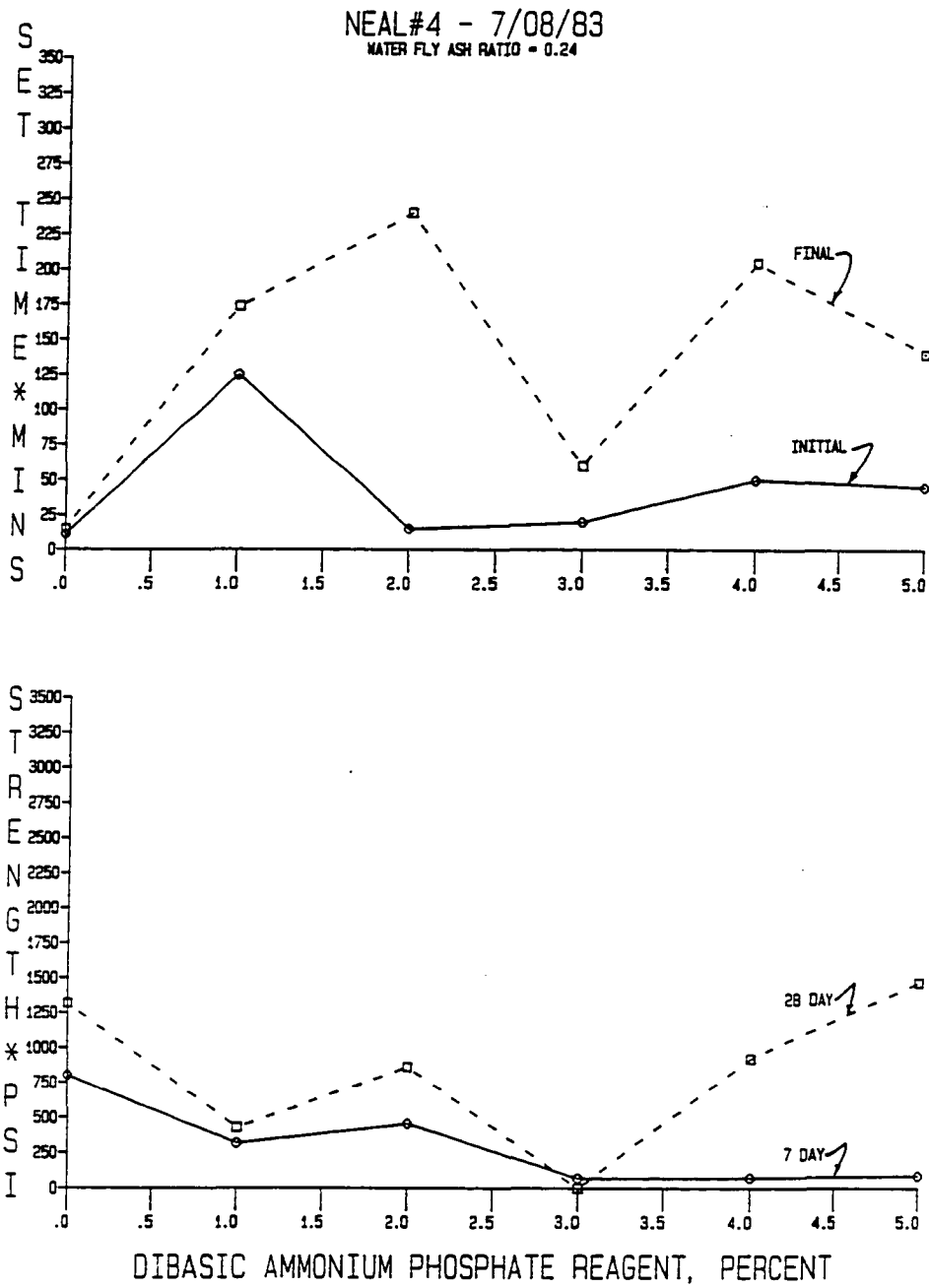


Figure 25. Set time and compressive strength of dibasic ammonium phosphate reagent and 7/08/83 Neal 4 fly ash

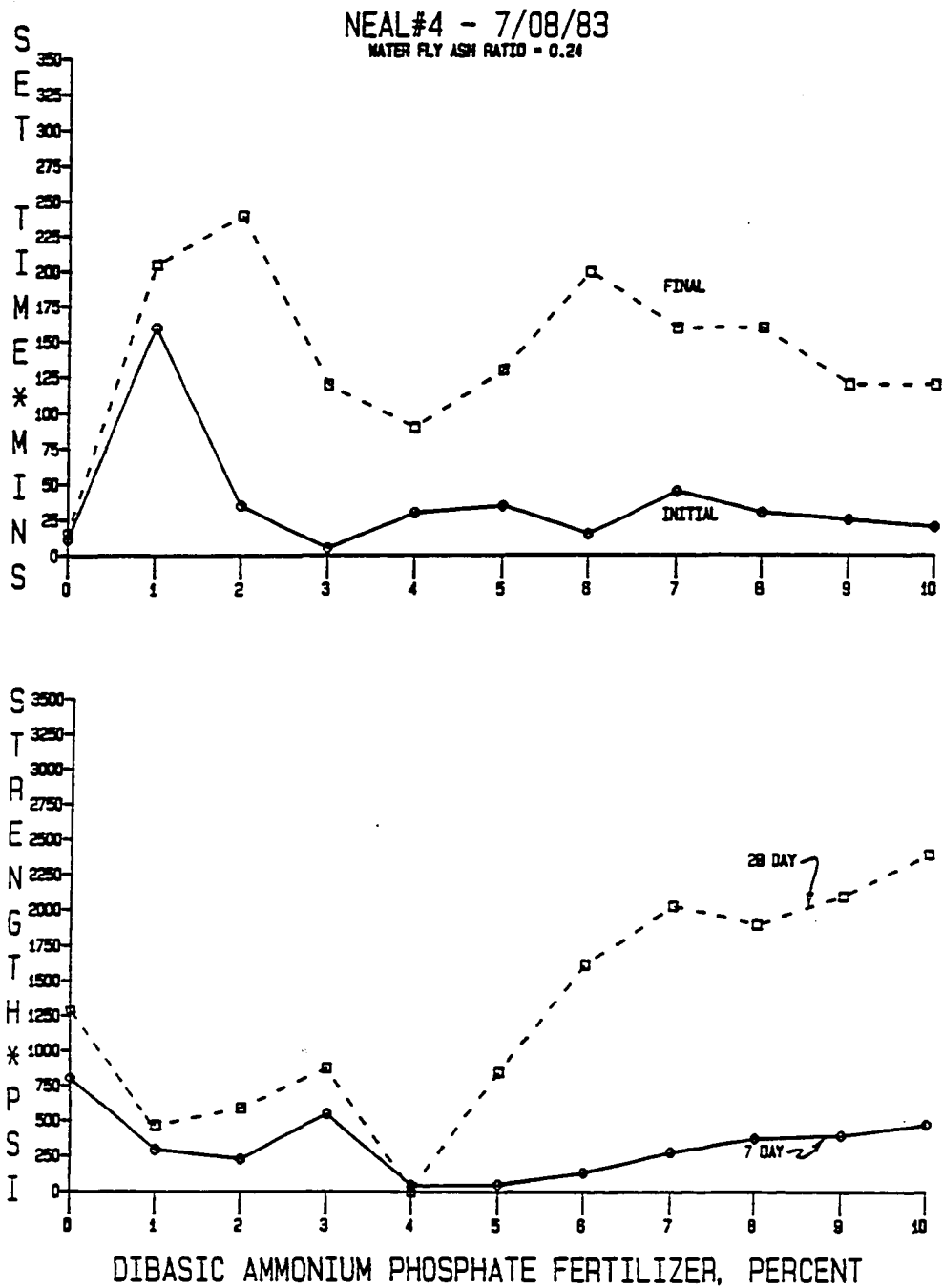


Figure 26. Set time and compressive strength of dibasic ammonium phosphate fertilizer and 7/08/83 Neal 4 fly ash

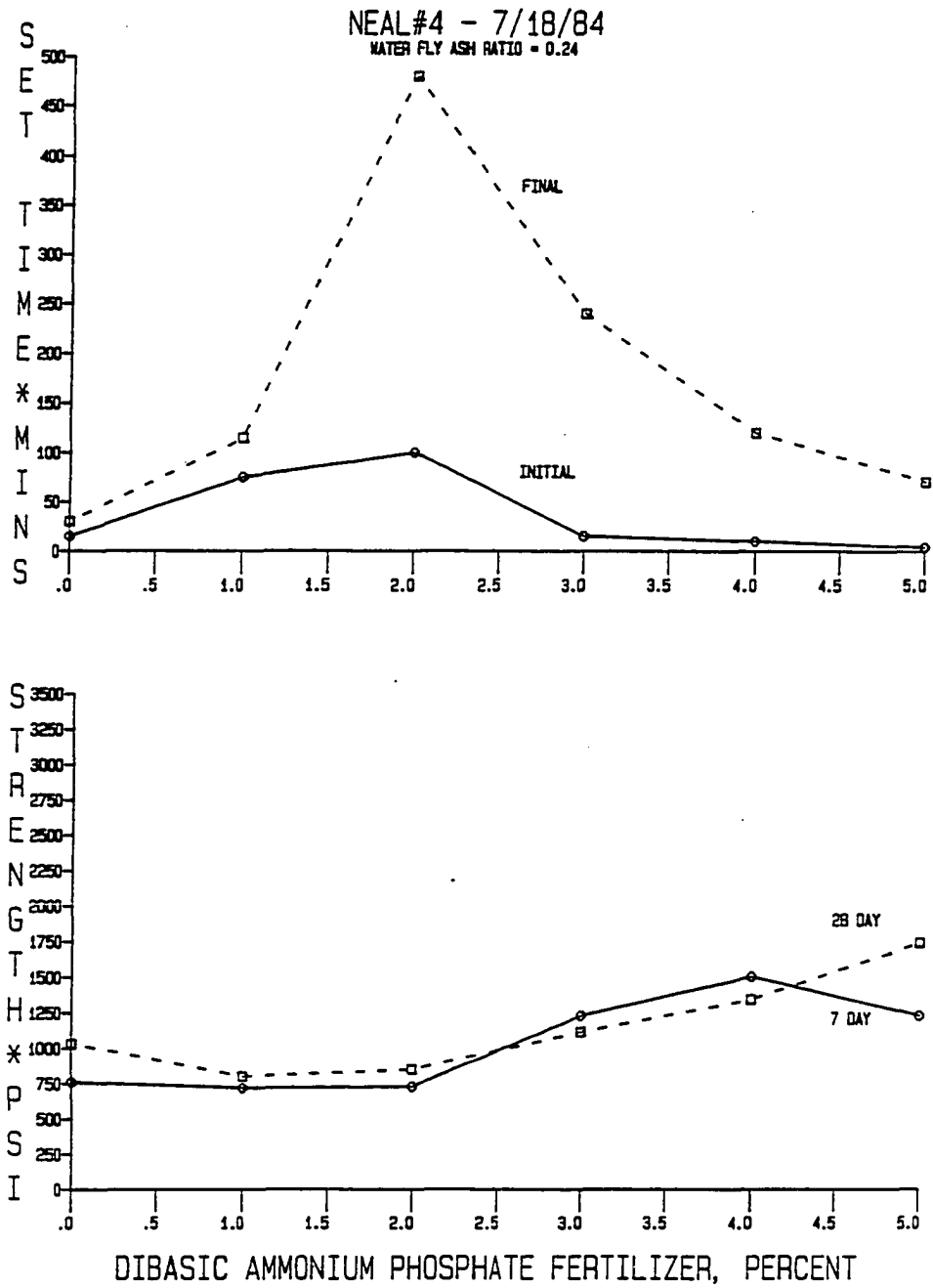


Figure 27. Set time and compressive strength of dibasic ammonium phosphate fertilizer and 7/18/84 Neal 4 fly ash

APF treatment of Neal 4 ash sampled on 7/18/84. The variation in response of the treated ashes from the same source but sampled at a different time is a cause for concern for their effective utilization. This variation in response will be discussed in detail under a following section on reaction mechanisms.

Ottumwa

Since ammonium nitrate was most effective with the Neal 2 ash and dibasic ammonium phosphate most effective with the Neal 4 ash the question arose as to which additive would be effective with ashes from other sources. For this phase of the study, fly ash from the Ottumwa generating station was selected. Its elemental and compound composition is an intergrade between Neal 2 and Neal 4 materials, but is more similar to the Neal 4 fly ash. Results of strength testing using reagent grade ammonium nitrate, showed a strength reduction with increased additive rate. Setting time was severely retarded past the 1 percent addition level. Similar trends were observed for fertilizer grade ammonium nitrate.

Reaction products were evaluated using x-ray diffraction. Results for untreated control and 5 percent reagent grade ammonium nitrate treated ash at about 130 days of age revealed that for the ammonium nitrate treated sample the characteristic hump produced by amorphous calcium aluminate silicate hydrate (CASH) and calcium aluminate hydrate (CAH)

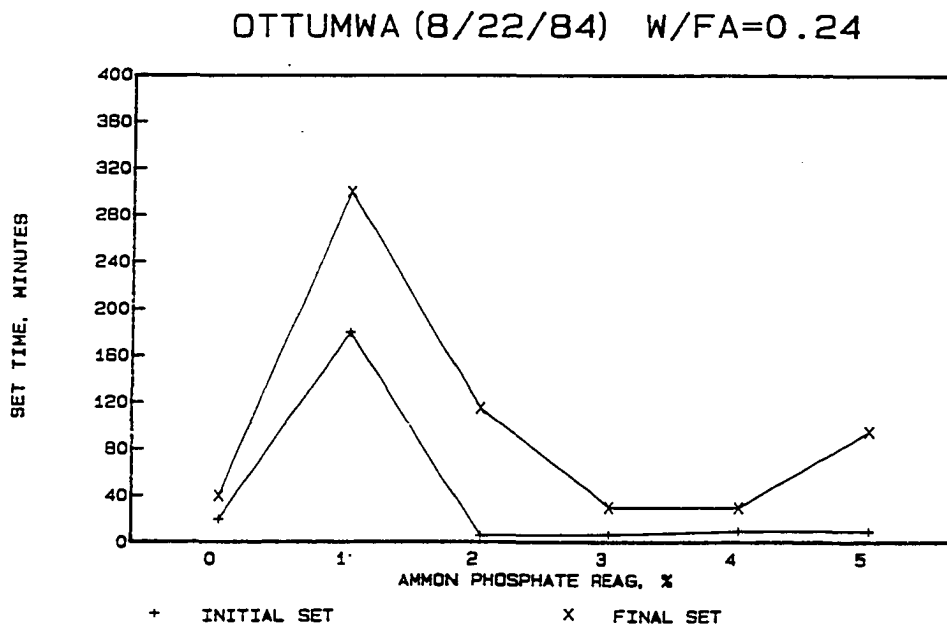
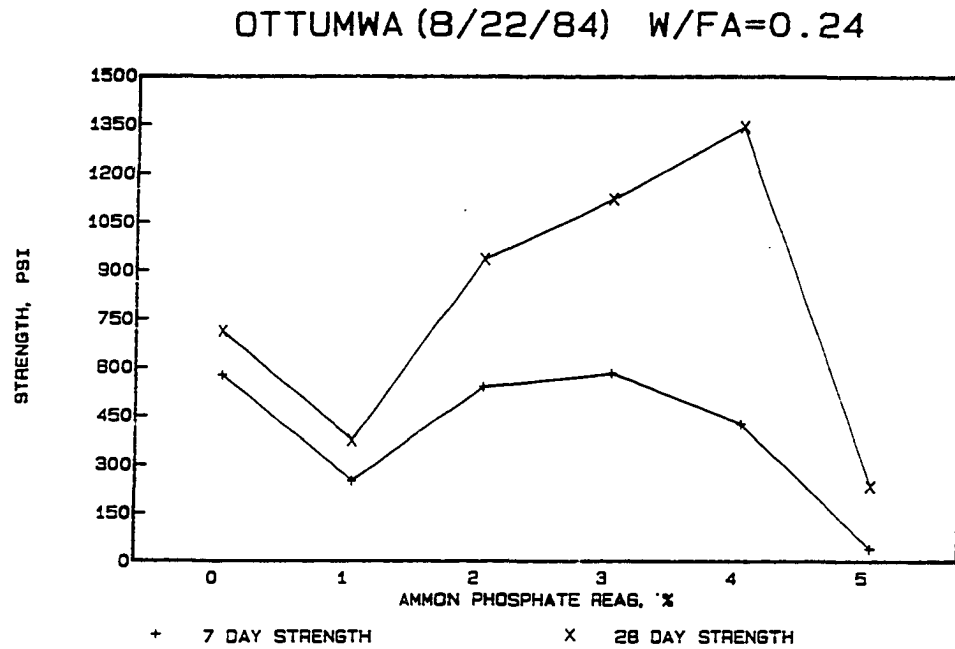


Figure 28. Set time and compressive strength of dibasic ammonium phosphate reagent and 8/22/84 Ottumwa fly ash

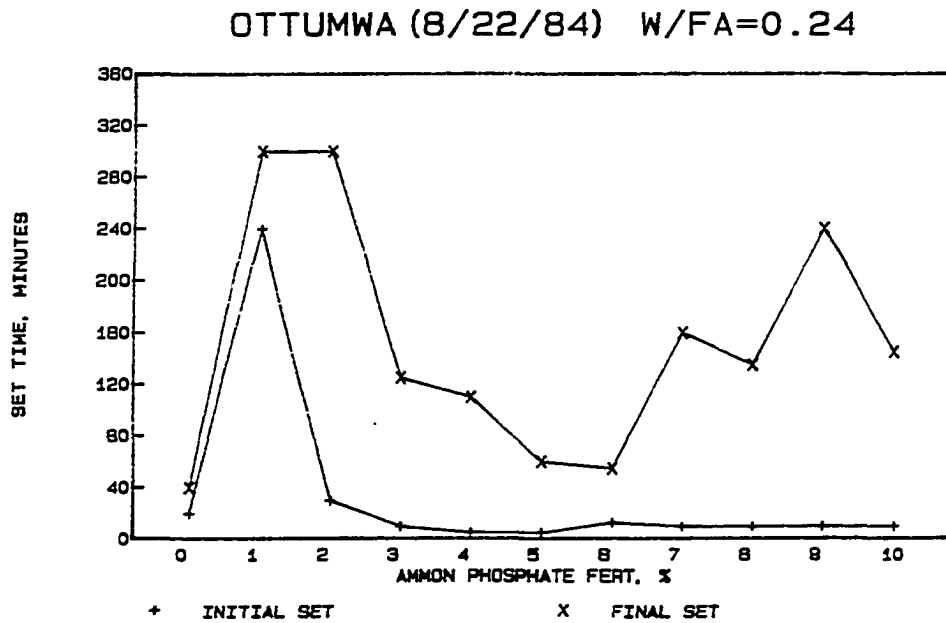
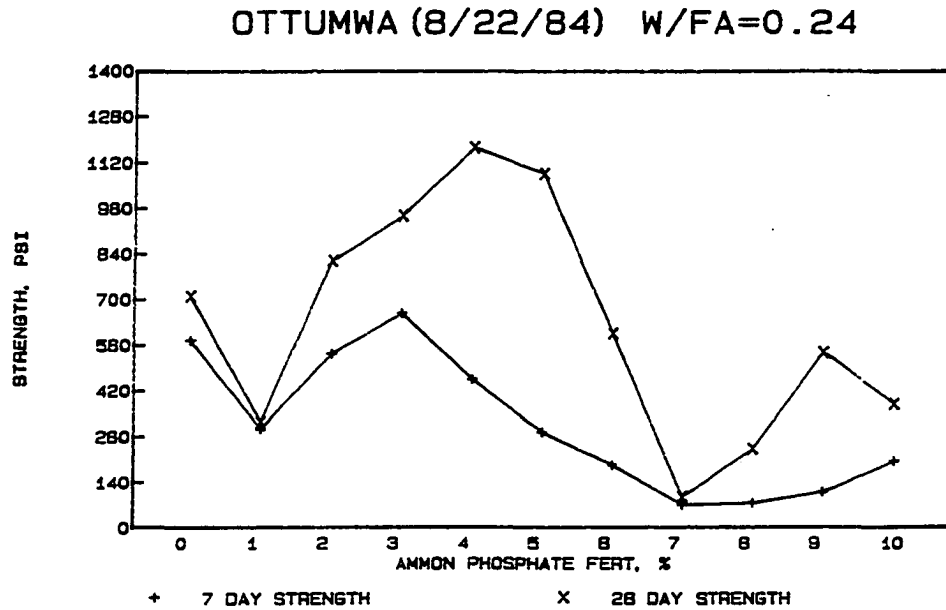


Figure 29. Set time and compressive strength of dibasic ammonium phosphate fertilizer and 8/22/84 Ottumwa fly ash

cementitious materials in the 9 to 11 degree two theta range were nearly absent. The hump produced by amorphous calcium silicate hydrate (CSH) cementitious materials in the 26 to 36 degree two theta range also appeared reduced. This indicated that the strength loss was apparently due to ammonium nitrate acting to severely reduce formation of cementitious reaction products in the Ottumwa fly ash.

Strength and setting properties of reagent grade ammonium phosphate treated Ottumwa ash are given on Figure 28. Strength decreased at a 1 percent addition level and increased to a maximum at a 4 percent treatment with strength enhanced by a factor of 1.9 times that of the untreated control. Set time was significantly retarded at the 1 percent treatment with final set values approaching that of the control at higher addition rates. Magnitude of strength enhancement and influence on setting properties were similar to those shown for the Neal 4 fly ash previously discussed.

Figure 29 presents the results of strength and setting times for fertilizer grade ammonium phosphate for additive rates up to 10 percent at a water fly ash ratio of 0.24. Strength trends were similar to reagent grade materials with a maximum developed at 4 percent treatment and a strength enhancement of 1.6 times that of untreated material. Set time trends were similar to reagent chemicals with the exception that final set was extended to

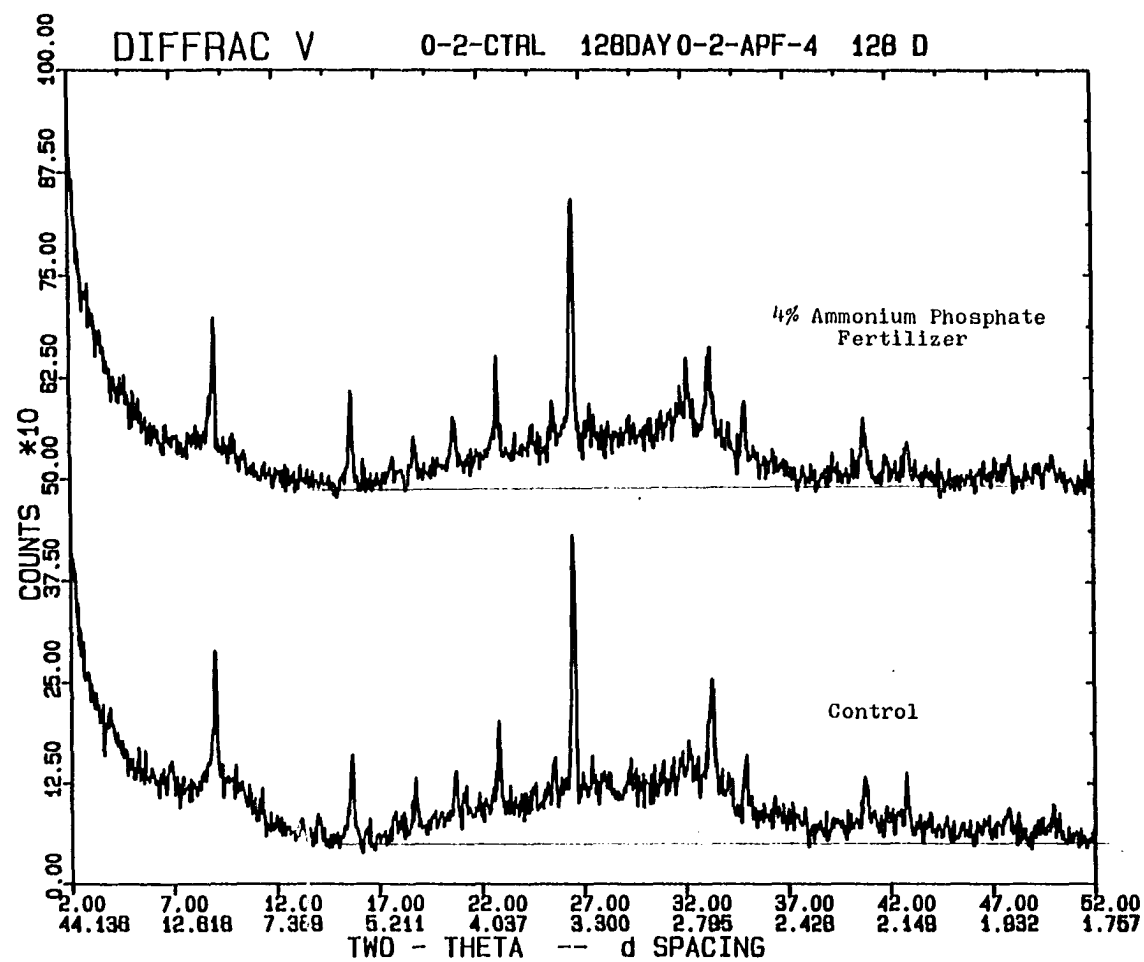


Figure 30. X-ray diffractograms of untreated and dibasic ammonium phosphate treated Ottumwa fly ash

approximately 55 minutes. These results indicate that the presence of the aluminum phosphate in the fertilizer grade ammonium phosphate chemical does not drastically alter strength enhancement and tends to retard final setting time. The retarding effect is desirable from a field application standpoint.

Diffraction traces for untreated and 4 percent ammonium phosphate treated materials at 0.24 water fly ash ratio are given on Figure 30. Previous work had shown that for ammonium nitrate treated fly ash a new unidentified cementitious compound was formed in the 10.4 angstrom range. For ammonium phosphate treated Neal 4 fly ash the formation of stratlingite was observed. From Figure 30, neither of these reaction products are evident. Intensity of crystalline compounds appear similar in magnitude. The CAH and CASH cementitious hump in the 9 to 11 degree two theta range appears reduced for the treated materials. The glassy halo produced by the glass phase of the fly ash in the 17 to 37 degree two theta range may be obscuring the detection of additional amorphous CSH cementitious materials that are generally recognizable by a hump in the background in the 26 to 36 two theta degree area. Careful examination, however, shows a shift of the halo from the 17-29 degree range to the 29-37 degree range with additional crystalization evident. This would seem to be the only reasonable explanation for the

strength increase observed. The differences in cementitious reaction products being developed between the ammonium phosphate treated Neal 4 and Ottumwa ash will be discussed in detail under the reaction mechanism section.

Summary

From this phase of the study, the following can be concluded.

1. Secondary chemical activators can be used to enhance compressive strength development by a factor of approximately 2 for high calcium ashes and factors of 5 to 6 times for intermediate calcium ashes.
2. Fertilizer grade chemical additives can be utilized.
3. Ammonium nitrate proved effective with the Neal 2 ash and dibasic ammonium phosphate proved effective with the Neal 4 and Ottumwa ashes for strength enhancement.
4. Secondary chemical activators can also be used to control setting properties. Ammonium nitrate acts to accelerate final setting time of Neal 2 ash while enhancing strength. Ammonium phosphate retards setting time of Neal 4 and Ottumwa ash with concurrent drop in strength depending on the amount of retardation desired.

REACTION MECHANISMS

Past research projects on Iowa fly ashes [29] and evaluation on the on-going ASTM C-618 data base from the Materials Analysis and Research Laboratory at Iowa State University has confirmed that the elemental composition of fly ash, from a given source, remains relatively consistent over time. This work had been initially predicated on the assumption that the physical properties of the fly ash from a given source would, therefore, also remain relatively consistent. As noted previously, however, the response to additive treatment of the Neal 4 ash varied widely depending on the date the ash was sampled. In order to formulate reasonable conclusions regarding effects of additive treatment and reaction mechanisms, it was first necessary to gain some insight into this behavior. It was observed that the untreated control strength of Neal 4 ash varied considerably for the same water fly ash ratio of fly ash sampled from the same source, but at different times. The additive variability effect is summarized for strength development of the Neal 4 fly ash on Figure 31, the upper half depicting 7 day strength gain and the lower half the 28 day strength response. The legend dates are the dates that samples of the ash were obtained for use in this study.

With respect to the 28 day strength values shown on the lower half of Figure 31, the following table summarizes

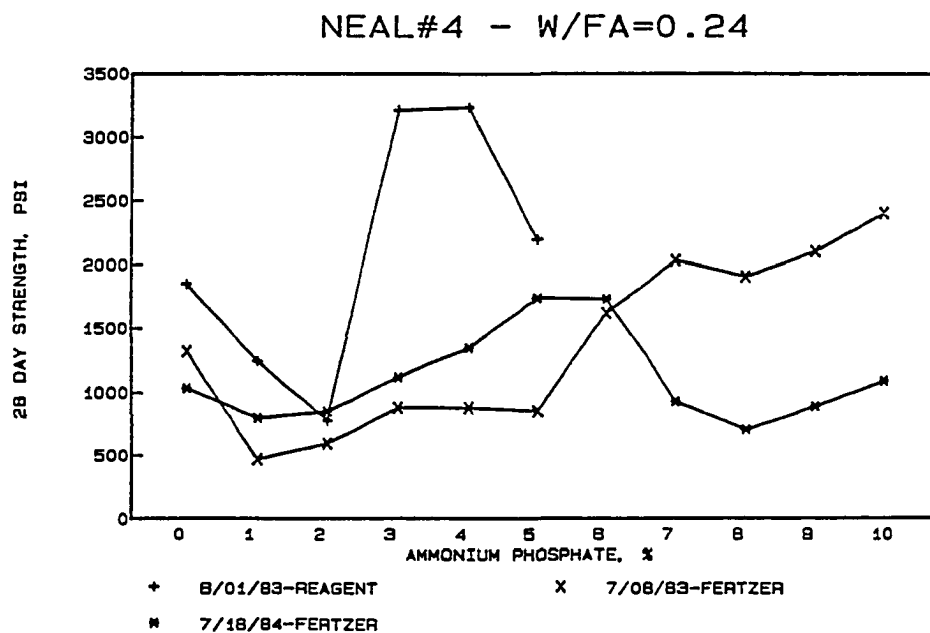
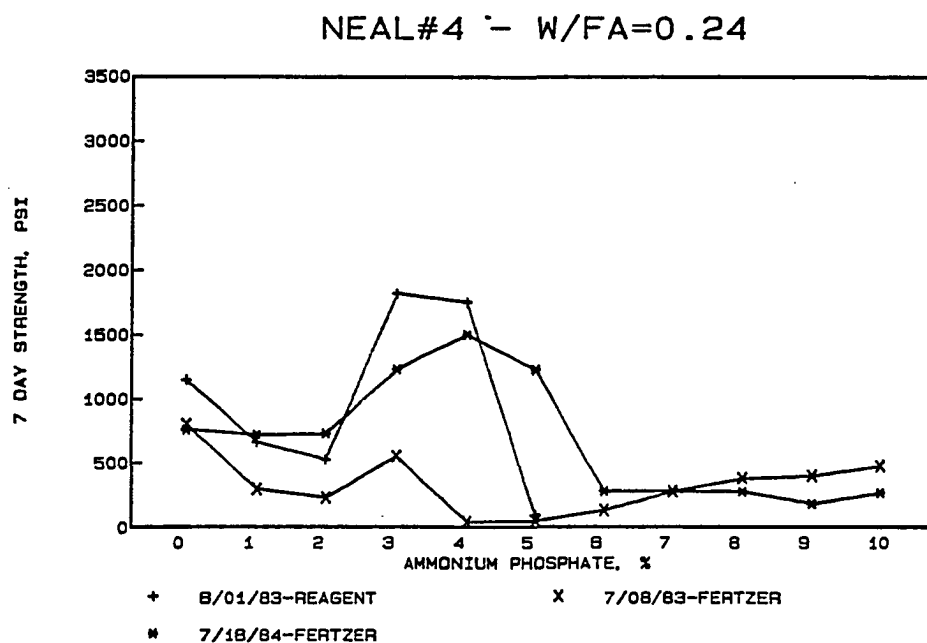


Figure 31. 7 day and 28 day compressive strength development of dibasic ammonium phosphate treatment of Neal 4 fly ashes

untreated and treated 28 day strength. The untreated control strengths are the average of at least 18 tests made in sets of six periodically. The treated results are usually the average of 6 tests unless sample damage was evident.

Table 9. Strength summary - Neal 4 fly ash, 28 day age

<u>Date Sampled</u>	<u>Untreated Control (psi)</u>	<u>Optimum Additive Rate %</u>	<u>Optimum Strength (psi)</u>	<u>Strength Gain Ratio</u>
6/01/83	1850	3-4	3250	1.8
7/08/83	1240	10	2400	1.9
7/18/84	1030	5-6	1740	1.7

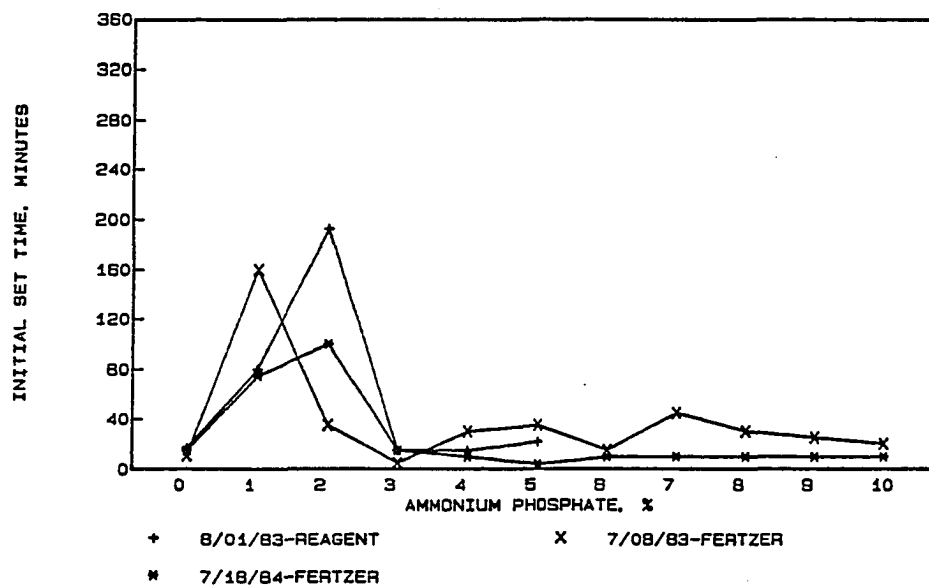
From Table 9, it is noted that the untreated control strength of the Neal 4 fly ash varied from a low of 1030 psi to a high of 1850 psi. Although not directly comparable since the 6/01/83 material was treated with reagent grade chemicals only, the strength gain achieved with chemical treatment appears to vary directly with untreated strength at an average gain ranging from 1.7 to 1.9 times that of the controls. The optimum additive rate to achieve this, however, appears to vary considerably for an ash from the same source especially comparing the response to fertilizer treatment of the 7/08/83 and 7/18/84 ash samples.

Setting properties of the Neal 4 untreated and treated fly ash are given on Figure 32. In general, the trends are similar for initial set time with a retarding effect at 1 to 2 percent addition levels and a concurrent drop in 7 and 28 day strengths as noted on Figure 31. The final set trends of the ashes are similar up to the 4 to 5 percent addition level.

In order to evaluate the cause of the varying untreated and treated strengths and variation in setting properties observed for the Neal 4 ash, elemental and compound analysis were conducted. Table 10 summarizes these data.

What is interesting from the data given on Table 10 is that from an elemental analysis standpoint, the ash from the Neal 4 plant does not appear to vary considerably with sampling date. The compound analysis data however, indicates the ash sampled on 7/18/84 contains approximately 22 percent crystalline compounds compared with 31 percent crystalline compounds for the 6/01/83 ash sample. Correspondingly, the 7/18/84 ash is estimated to be 78 percent glass while the 6/01/83 ash is approximately 69 percent glass. The average composition of the glassy phase appears to remain relatively consistent and may be independent of sampling date. The data in Table 10 and the foregoing discussion imply that for the Neal 4 fly ash, elemental composition and average composition of the glassy phase does not appear to vary substantially

NEAL#4 - W/FA=0.24



NEAL#4 - W/FA=0.24

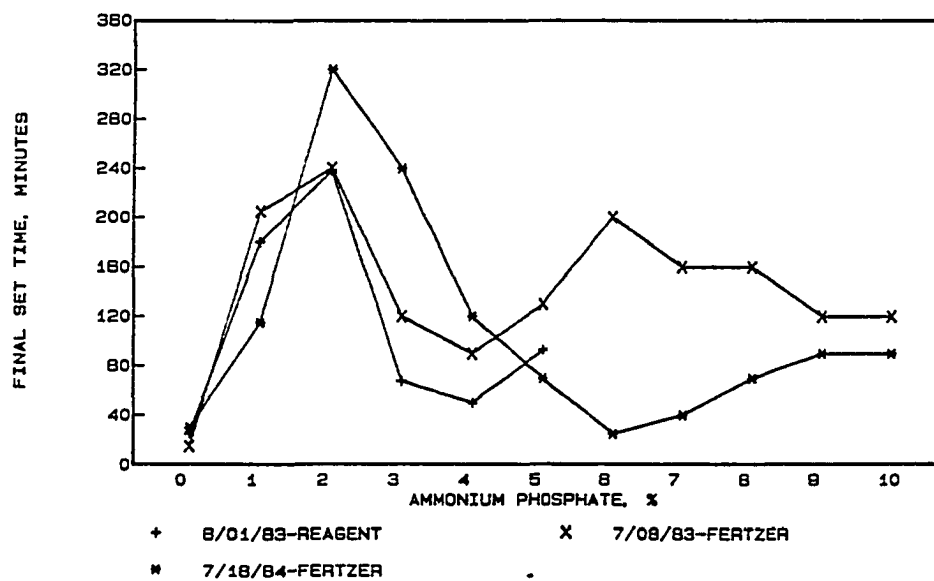


Figure 32. Initial and final set times of dibasic ammonium phosphate treatments of Neal 4 fly ashes

Table 10. Elemental and compound composition of Neal 4 ash

	Dates Sampled		
	6/01/83	7/08/83	7/18/84
<u>Elemental Analysis</u>			
Silicon Oxide	36.09	39.91	34.66
Aluminum Oxide	15.49	16.59	16.61
Iron Oxide	6.22	5.37	5.88
Total	57.80	61.87	57.15
Magnesium Oxide	5.98	5.71	6.00
Calcium Oxide	26.16	24.01	25.73
Titanium Oxide	1.07	1.05	1.13
Sulphur Trioxide	3.65	2.23	3.21
Phosphorous Pentoxide	0.69	0.71	1.29
Potassium Oxide	0.28	0.43	0.30
Sodium Oxide	2.09	2.19	2.38
Total	97.72	98.20	97.20
<u>Compound Analysis</u>			
Mullite	0.6	2.7	1.4
Quartz	9.9	10.1	7.2
Ca. Alum. Sulphate	1.3	0.2	1.4
Calcium Sulphate	3.1	1.6	3.2
Magnetite	5.7	2.4	4.0
Calcium Oxide	1.1	0.5	0.7
Magnesium Oxide	4.6	2.6	2.8
Tricalcium Alum.	4.3	3.4	1.0
Total	30.6	23.4	21.7
Percent Glass	69.4	76.6	78.3
<u>Glass Composition</u>			
Silicon Oxide	26	29	27
Aluminum Oxide	13	13	14
Calcium Oxide	21	21	23
Magnesium Oxide	1.4	3.1	3.2

with time. The ratio of the amount of crystalline compounds and amount of glass, however, may change. If it is then assumed that crystalline compounds present in fly ash are available and responsible for initial and short term hydration reactions then the presence of an increased total and individual amount of crystalline compounds would be important.

The fluctuation in compressive strength and reaction product development, noted for the Neal 4 ashes of similar elemental composition but sampled at different dates, makes it difficult to interpret the effects and reaction mechanisms associated with incorporation of secondary chemical activators in the system. It is also a cause for concern regarding practical engineering application in the use of fly ash for soil and subbase stabilization either in a treated or untreated condition.

In order to investigate this further, a series of experiments were initiated with the Ottumwa fly ash using the Materials Research and Analysis library of small samples of fly ash received during 1985. The size of the samples was limited, therefore, special molds were fabricated to form 1"x1"x1" cubes of the paste mixes for compressive strength testing. Sealed vial samples were also made for reaction product evaluation. All samples were prepared at a water to fly ash ratio of 0.27. A series of five Ottumwa ash samples

obtained at various dates in 1985 were selected for testing. Results of compressive strength testing shown on Figure 33 showed extreme variations in strength ranging from 600 psi to 5200 psi at 28 days. This was particularly disturbing since elemental composition of the ashes are very similar. The high strength and low strength raw fly ash samples were tested by XRD and results given on Figure 34a. This again was found disturbing, for there were no significant differences readily apparent in crystalline compounds or the glass. However, XRD analysis of hydrated samples given in Figure 34b produced very interesting results clearly indicating that in the high strength sample the glassy halo was significantly reduced upon hydration. This implies that the dissolution of the glassy phase and reformation of the disassociated elements into cementitious materials were responsible for the strength differential. It is also obvious that there are significant differences in the type of reaction products occurring in the 7 to 11 two theta degree range. The results of these significant findings formed the basis for a research proposal submittal to, and acceptance by, the Iowa Highway Research Board.

The foregoing discussion is being included in this section because it is the writer's opinion that in order to develop a meaningful explanation of the reaction mechanisms of including secondary chemical activators into the fly ash

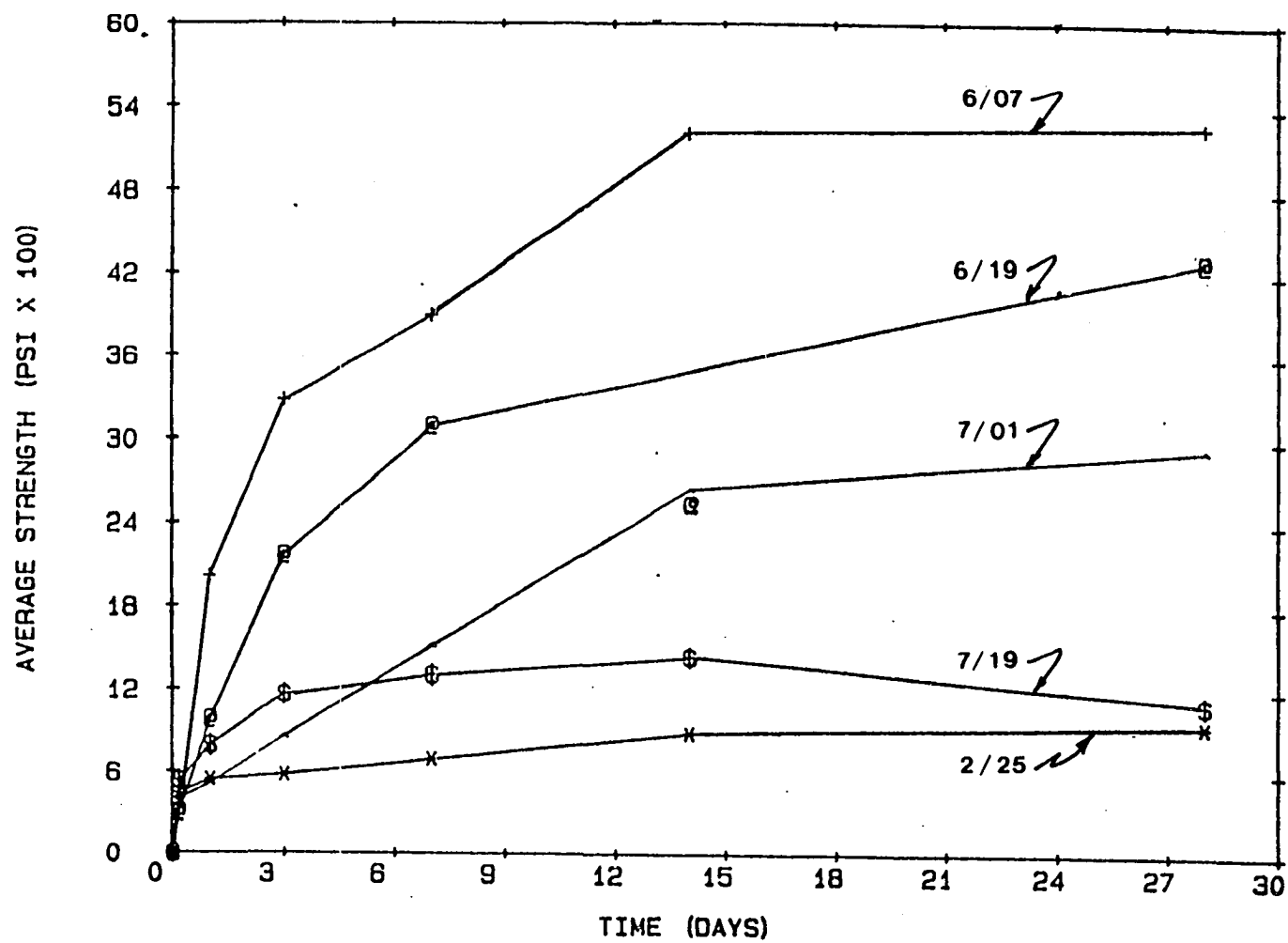


Figure 33. Compressive strength variation of Ottumwa fly ash sampled at different times

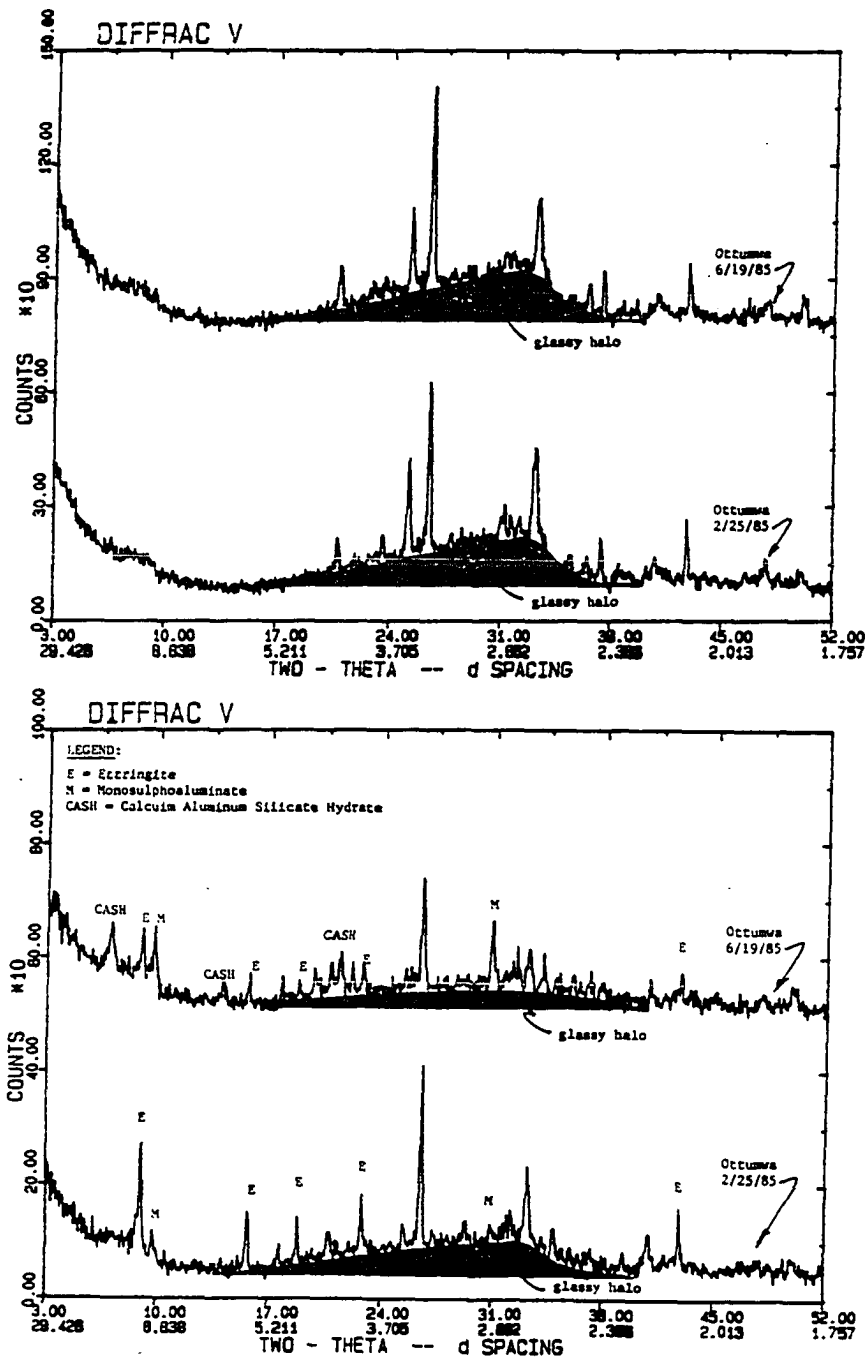


Figure 34. X-ray diffractograms of raw and hydrated Ottumwa fly ashes

system it is first necessary to have some understanding of the reaction mechanisms of the fly ash system itself. This is an extremely complex subject of which little is yet known and extensive additional investigations are needed. It is the writer's opinion, at present, that it is extremely important to our understanding of the system and perhaps can provide some clues to the reaction mechanism involved with secondary chemical activators.

To provide some additional insight into the Ottumwa ash behavior, and possible reasons for it, three of the ashes exhibiting low, medium, and high strength in the previous work were selected for additional indepth study.

Figure 35 presents compressive strength development curves for the three Ottumwa ashes. Table 11 presents elemental, compound, and glassy phase compositions for the low and high strength ash and shows the similarity in elemental composition (expressed as oxides).

Figures 36 through 39 show XRD diffractograms for hydrated samples of the three ashes at various ages. Analysis of these figures show that what is believed to be stratlingite was formed in the 6/07 ash and in addition to this, ettringite which was initially formed in all three ashes at one day of age was converted to monosulfoaluminate. This also occurred in the 7/08 (medium strength) ash but to a lesser extent. The 2/25 ash showed little to no evidence of

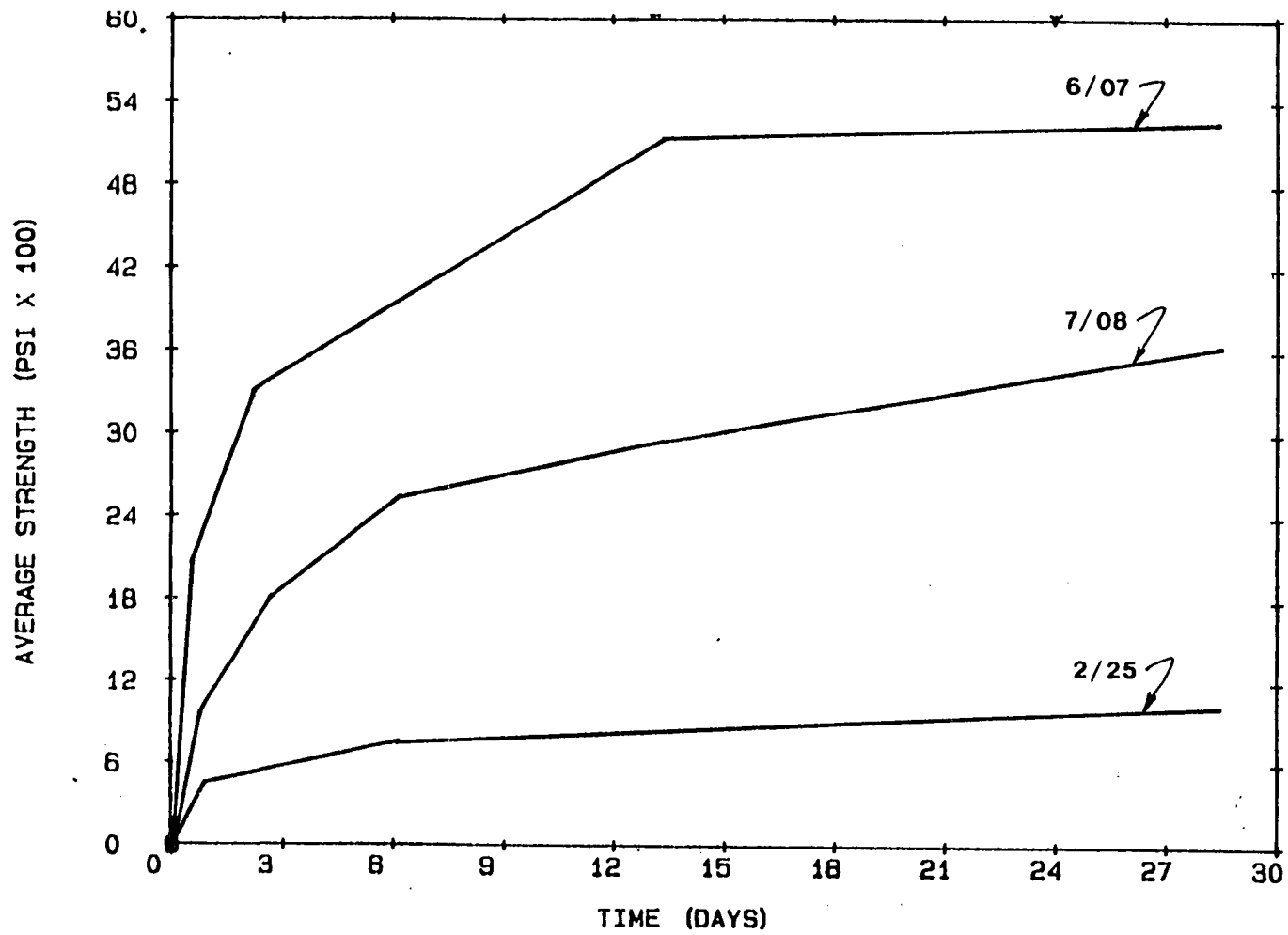


Figure 35. Compressive strength development of Ottumwa fly ashes

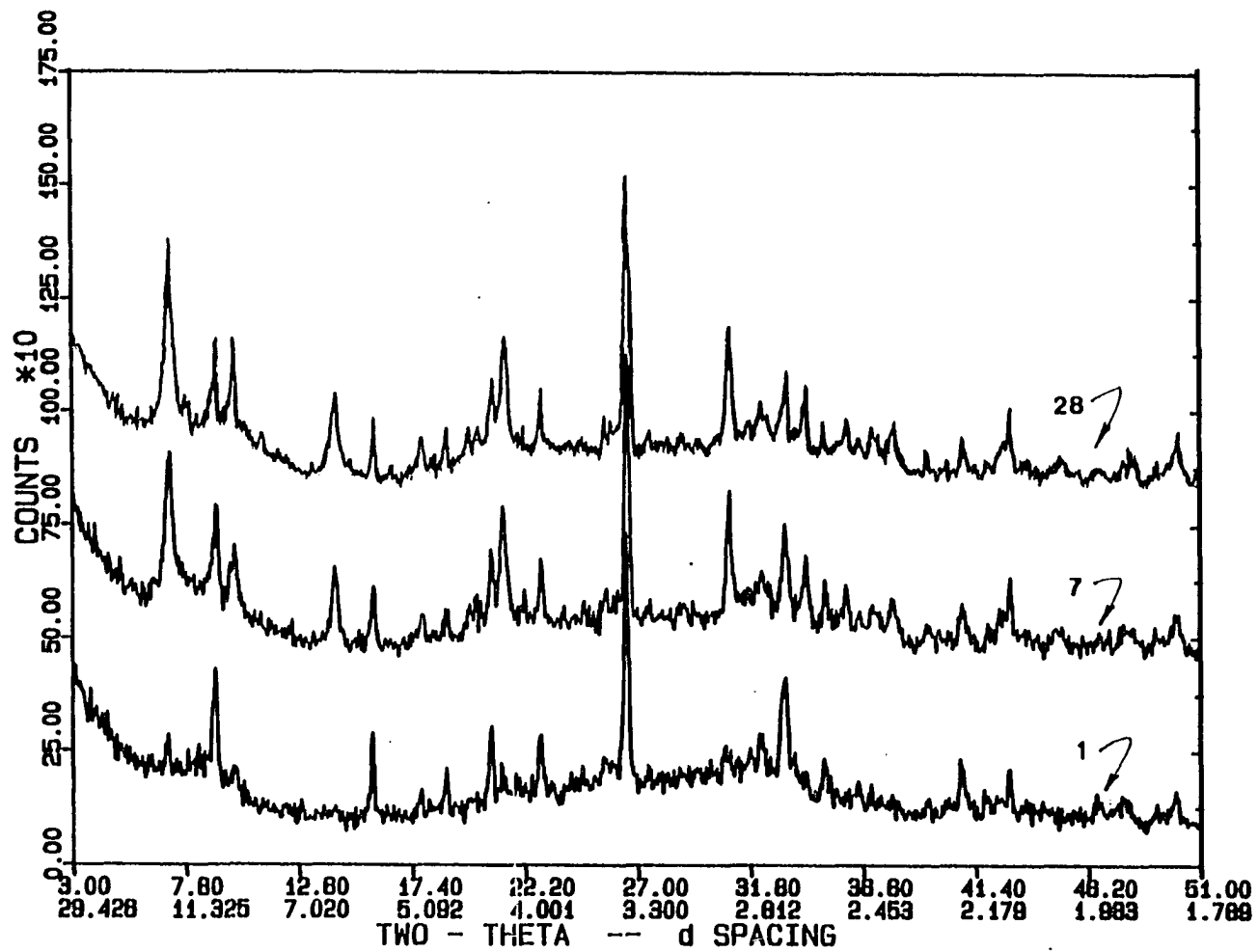


Figure 36. X-ray diffractograms of 6/07/85 hydrated Ottumwa fly ash

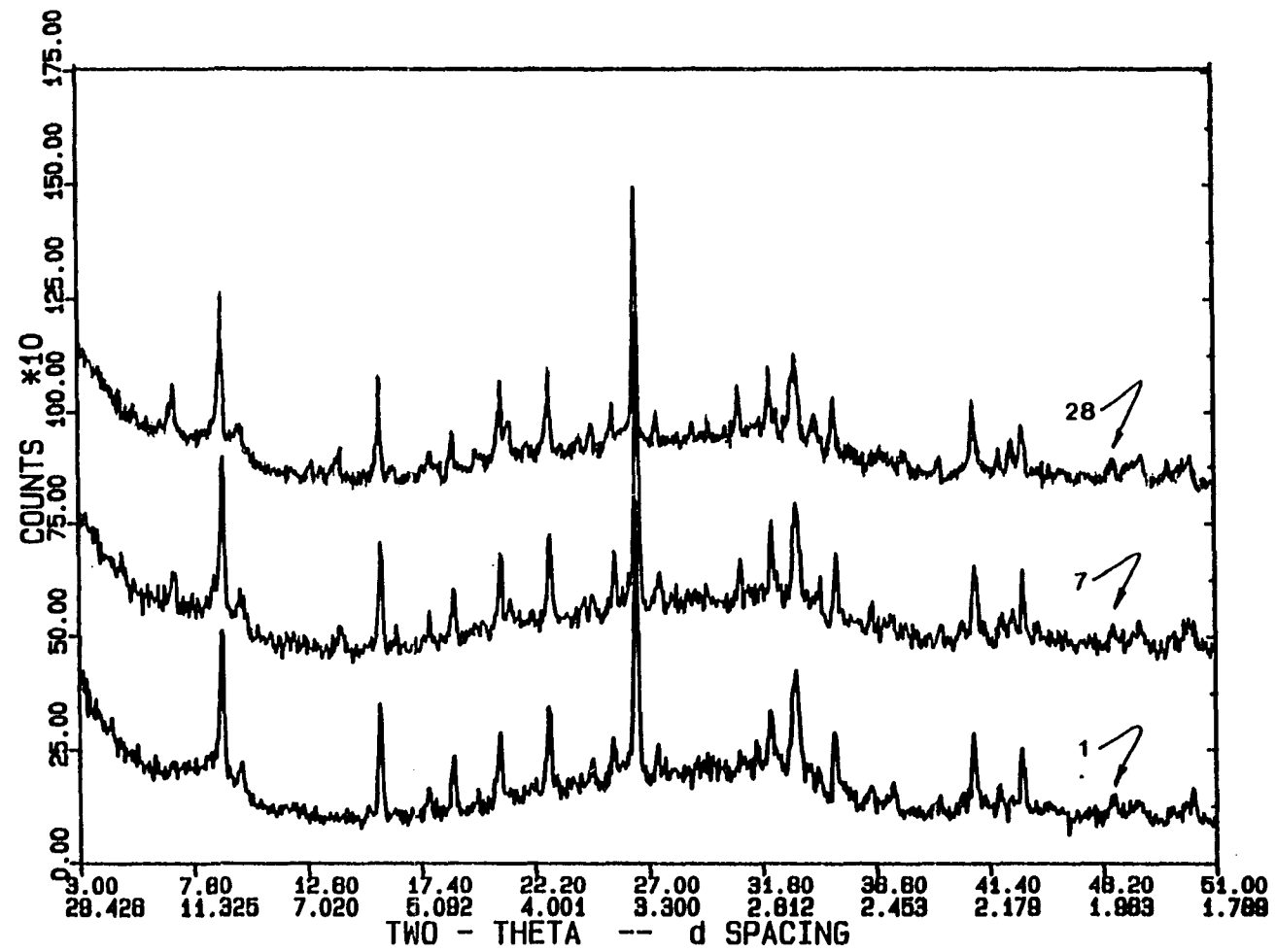


Figure 37. X-ray diffractograms of 7/08/85 hydrated Ottumwa fly ash

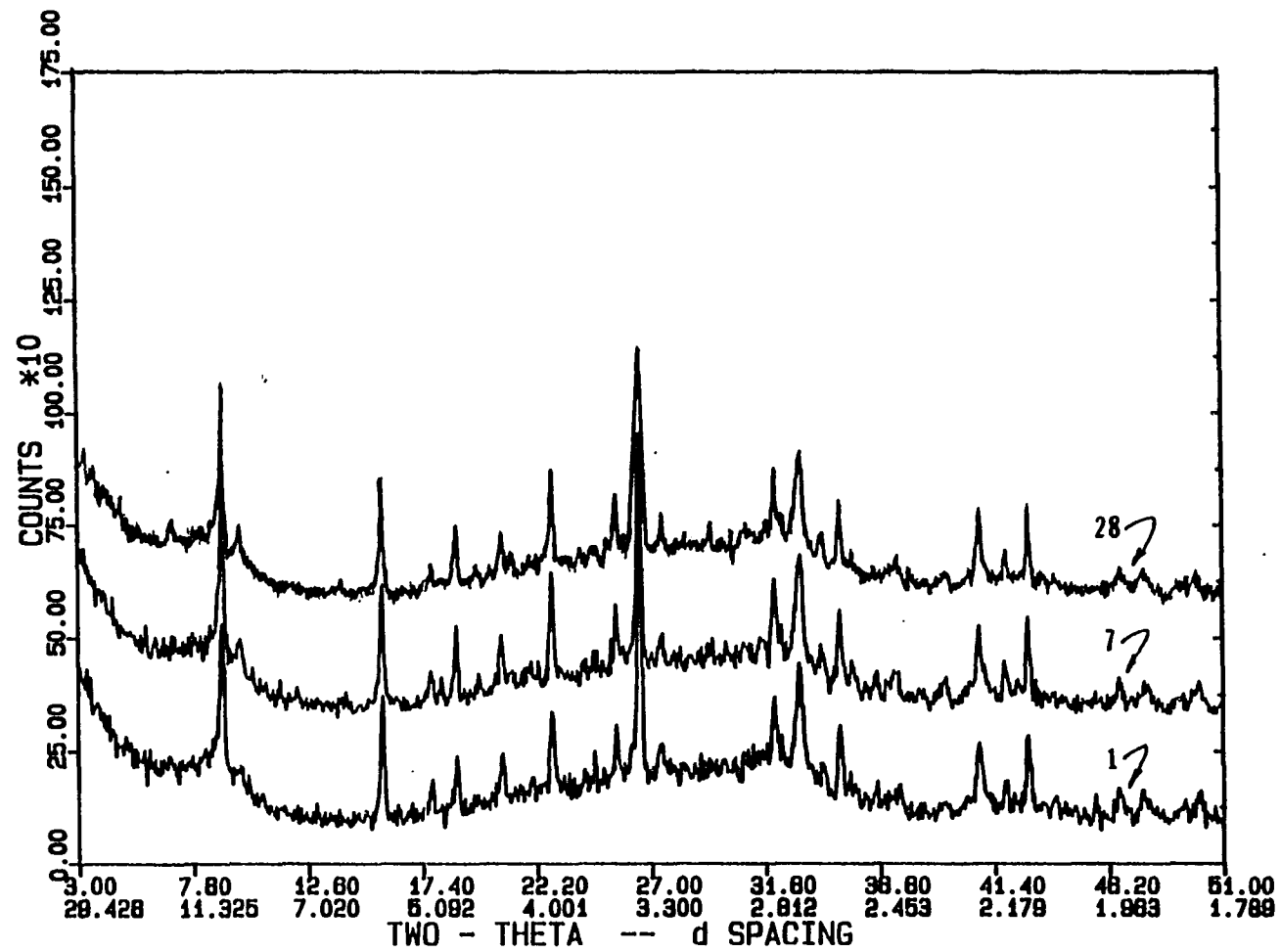


Figure 38. X-ray diffractograms of 2/25/85 hydrated Ottuwma fly ash

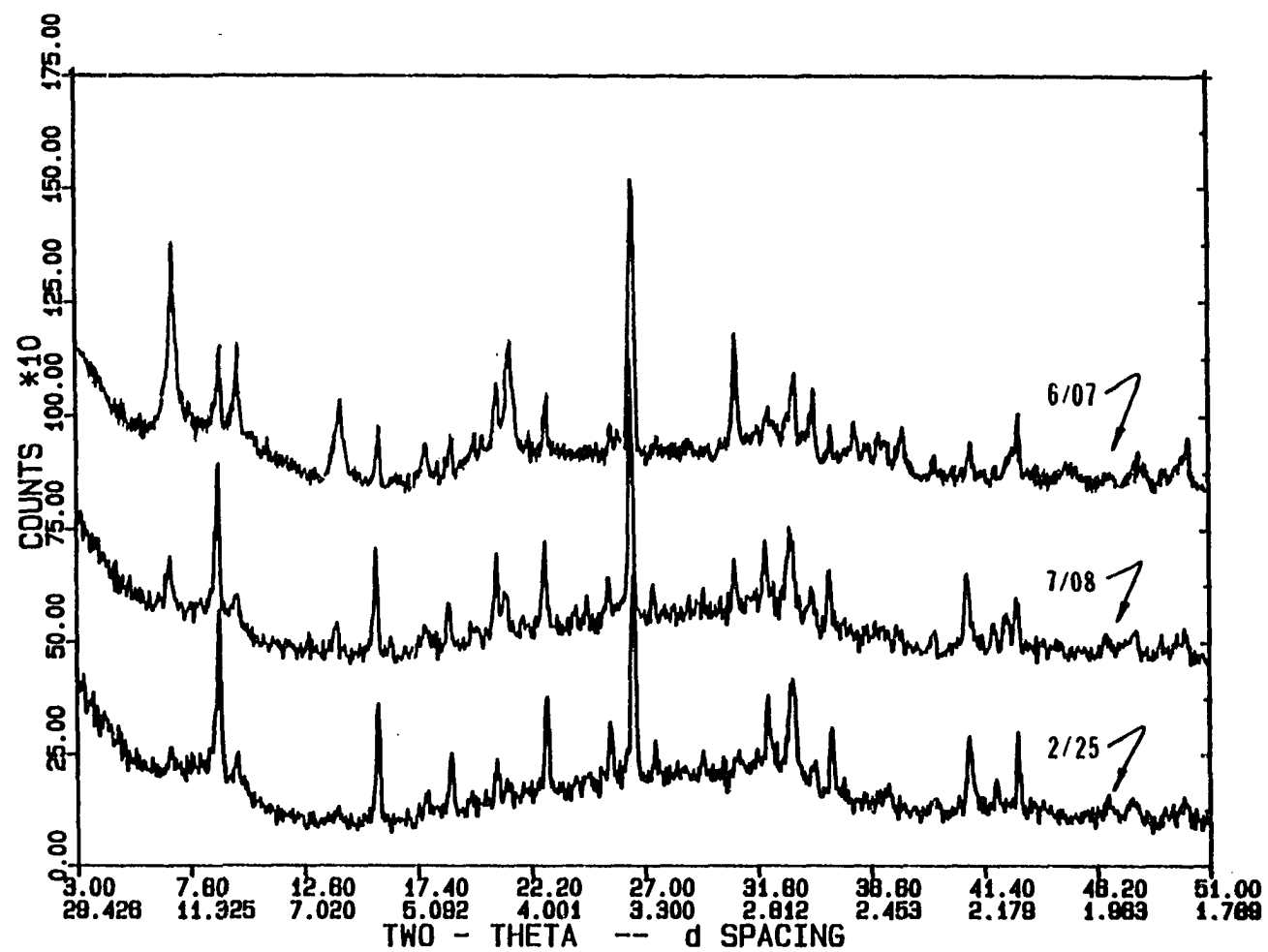


Figure 39. X-ray diffractograms comparing reaction products at 28 days for Ottumwa fly ashes

Table 11. Chemical composition of Ottumwa ash

<u>Elemental Composition (as oxides)</u>		<u>2/25/85</u>	<u>6/07/85</u>
SiO ₂		32.7	31.8
Al ₂ O ₃		19.0	19.0
Fe ₂ O ₃		5.5	6.5
CaO		26.3	27.6
MgO		4.9	4.6
K ₂ O		1.1	2.0
Na ₂ O		2.8	1.8
TiO ₂		1.1	1.1
SO ₃		3.2	2.4
<u>Crystalline Compound Composition</u>			
Lime		1.7	0.5
Quartz		2.8	6.6
Tricalcium aluminate		2.9	4.4
Anhydrite		3.5	1.4
Periclase		3.9	1.7
<u>Glass Composition (as oxides)</u>			
SiO ₂		25.2	29.8
Al ₂ O ₃		17.9	17.3
CaO		21.3	23.8
MgO		1.0	2.8
Total		65.4	73.7

stratlingite formation. It is recalled that in dibasic ammonium phosphate treatment of Neal 4 ash, which resulted in increased strength, stratlingite was also identified. The presence of stratlingite is believed to be the principal reason for the differences in strength noted for the Ottumwa samples. The hydration of tricalcium aluminate involves reactions with sulphate ions present in the system. The

sulphate ions are believed to be supplied principally by anhydrite and the resultant reaction product is ettringite. Ettringite is stable only if there is an excess supply of sulphate ions in the hydrating system. If the supply of sulphate ions is depleted before the hydration of all the tricalcium aluminate, then ettringite undergoes a transformation into monosulfoaluminate. From Table 11, the molar ratios of anhydrite to tricalcium aluminate for the 6/07 ash is 0.64 and for the 2/25 ash is 2.4. Therefore, ettringite would be expected to be a stable reaction product in the 2/25 ash. This is confirmed by Figure 38. Figure 36 for the 6/07 ash shows the reduction in ettringite, with time, and the conversion to monosulfoaluminate.

Reviewing the data of Table 11, it is seen that the composition of the glassy phase is similar between the two ashes. The modifier/former ratio is 0.52 and 0.56, respectively, for the 2/25 and 6/07 ashes which implies similar reactive states. The difference between the ashes is the amount of glass present. The relative difference in the type and amount of calcium bearing crystalline compounds present and the amount of glass present is believed to be the cause of the strength variations.

Considering the foregoing, it is apparent that the hydraulic properties of a fly ash is both a function of the crystalline phases present, and type and amount of glass

present. Although much more research is needed, it would seem possible to develop a "hydraulic reactivity index" for fly ashes. The "hydraulic reactivity index" is envisioned as being a function of both the type and amount of calcium bearing crystalline compounds present, and the amount and reactivity of the glassy phase. The ratio of anhydrite to tricalcium aluminate may be an appropriate indicator of the crystalline phase reactivity. The index might be a function of the ratio of anhydrite/tricalcium aluminate times the weight percent of crystalline calcium bearing compounds plus the reactivity index of the glassy phase times the weight percent of glass present.

CONCLUSIONS

It is proposed that the reactivity of the glassy phase of Iowa fly ashes can be characterized by a reactivity index which is the ratio of modifiers to formers expressed by $(\text{CaO}+\text{MgO})/(\text{SiO}_2+\text{Al}_2\text{O}_3)$ in the glass. It has been shown that this relationship is nearly linear to this same ratio based on elemental composition which allows a rapid evaluation of reactivity based on ASTM C-618 analysis.

It has been shown that the elemental analysis consistency of Iowa ashes, from a given generating station, is not a valid indicator of its fundamental physical properties. The variability in physical properties (e.g., compressive strength development, setting time, etc.) has been shown to be a function of the amount of calcium bearing crystalline compounds present and correspondingly, the amount of reactive glass present. The critical point being that when water is introduced into the system then the hydrous solution formed must be both capable of dissolution of the glassy phase and provide for concurrent reformation of dissolved elements into cementitious products. If this occurs then this in turn depletes the hydrous solution of those elements and allows for further attack and dissolution of the glassy phase.

It has been shown that for a high calcium ash, from a given generating station, that the glassy phase is an integral and necessary contributor to early (28 day strength)

gain.

The hypothesis that addition of minute amounts of secondary chemical additives can enhance cementitious reaction product development has been demonstrated. It is believed that the dibasic ammonium phosphate additive acts to enhance dissolution of the glassy phase of high calcium, Iowa ashes possibly by complex formation and to "seed" cementitious reaction product development possibly by activating tetrahedral coordination.

BIBLIOGRAPHY

1. Benton, Elton J. "Cement-Pozzolan Reactions." Highway Research Board Bulletin 239, (1960), 56-65.
2. Bergeson, K. L., J. M. Pitt and T. Demirel. "Increasing Cementitious Products of a Class C Fly Ash." Transportation Research Record No. 998, July 1985.
3. Buri, A., F. Branda, D. Caferri and A. Marotta. "Structure and Devitrification Behavior of $\text{CaO-Al}_2\text{O}_3\text{-SiO}_2$ Glasses." Silicates Industriels, 3 (1981), 59-63.
4. Daugherty, K. E., B. Saad, C. Weirich and A. Eberendu. "The Glass Content of Slag and Hydraulic Activity." Silicates Industriels, 4-5 (1983), 107-110.
5. Diamond, Sidney. "The Characterization of Flyashes." In Proceedings Symposium N, Effects of Fly Ash Incorporation in Cement and Concrete. Editor S. Diamond. University Park, Pennsylvania: Materials Research Society, 1982, pp. 12-23.
6. Diamond, Sidney. "On the Glass Present in Low-Calcium and High Calcium Flyashes." Cement and Concrete Research, 13 (1983), 459-464.
7. Diamond, S. "Characterization and Classification of Flyashes in Terms of Certain Chemical and Physical Parameters." In International Symposium on the Use of PFA in Concrete, 2. Editors J. Cabrera and A. Cusens. Leeds, England: University of Leeds, April 1982, pp. 9-22.
8. Diamond, Sidney and Federico Lopez-Flores. "On the Distinction in Physical and Chemical Characteristics Between Lignitic and Bituminous Fly Ashes." In Proceedings Symposium N, Effects of Fly Ash Incorporation in Cement and Concrete. Editor S. Diamond. University Park, Pennsylvania: Materials Research Society, 1982, pp. 34-44.

9. Dunstan, E. R., Jr. "A Possible Method for Identifying Fly Ashes That Will Improve the Sulphate Resistance of Concretes." Cement Concrete and Aggregates, 2, No. 1 (1980), 20-30.

10. Engelhardt, G., M. Nofz, K. Forkel, F. Wihsmann, M. Magi, A. Samoson and E. Lippmaa. "Structural Studies of Calcium Aluminosilicate Glasses by High Resolution Solid State Si and Al Magic Angle Spinning Nuclear Magnetic Resonance." Physics and Chemistry of Glasses, 26, No. 5 (October 1985), 157-165.

11. Faber, J. H. and H. T. Stirling. "Coal and Ash Characteristics That Affect the Use of Pozzolans in the United States." In International Symposium on the Use of PFA in Concrete. Editors J. Cabrera and A. Cusens. Leeds, England: University of Leeds, April 1982, pp. 23-33.

12. Gibbon, D. L. "Microcharacterization of Fly-Ash and Analogs: The Role of SEM and TEM." Scanning Electron Microscopy, 2 (1979), 501-510.

13. Idorn, G. M. "30 Years With Alkalies in Concrete." Keynote address to Alkalies in Concrete Research and Practice. Copenhagen, (June 1983).

14. Idorn, G. M. "International Aspects of Development of the Uses of Fly Ash with Cement." In Proceedings Symposium N, Effects of Fly Ash Incorporation in Cement and Concrete. Editor S. Diamond. University Park, Pennsylvania: Materials Research Society, 1982, pp. 244-259.

- 14a. Iowa Department of Transportation. Fly ash monitoring data base. Iowa Highway Research Board Project HR-260.

15. Johansson, Sven-Erik. "Relation Between Strengths of Slag Cement and Properties of Slag." Silicates Industriels, 7-8 (1978), 139-143.

16. Joshi, R. C. and M. A. Ward. "Cementitious Flyashes-Structural and Hydration Mechanism." In CRI Abstracts of Seventh Intern. Cong. on the Chem. of Cement, October 1980, pp. 87-88.

17. Joshi, R. C., G. S. Natt, R. L. Day and D. D. Tilleman. "Scanning Electron Microscopy and X-Ray Diffraction Analysis of Various Size Fractions of Fly Ash." Fly Ash and Coal Conversion By-Products: Characterization, Utilization and Disposal I, 43. Editors G. J. McCarthy and R. L. Lauf. Pittsburgh: Materials Research Society, 1985, pp. 32-39.

18. Kingery, W. D. Introduction to Ceramics. New York: John Wiley and Sons, Inc., 1960.

19. Lee, Chau, S. Schlorholtz and T. Demirel. "Available Alkalis in Fly Ash." University Park, Pennsylvania: Materials Research Society, 1986, in publication.

20. Litvan, G. G. "Volume Instability of Porous Solids. Part 2. Dissolution of Porous Silica Glass in Sodium Hydroxide." Journal of Materials Science, 19 (1984), 2473-2480.

21. Locher, F. W. "Hydraulic Properties and Hydration of Glasses of the System $\text{CaO-Al}_2\text{O}_3\text{-SiO}_2$." In Proceedings of Fourth International Symposium on the Chemistry of Cement, Monograph No. 43. Washington, D. C.: U. S. National Bureau of Standards, 1960, pp. 267-276.

22. Malek, R. I. A. and D. M. Roy. "Electrokinetic Phenomena and Surface Characteristics of Fly Ash Particles." Fly Ash and Coal Conversion By-Products: Characterization, Utilization and Disposal I, 43. Editors G. J. McCarthy and R. L. Lauf. Pittsburgh: Materials Research Society, 1985, pp. 41-50.

23. Mather, Kathanne, C. R. Hallford, J. P. Burkes and A. D. Buck. "Investigation of Cement Pastes and Related Materials by Scanning Electron Microscopy and X-Ray Diffraction." U.S. Army Waterways Experiment Station, Vicksburg, Mississippi, Miscellaneous Paper SL-83-6, May, 1983.
24. Mehta, P. K. "Pozzolanic and Cementitious By-Products as Mineral Admixtures for Concrete - A Critical Review." ACI Special Publication No. 79, 1983.
25. Mings, M. L., S. Schlorholtz, J. M. Pitt and T. Demirel. "Characterization of Fly Ash by X-ray Analysis Methods." Transportation Research Record No. 941, 1983, 5-11.
26. Mitchell, Richard S. and H. J. Gluskoter. "Minerology of Ash of Some American Coals: Variations with Temperature and Source." Fuel, 55 (April 1976), 90-96.
27. Narang, K.C. and Chopra, S.K. "Studies on Alkaline Activation of BF, Steel and Alloy Slags." Silicates Industriels, 9 (1983), 175-182.
28. Paul, A. Chemistry of Glasses. New York: Chapman and Hall, 1982.
29. Pitt, J. M., T. Demirel, S. Schlorholtz, R. Hammerburg and R. Allenstein. "Final Report: Characterization of Fly Ash for Use in Concrete." Iowa Highway Research Board, Ames, Iowa, Project HR-225, September 1983.
30. Pitt, J. M., M. L. Mings and S. Schlorholtz. "Characterization and Techniques for Rapid Evaluation of Iowa Fly Ashes." Transportation Research Record No. 941, 1983, 12-17.

31. Raask, E. "Pulvensed Fuel Ash Constituents and Surface Characteristics in Concrete Applications." In International Symposium on the Use of PFA in Concrete, 1. Editors J. Cabrera and A. Cusens. Leeds, England: University of Leeds, April 1982, pp. 5-16.
32. Regourd, M., J. H. Thomassin, P. Baillif and J. C. Touray. "Blast-Furnace Slag Hydration, Surface Analysis." Cement and Concrete Research, 13 (1983), 549-556.
33. Roy, D. M. and G. M. Idorn. "Hydration, Structure, and Properties of Blast Furnace Slag Cements, Mortars and Concrete." ACI Journal, (Nov.-Dec., 1982), 444-457.
34. Roy, Della M., Karen Luke and Sidney Diamond. "Characterization of Fly Ash and its Reactions in Concrete." Fly Ash and Coal Conversion By-Products: Characterization, Utilization and Disposal I, 43. Editors G. J. McCarthy and R. L. Lauf. Pittsburgh: Materials Research Society, 1985, pp. 3-20.
35. Run-Zhang, Yuan and Gao Qiong-Ying. "Influence of Structural Features of Slags on Their Hydraulic Activity." Silicates Industriels, 12 (1982), 279-281.
36. Run-Zhang, Yuan, Zhu Jie-An and Zhang Li-Yun. "Composition and Structure of Fly Ashes and Their Pozzolanic Reactivity." In International Symposium on the Use of PFA in Concrete. Editors J. Cabrera and A. Cusens. Leeds, England: University of Leeds, April 1982, pp. 61-69.
37. Run-Zhang, Yuan, Ouyans Shi-Xi and Gao Qiong-Ying. "Structure and Hydraulic Activity of Slags in the System $\text{CaO-MgO-Al}_2\text{O}_3\text{-SiO}_2$." Silicates Industriels, 1 (1983), 3-6.

38. Scheetz, Barry E. and William B. White. "Characterization of Crystalline Phases in Fly Ash by Micro-focus Ramon Spectroscopy." Fly Ash and Coal Conversion By-Products: Characterization, Utilization and Disposal I, 43. Editors G. J. McCarthy and R. L. Lauf. Pittsburgh: Materials Research Society, 1985, pp. 53-60.
39. Schlorholtz, S. and M. Boybay. "Quantitative X-ray Fluorescence Analysis for Fly Ash Samples." Advances in X-ray Analysis, 27 (1984), 497-504.
40. Schlorholtz, S. and T. Demirel. "Autoclave Expansion of Portland Cement - Fly Ash Pastes." Fly Ash and Coal Conversion By-Products: Characterization, Utilization and Disposal I, 43. Editors G. J. McCarthy and R. L. Lauf. Pittsburgh: Materials Research Society, 1985, pp. 85-94.
41. Schlorholtz, S., T. Demirel and J. M. Pitt. "An Examination of the ASTM Lime Pozzolanic Activity Test for Class C Fly Ashes." Cement and Concrete Research, 14, No. 4 (July 1984), 499-504.
42. Shiyuan, Huang. "The Effect of Addition of Gypsum on the Hydration of Fly Ash Cement: Theme II Discussion." In International Symposium on the Use of PFA in Concrete, 2. Editors J. Cabrera and A. Cusens. Leeds, England: University of Leeds, April 1982, pp. 53-77.
43. Sugama, T. and L. E. Kukacka. "Magnesium Monophosphate Cements Derived from Diammonium Phosphate Solutions." Cement and Concrete Research, 13 (1983), 407-416.
44. Sun, K. H. "Fundamental Condition of Glass Formation." Journal of American Ceramic Society, 30 (1947), 277-281.

45. Thorne, D. J. and J. D. Watt. "Composition and Pozzolanic Properties of Pulverised Fuel Ashes II. Pozzolanic Properties of Fly Ashes as Determined by Crushing Strength Tests on Lime Mortars." Journal Applied Chemistry, 15, No. 12 (December 1965), 595-604.

46. Van Vlack, L. H. Physical Ceramics for Engineers. Amsterdam: Addison-Wesley Publishing Company, 1965.

47. Volf, M. B. Chemical Approach to Glass: Glass Science and Technology 7. New York: Elsevier Publishing Company, 1984.

48. Watt, J. D. and D. J. Thorne. "Composition and Pozzolanic Properties of Pulverised Fuel Ashes I. Composition of Fly Ashes from Some British Power Stations and Properties of Their Component Particles." Journal Applied Chemistry, 15, No. 12 (December 1965), 585-594.

49. Watt, J. D. and D. J. Thorne. "The Composition and Pozzolanic Properties of Pulverised Fuel Ashes III. Pozzolanic Properties of Fly Ashes as Determined by Chemical Methods." Journal Applied Chemistry, 16, No. 2 (February 1966), 33-39.

50. Zacharisen, W. H. "The Atomic Arrangement in Glass." Journal of American Chemical Society, 54 (1932), 3841-3851.

ACKNOWLEDGEMENTS

This research effort was supported by Iowa Highway Research Board Project HR-260, "Optimization of Soil Stabilization with Class C Fly Ash," and Iowa Highway Research Board Project HR-285, "Development of a Rational Characterization Method for Iowa Fly Ashes."

The assistance and help of Scott Schlorholtz, Glenn Oren, and Jerry Amenson in operation of the Materials Analysis and Research Laboratory equipment is gratefully appreciated. In addition, Scott Schlorholtz is very highly commended for his diligent efforts to keep the Materials Laboratory Library and personnel updated on recent research publications in a wide variety of areas.

The writer is forever indebted to his major professor, Dr. Turgut Demirel without whose interest, concern, guidance, and patience this work would not have been accomplished. The author is also grateful to his co-major professor, Dr. John Pitt for his support, encouragement, and contributions throughout this effort.

APPENDIX: FIGURES

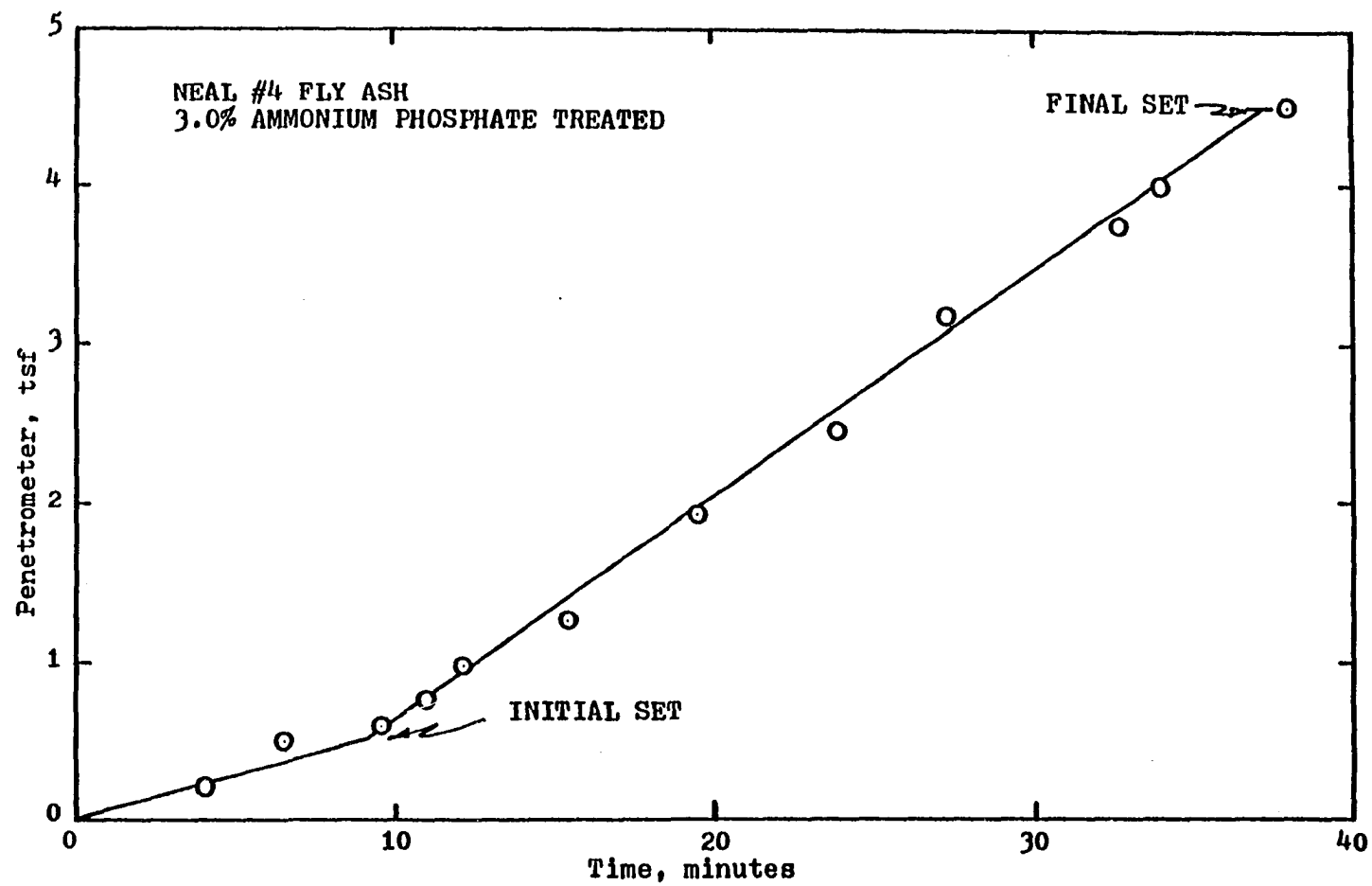


Figure 1. Setting times of dibasic ammonium phosphate treated Neal 4 fly ash

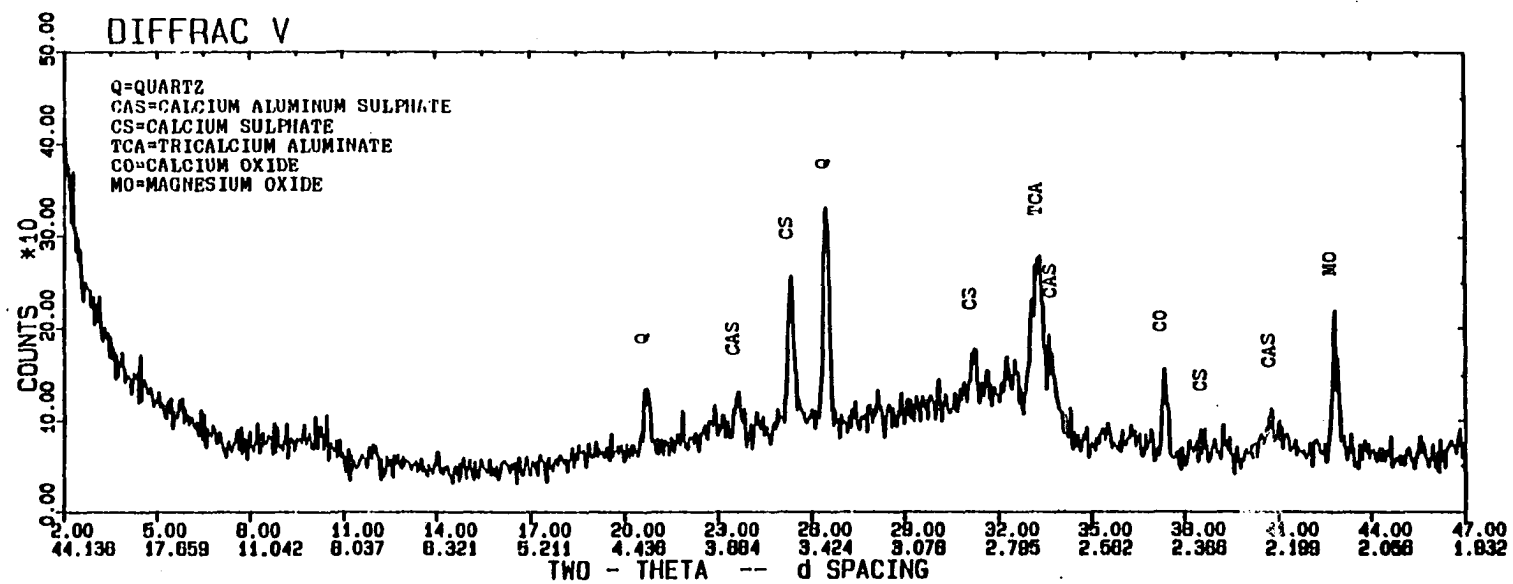


Figure 2. X-ray diffraction trace, raw Neal 4 fly ash, air dry

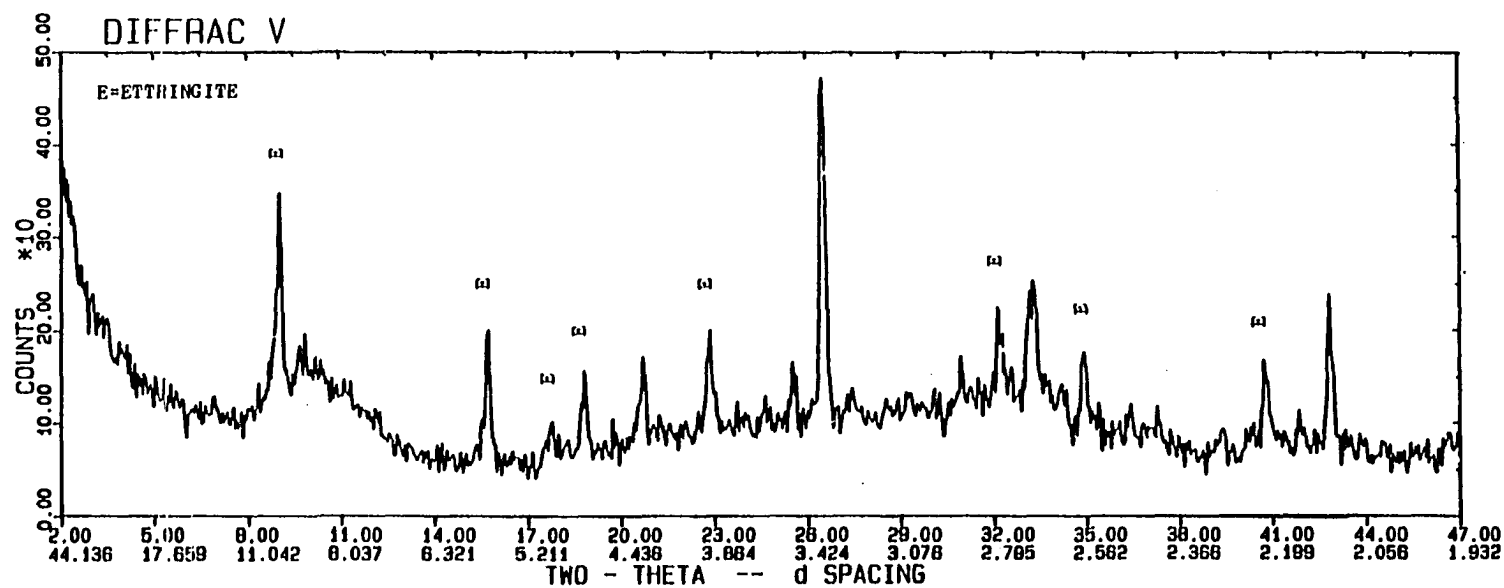


Figure 3. X-ray diffraction trace, Neal 4 fly ash, hydrated with water, cured at room temperature, sealed from air, age 36 days

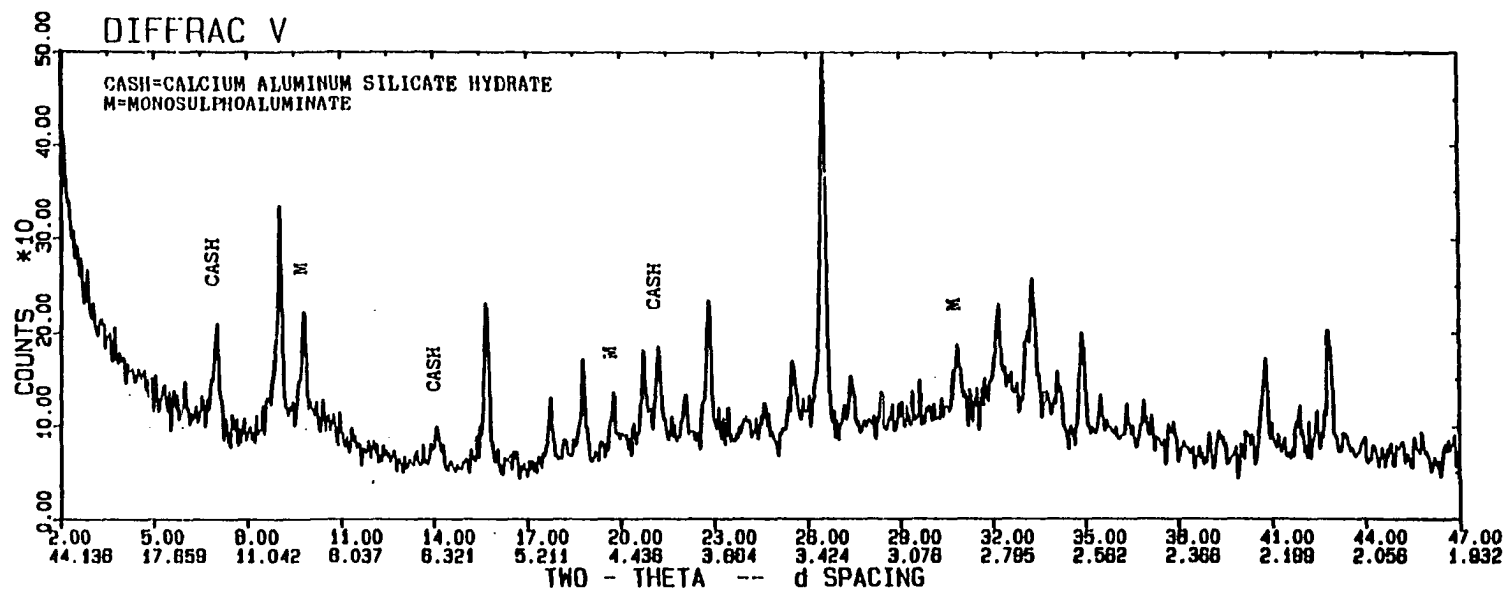


Figure 4. X-ray diffraction trace, Neal 4 fly ash, 3.0% dibasic ammonium phosphate treated, cured at room temperature, sealed from air, age 35 days

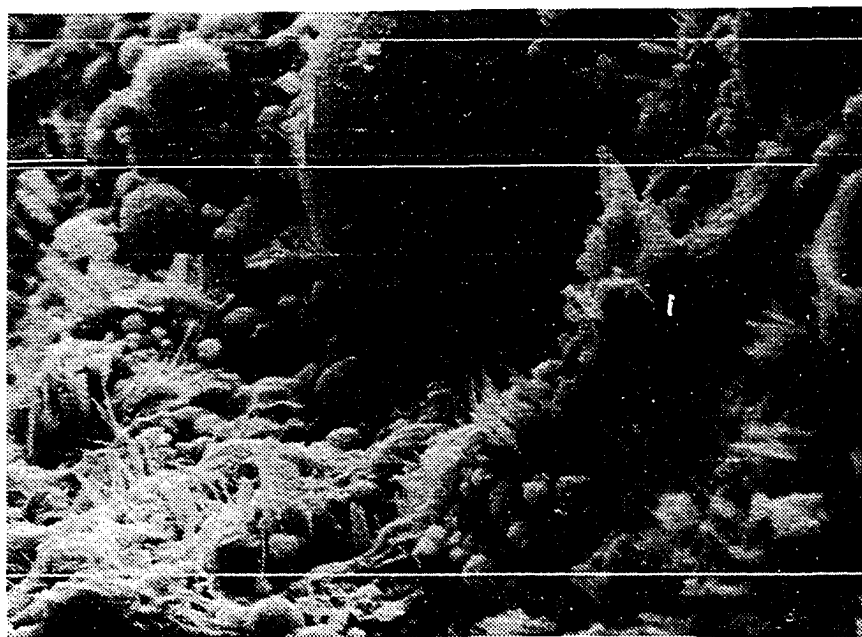


Figure 5. Scanning electron micrograph, Neal 4 fly ash, hydrated with water, cured at room temperature, sealed from air, age 36 days, 1900X

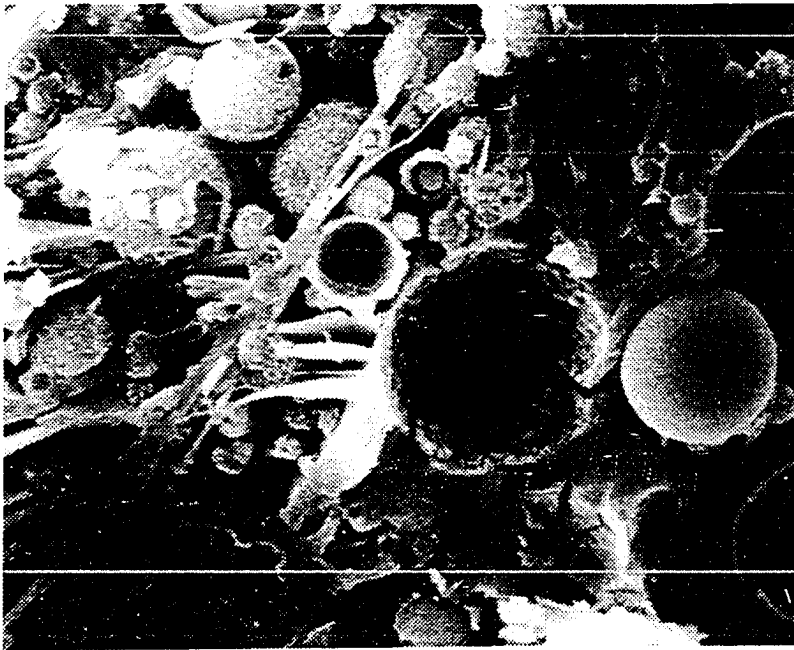


Figure 6. Scanning electron micrograph, Neal 4 fly ash, 3.0% ammonium phosphate treated, cured at room temperature, sealed from air, age 35 days, 1900X

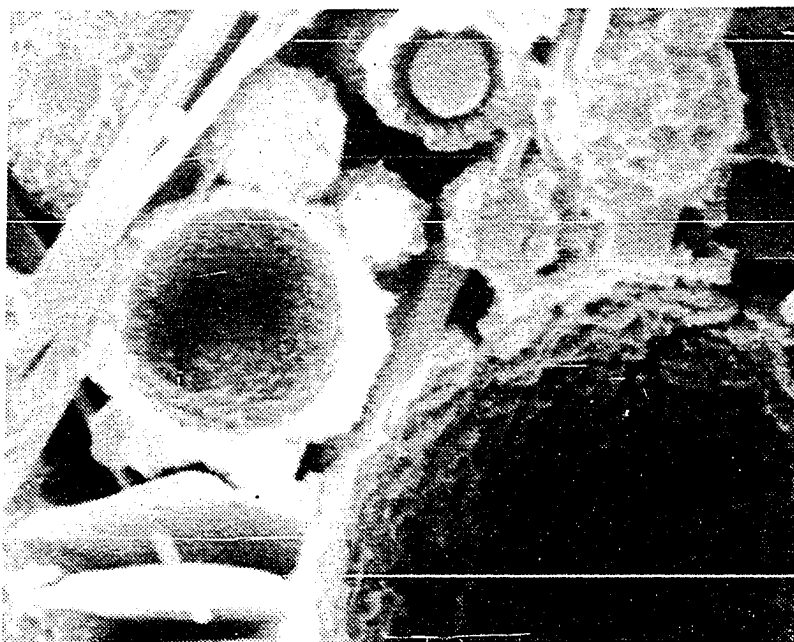


Figure 7. Scanning electron micrograph, Neal 4 fly ash, 3.0% ammonium phosphate treated, cured at room temperature, sealed from air, age 35 days, 5000X

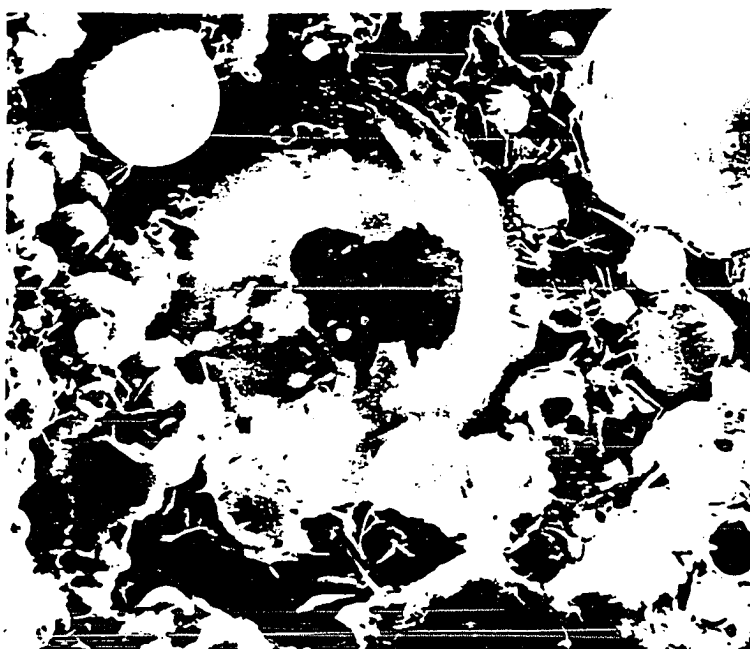
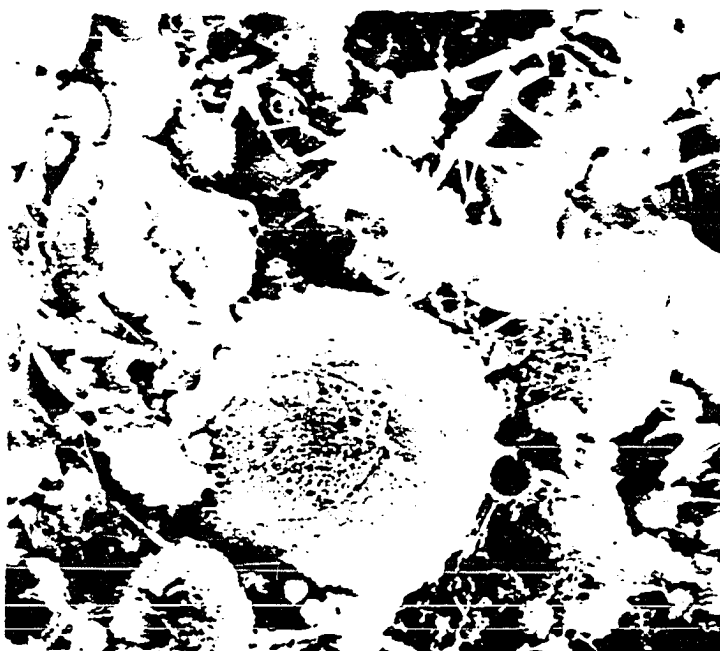


Figure 8. Scanning electron micrographs, Neal 2 fly ash, hydrated with water (top) and hydrated with 3.0% ammonium nitrate (bottom), cured at room temperature, sealed from air, age 28 days, 2500X